



US007348977B2

(12) **United States Patent**  
**West et al.**

(10) **Patent No.:** **US 7,348,977 B2**  
(45) **Date of Patent:** **Mar. 25, 2008**

(54) **SUBSURFACE SCATTERING  
APPROXIMATION METHODS AND  
APPARATUS**

6,252,608 B1 6/2001 Snyder et al.  
6,342,887 B1 1/2002 Munroe  
6,897,865 B2 \* 5/2005 Higashiyama ..... 345/426  
6,961,058 B2 \* 11/2005 Guo et al. .... 345/426

(75) Inventors: **Bradley S. West**, Seattle, WA (US);  
**Thomas Lokovic**, Richmond, CA (US);  
**David Batte**, Albany, CA (US)

(73) Assignee: **Pixar**, Emeryville, CA (US)

(\* ) Notice: Subject to any disclaimer, the term of this patent is extended or adjusted under 35 U.S.C. 154(b) by 30 days.

(21) Appl. No.: **10/810,064**

(22) Filed: **Mar. 25, 2004**

(65) **Prior Publication Data**

US 2004/0263511 A1 Dec. 30, 2004

**Related U.S. Application Data**

(63) Continuation-in-part of application No. 09/619,064, filed on Jul. 19, 2000, now Pat. No. 6,760,024.

(51) **Int. Cl.**  
**G06T 15/50** (2006.01)

(52) **U.S. Cl.** ..... **345/426**

(58) **Field of Classification Search** ..... 345/421  
See application file for complete search history.

(56) **References Cited**

**U.S. PATENT DOCUMENTS**

5,742,749 A 4/1998 Foran et al.  
5,870,097 A 2/1999 Snyder et al.  
5,959,731 A 9/1999 Jones  
6,016,150 A 1/2000 Lengyel et al.  
6,111,582 A 8/2000 Jenkins

**OTHER PUBLICATIONS**

Agrawala et al., Efficient image-based methods for rendering soft shadows, *Computer Graphics, (SIGGRAPH 2000 Proceedings)* pp. 375-384.

Chang et al., LDI tree: a hierarchical representation for image-based rendering, *Computer Graphics (SIGGRAPH 99 Proceedings)* pp. 291-298.

Heckbert, Survey of texture mapping, *IEEE Computer Graphics and Applications*, 6(11):56-67, Nov. 1986.

(Continued)

*Primary Examiner*—Mark Zimmerman

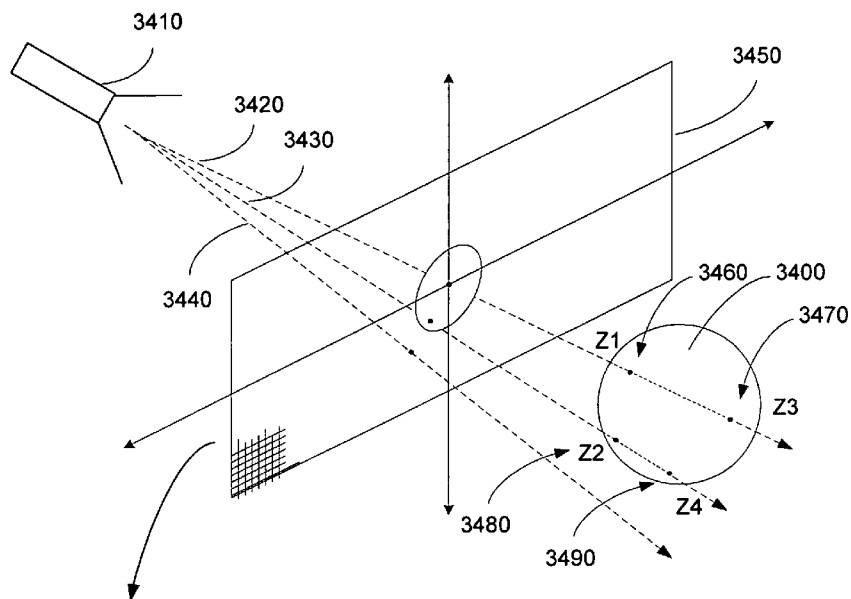
*Assistant Examiner*—Andrew Yang

(74) *Attorney, Agent, or Firm*—Townsend and Townsend and Crew LLP

(57) **ABSTRACT**

A method for determining illumination of surface points of an object in a scene from lighting sources includes determining a first thickness map for a first lighting source for the scene, wherein the first thickness map includes a first plurality of thickness values of the object with respect to distance from the first lighting source, determining a surface point on the object, determining a first plurality of thickness values associated with the surface point on the object in response to the first thickness map, determining a first filtered thickness value associated with the surface point on the object in response to the first plurality of thickness values, and determining an illumination contribution from the first lighting source at the surface point in response to the first filtered thickness value.

**28 Claims, 32 Drawing Sheets**



OTHER PUBLICATIONS

Kajiya et al., Rendering fur with three dimensional textures. In *Computer Graphics (SIGGRAPH '89 Proceedings)*, vol. 23, pp. 271-280, Jul. 1989.

Kajiya et al., Ray tracing volume densities. In *Computer Graphics (SIGGRAPH '84 Proceedings)*, vol. 18, pp. 165-174, Jul. 1984.

Keating et al., Shadow penumbras for complex objects by depth-dependent filtering of multi-layer depth images. In *Eurographics Rendering Workshop 1999*, pp. 205-220, New York, Jun. 1999. Springer-Verlag.

Levoy, *Display of Surfaces from Volume Data*. Ph.D. thesis, University of North Carolina at Chapel Hill, 1989.

Levoy et al., Light Field Rendering, *Computer Graphics (SIGGRAPH '96 Proceedings)* pp. 31-42.

Max, Hierarchical rendering of trees from precomputed multi-layer Z-buffers. In *Eurographics Rendering Workshop 1996*, pp. 165-174, New York, Jun. 1996.

Shade et al., Layered depth images. In *SIGGRAPH 98 Proceedings*, pp. 231-242. Addison Wesley, Jul. 1998.

Soler et al, Fast calculation of soft shadow textures using convolution, *Computer Graphics (SIGGRAPH 98 Proceedings)* pp. 321-322.

Williams, Casting curved shadows on curved surfaces. *Computer Graphics (SIGGRAPH '78 Proceedings)*, 12(3):270-274, Aug. 1978.

Williams, Pyramidal parametrics. *Computer Graphics (SIGGRAPH '83 Proceedings)*, 17(3):1-11, Jul. 1983.

Woo et al., A survey of shadow algorithms. *IEEE Computer Graphics and Applications*, 10(6):13-32, Nov. 1990.

Lokovic et al., *Deep Shadow Maps*. In Proceedings of SIGGRAPH 2000, *Computer Graphics Proceedings, Annual Conference Series*, pp. 385-392, 2000. K. Akeley, editor, <http://graphics.stanford.edu/papers/deepshadows>, printed Sep. 1, 2004.

Mitchell, Consequences of Stratified Sampling in Graphics, (SIGGRAPH) '96 Proceedings, pp. 277-280, Addison Wesley, 1996.

Reeves et al., Rendering Antialiased Shadows with Depth Maps, *Computer Graphics (SIGGRAPH) '87 Proceedings*, vol. 21, pp. 283-291, 1987.

\* cited by examiner

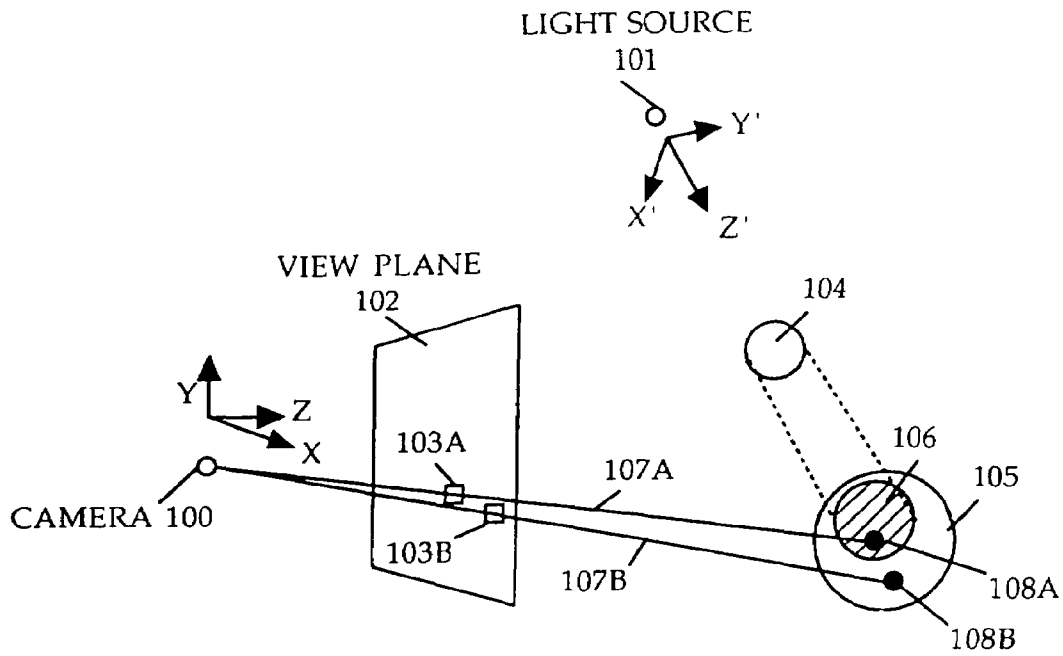


FIGURE 1  
PRIOR ART

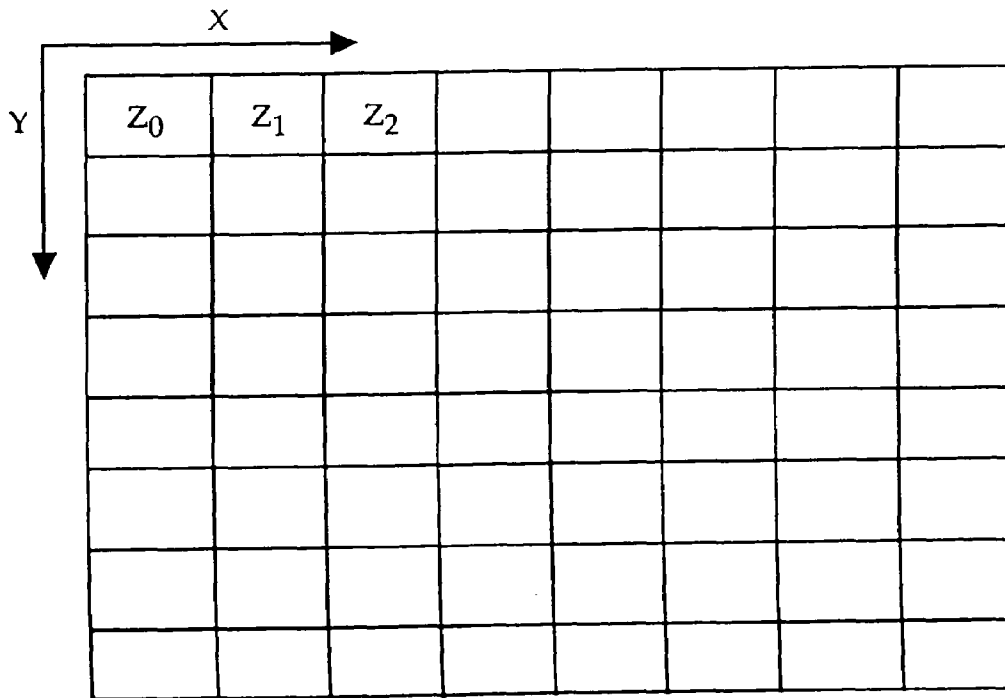


FIGURE 2  
PRIOR ART

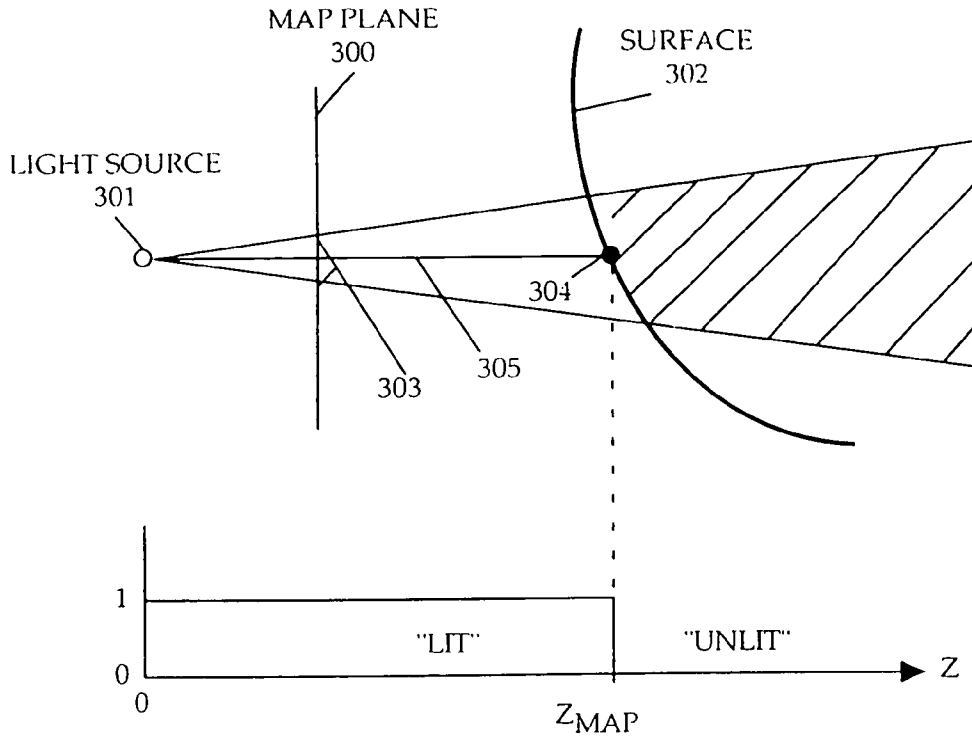


FIGURE 3  
PRIOR ART

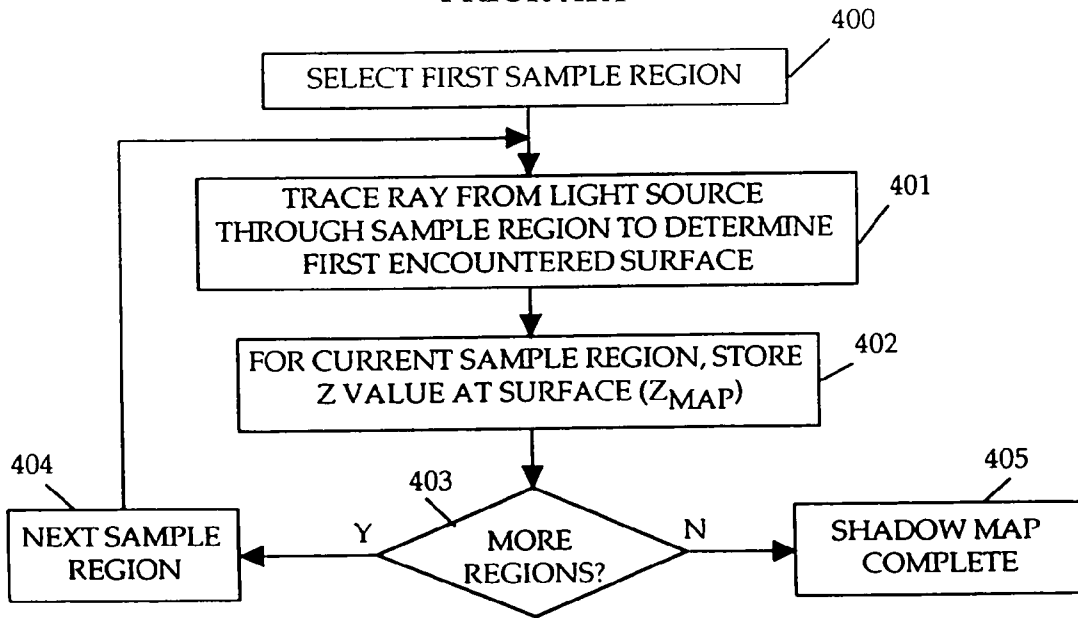
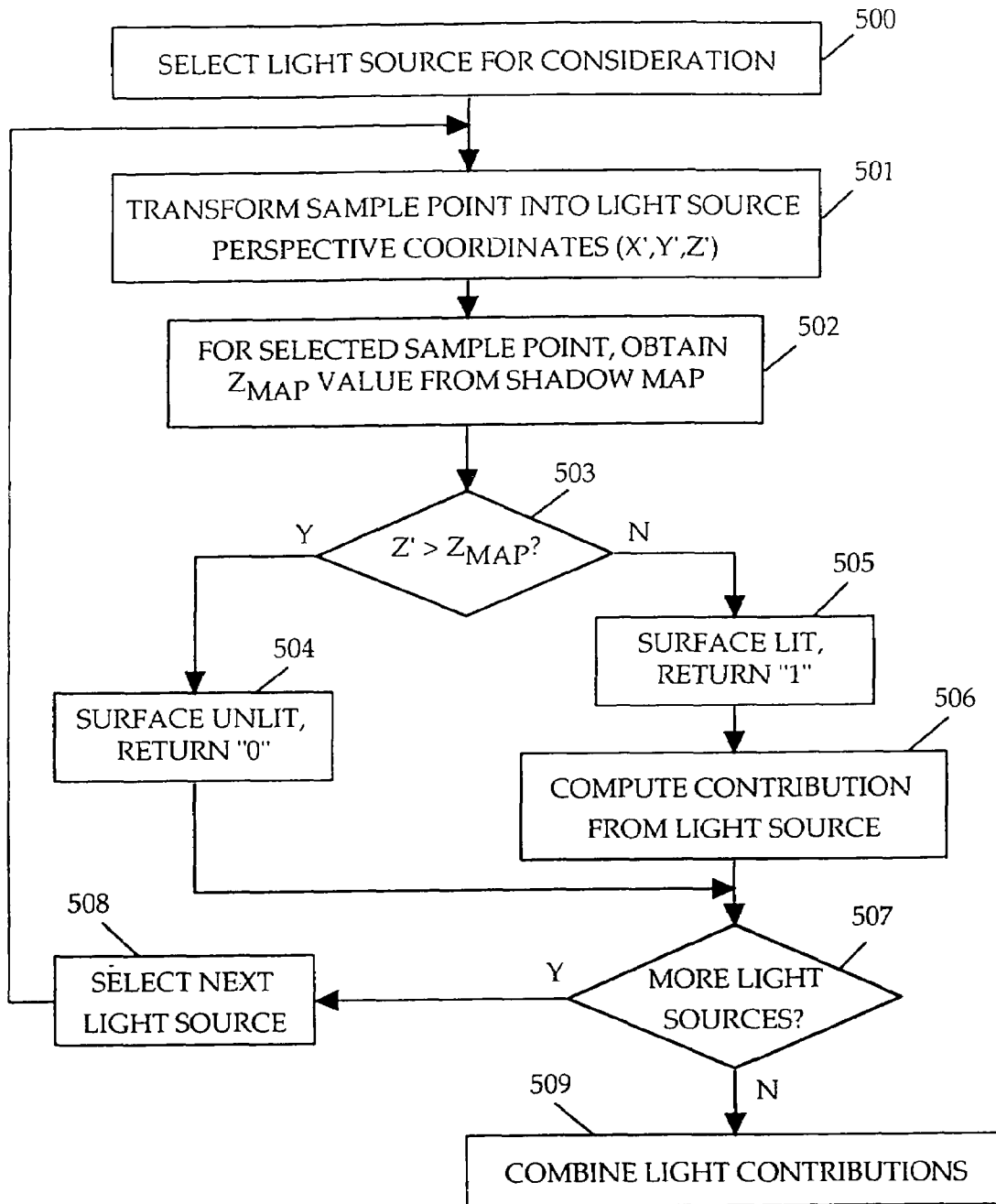
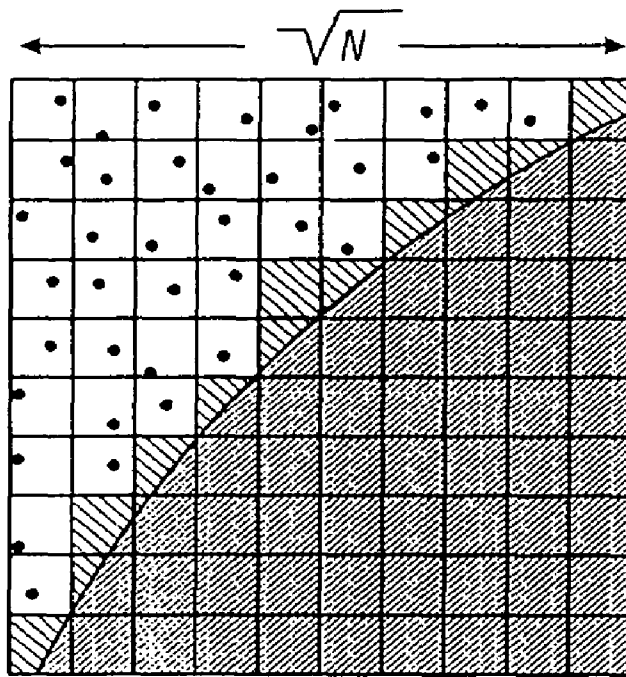


FIGURE 4  
PRIOR ART

FIGURE 5



PRIOR ART



**FIGURE 6A**  
**PRIOR ART**

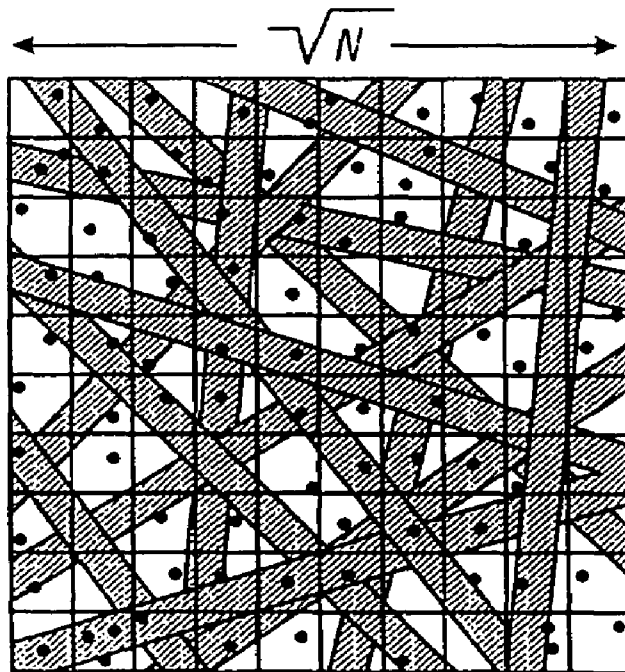


**FIGURE 6B**  
**PRIOR ART**

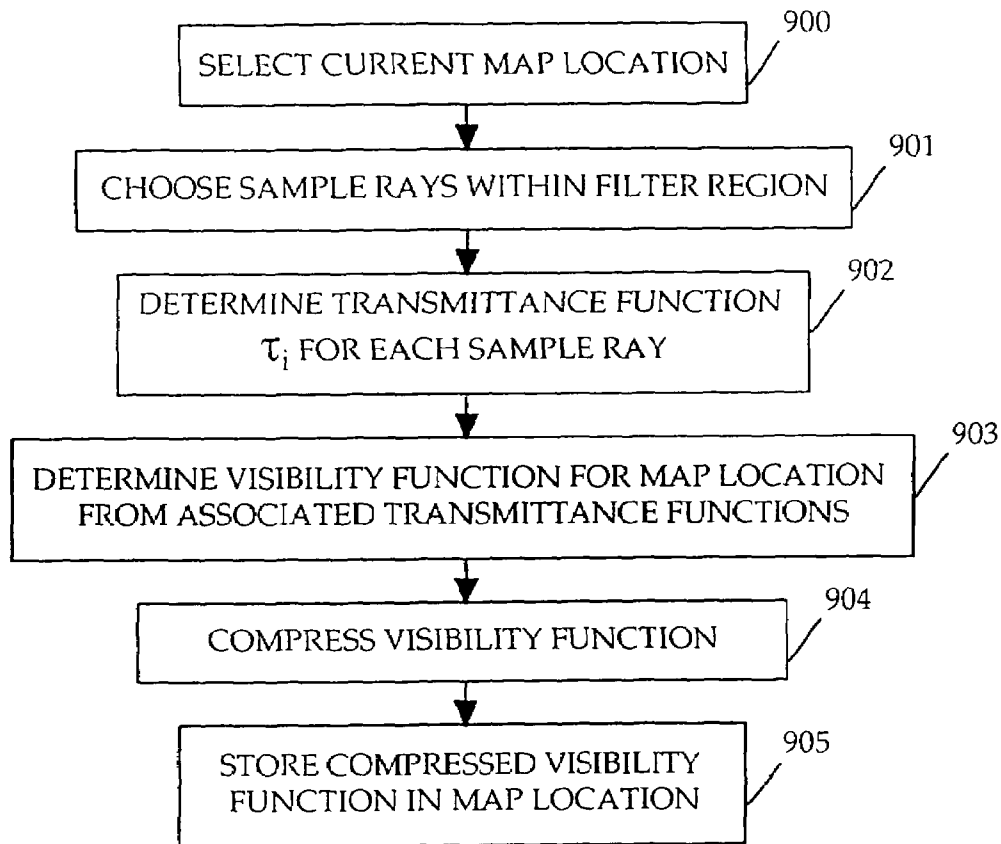


FIGURE 9

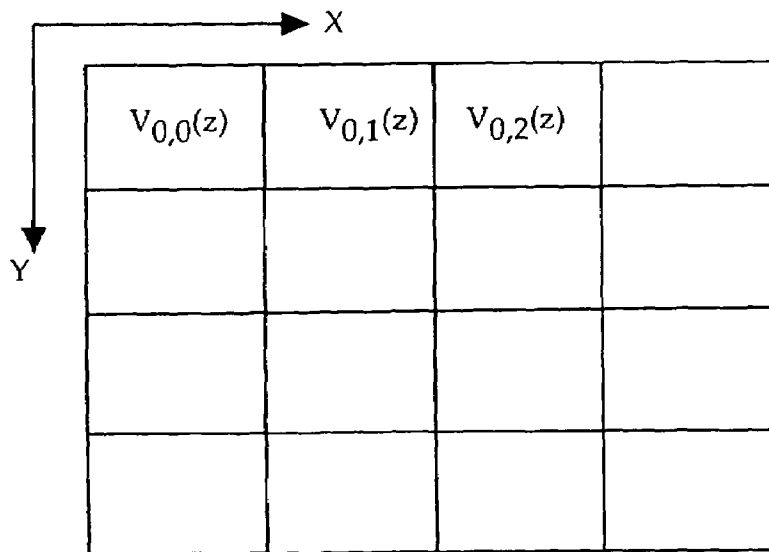


FIGURE 7

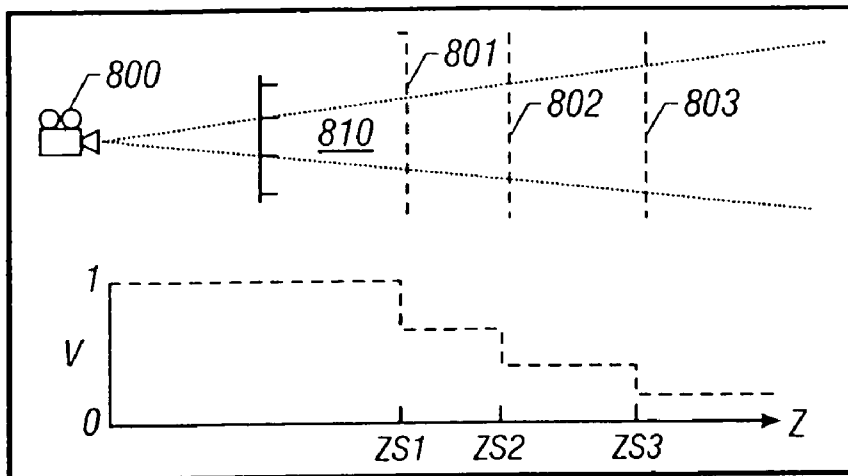


FIGURE 8A

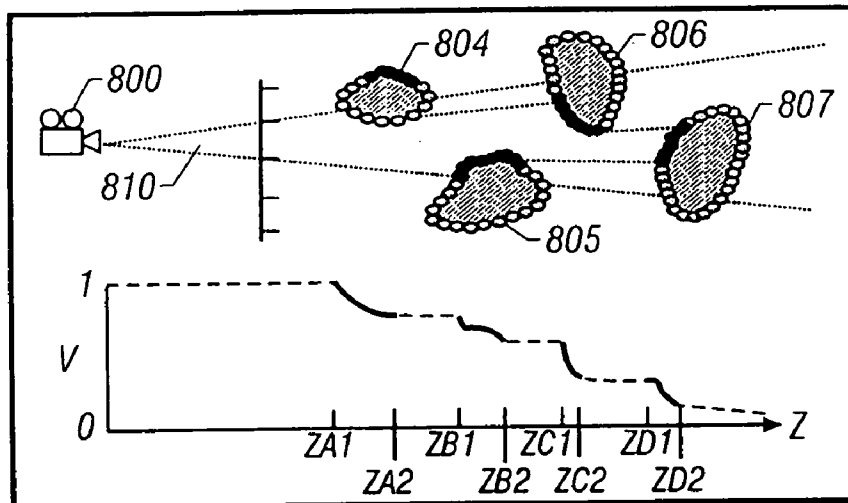


FIGURE 8B

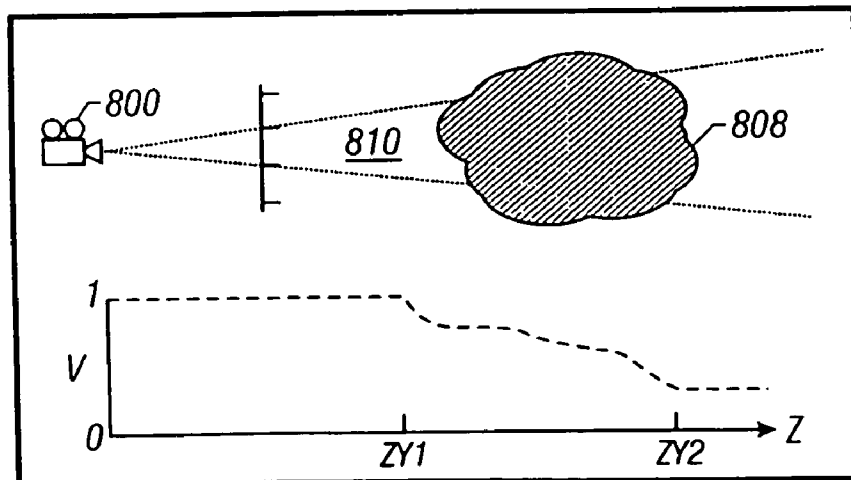


FIGURE 8C



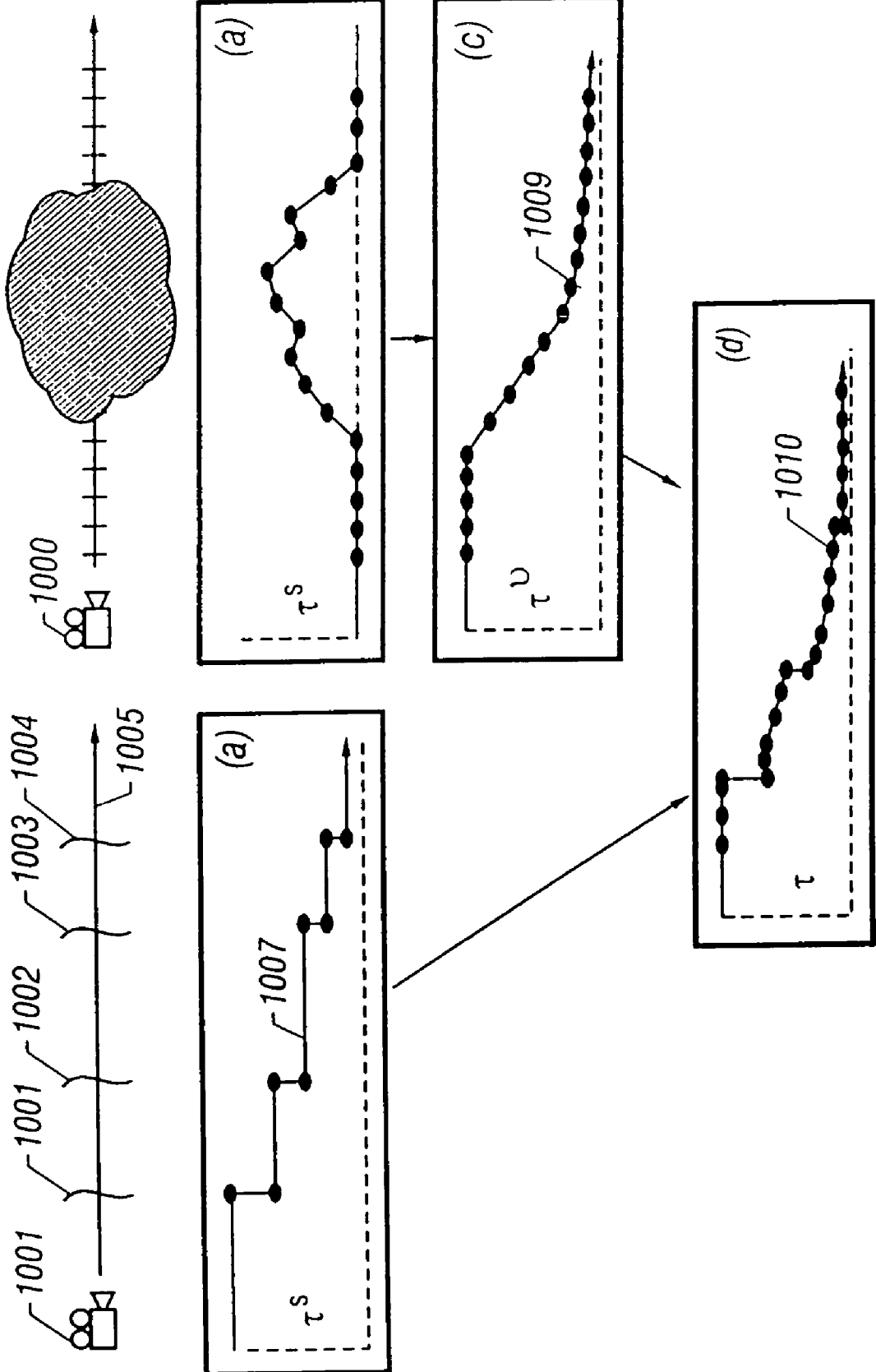


FIGURE 10

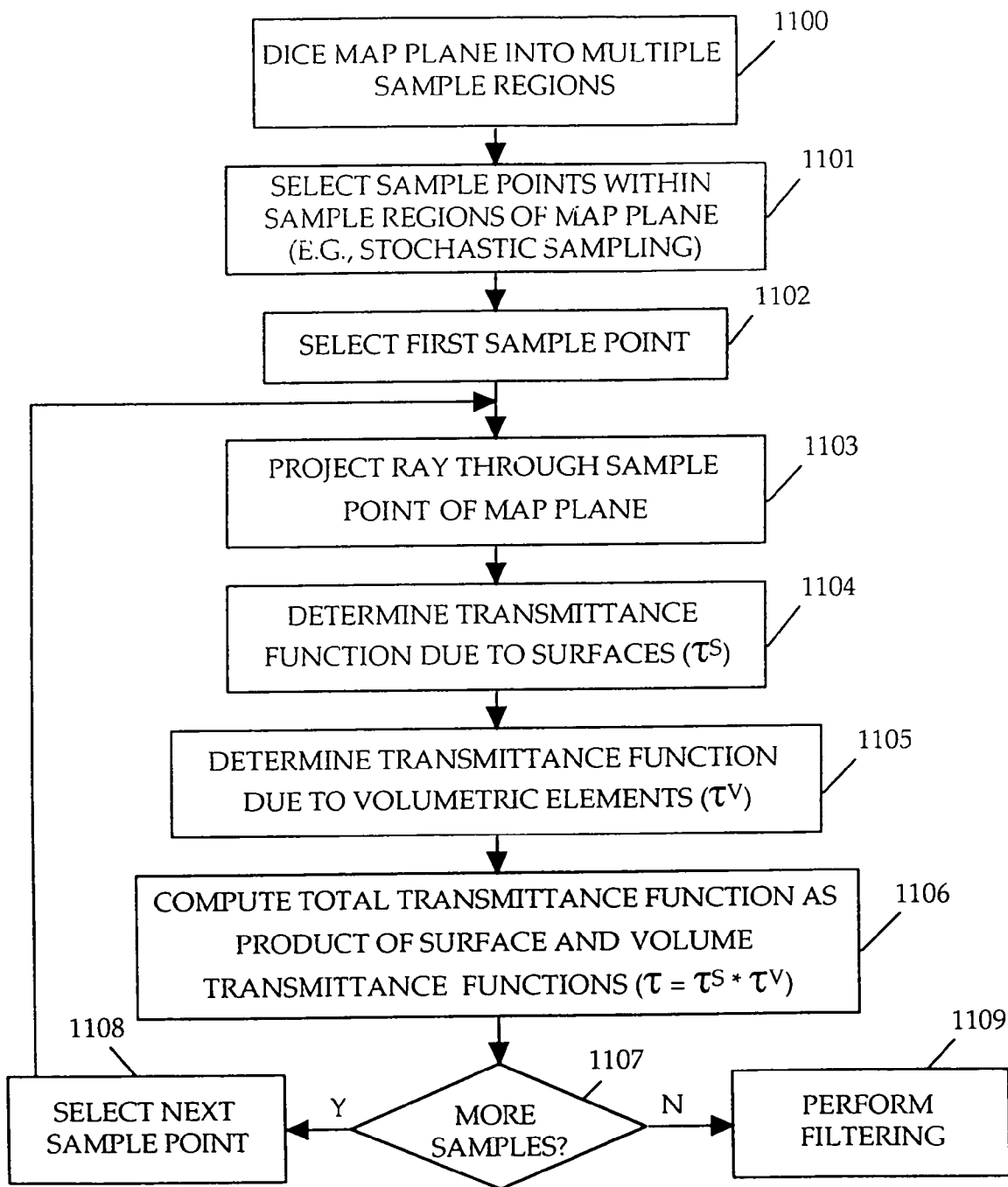


FIGURE 11A

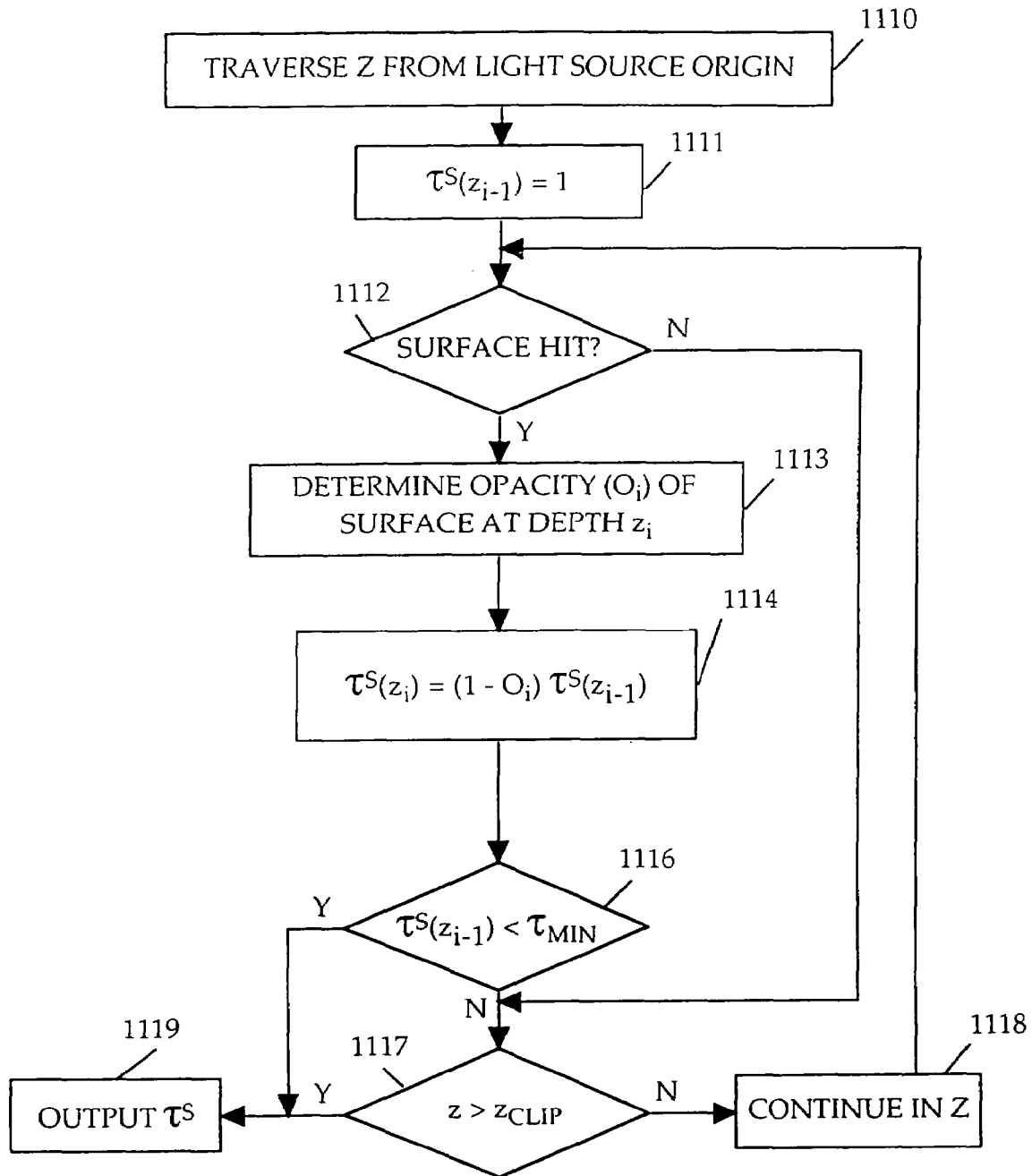


FIGURE 11B

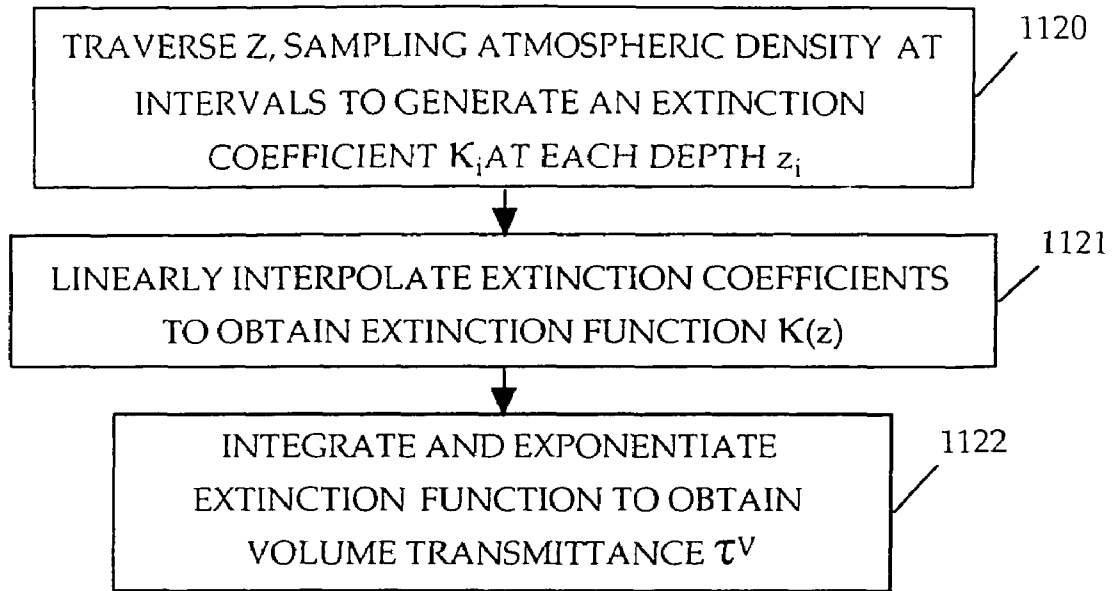


FIGURE 11C

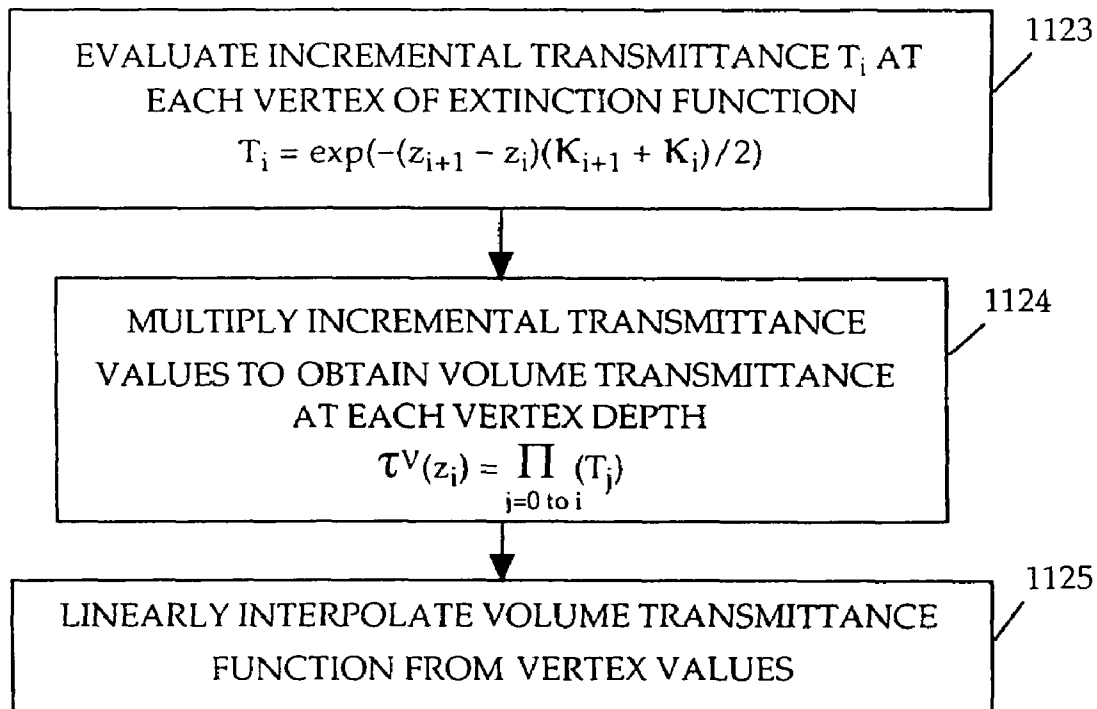


FIGURE 11D

C	B	B	C
B	A	A	B
B	A	A	B
C	B	B	C

FIGURE 12

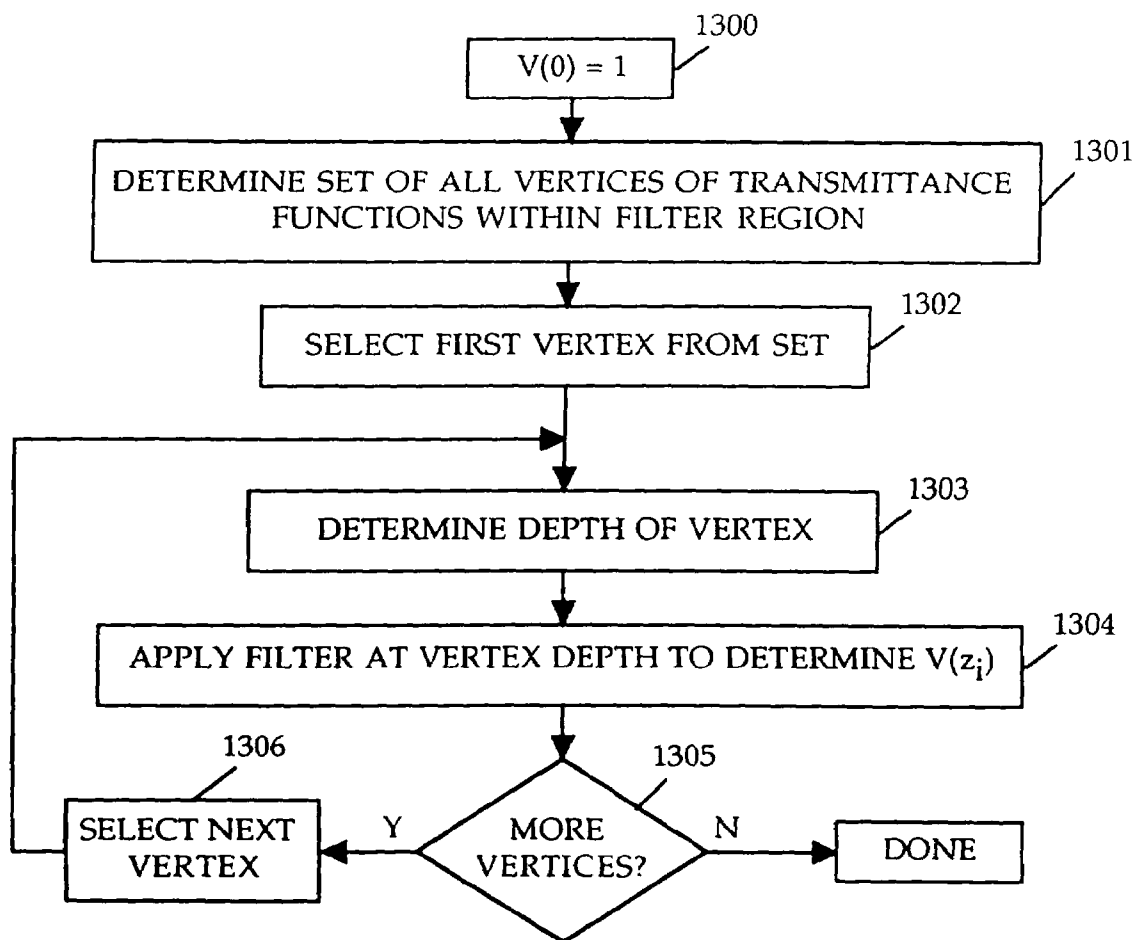


FIGURE 13A

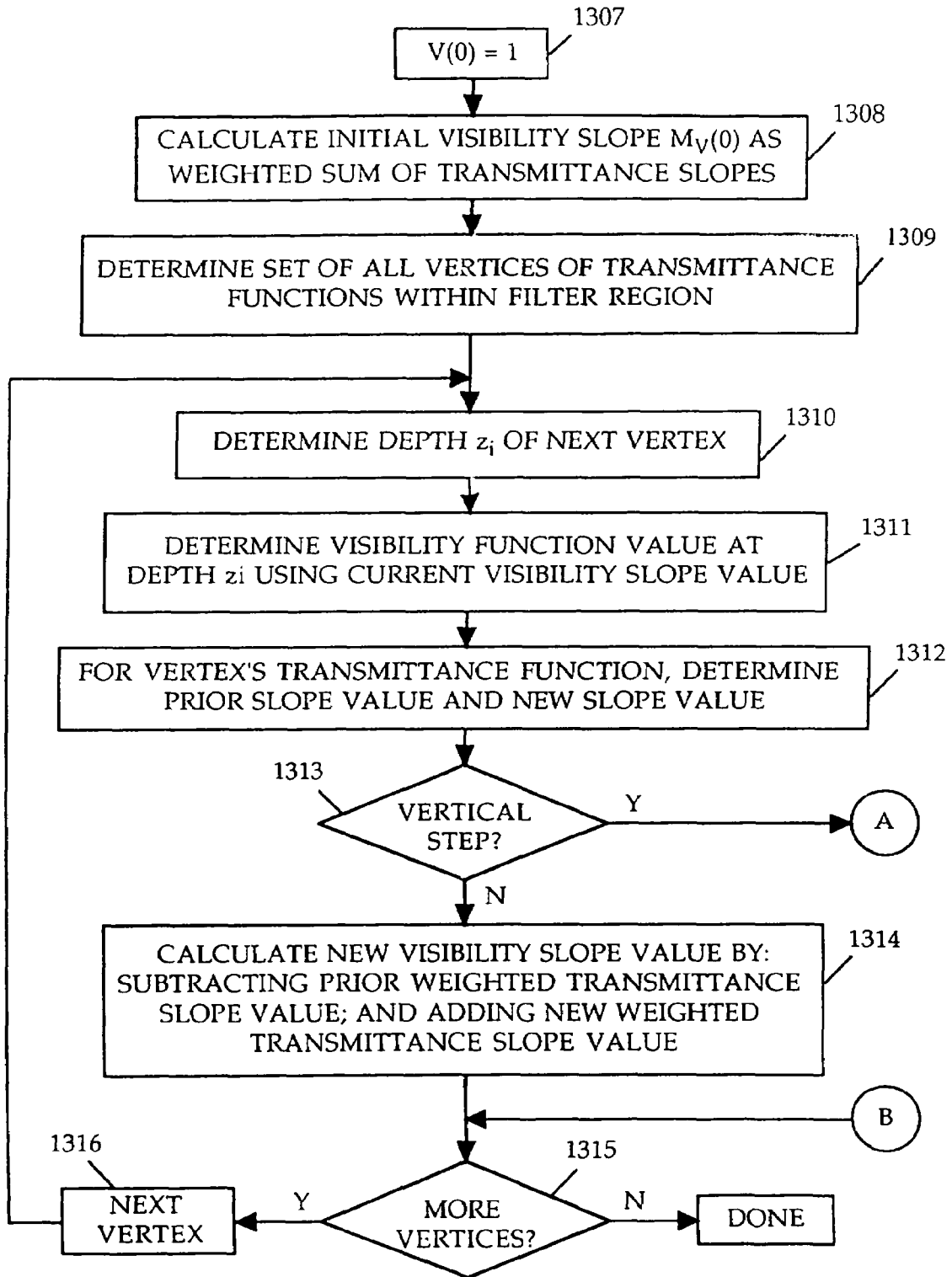


FIGURE 13B

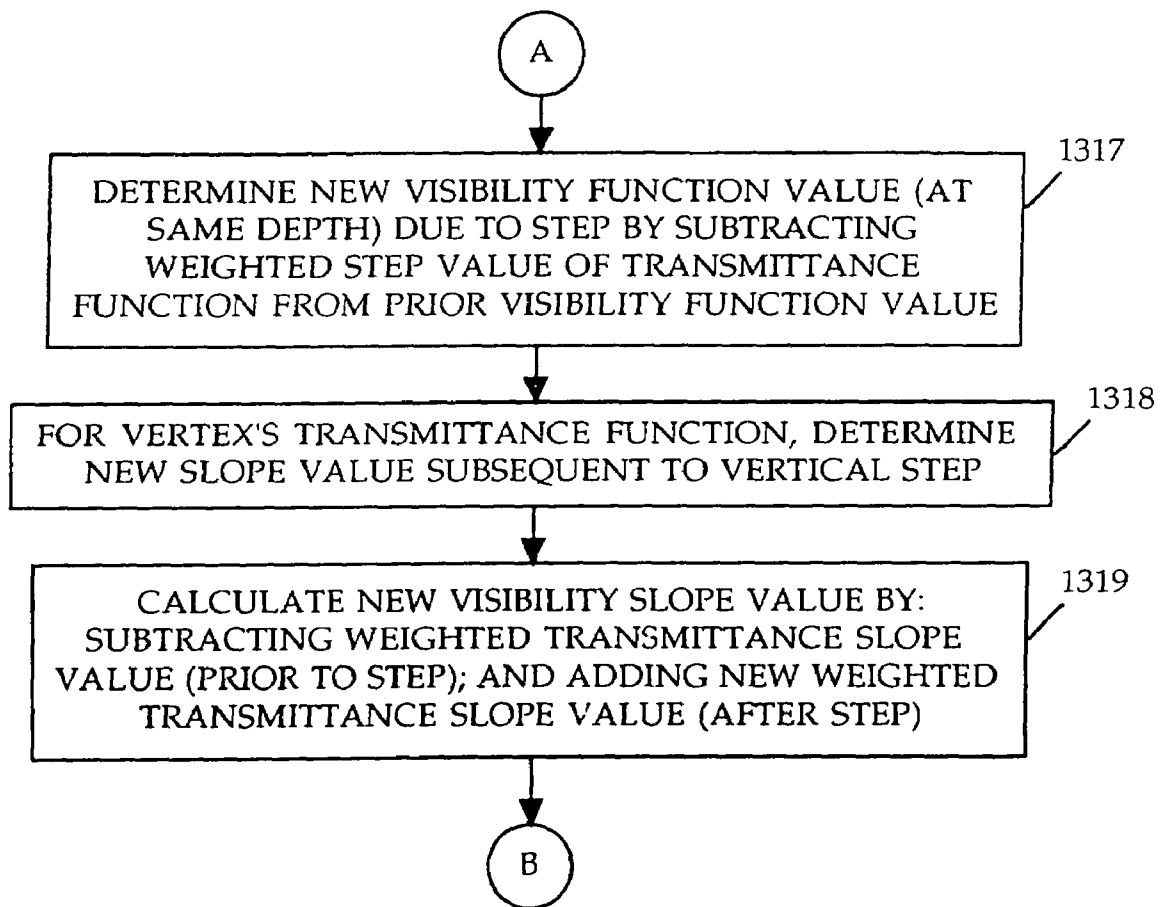


FIGURE 13C

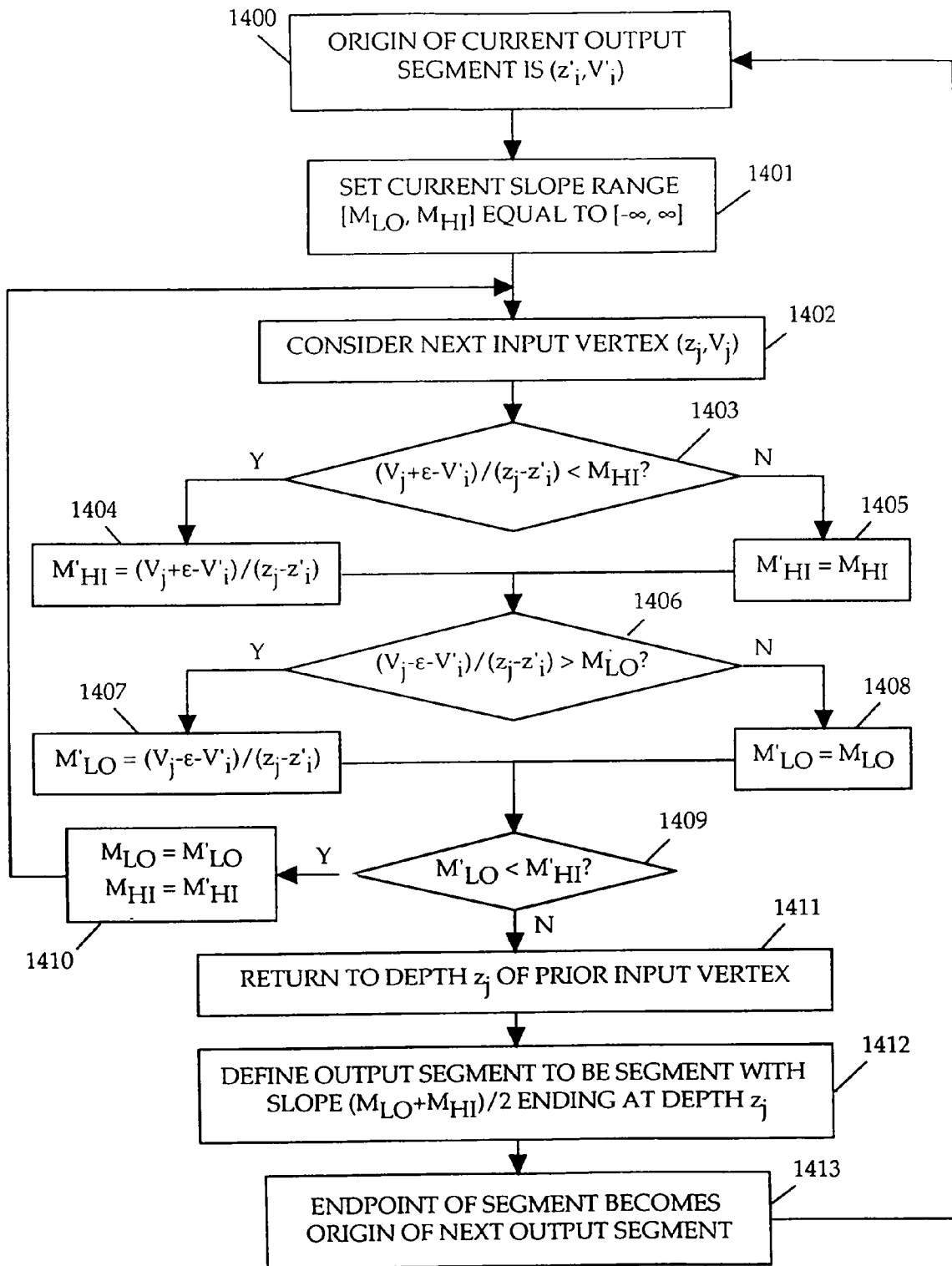
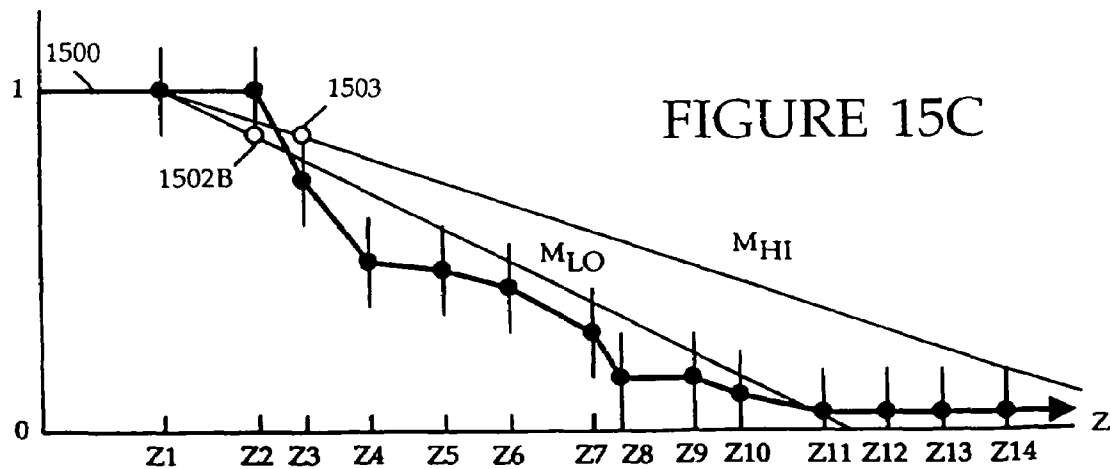
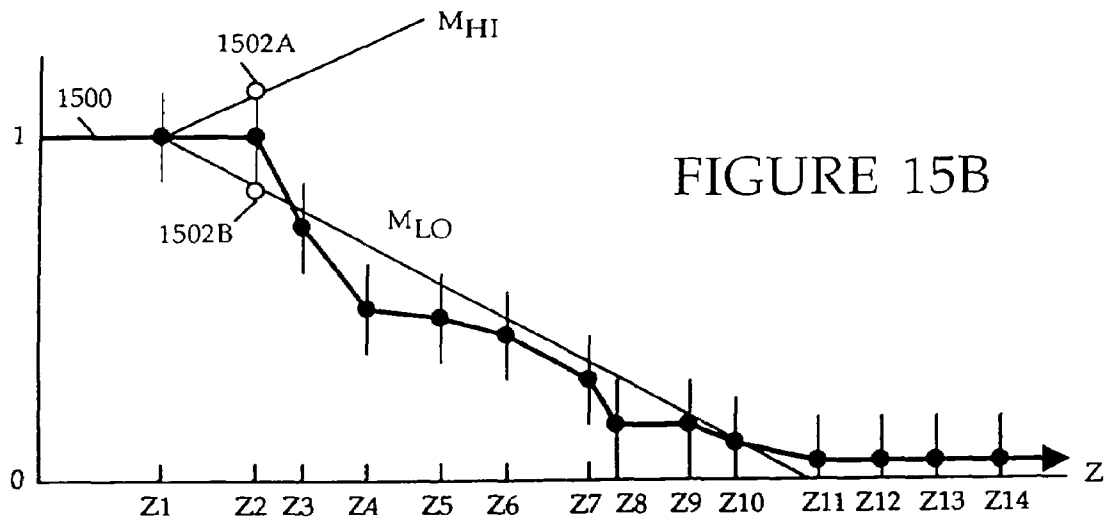
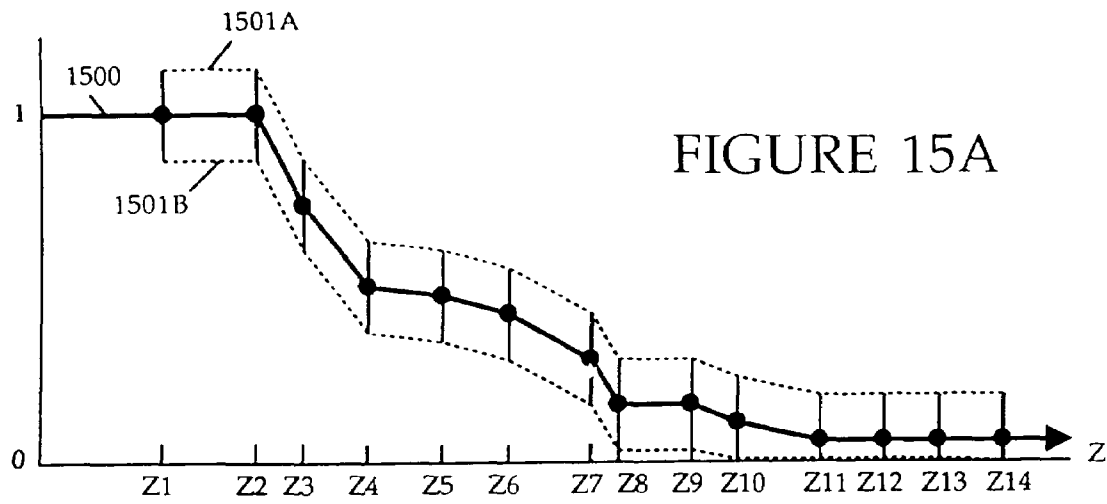
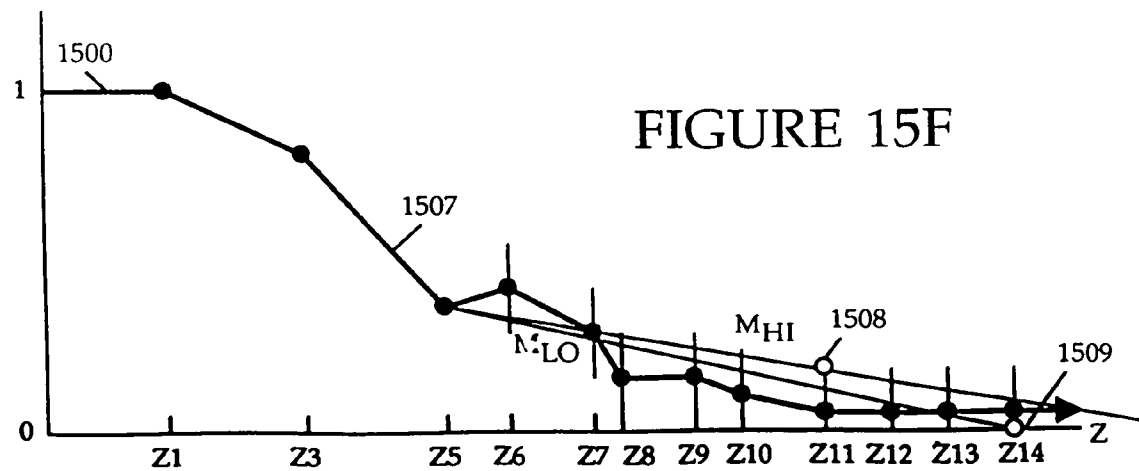
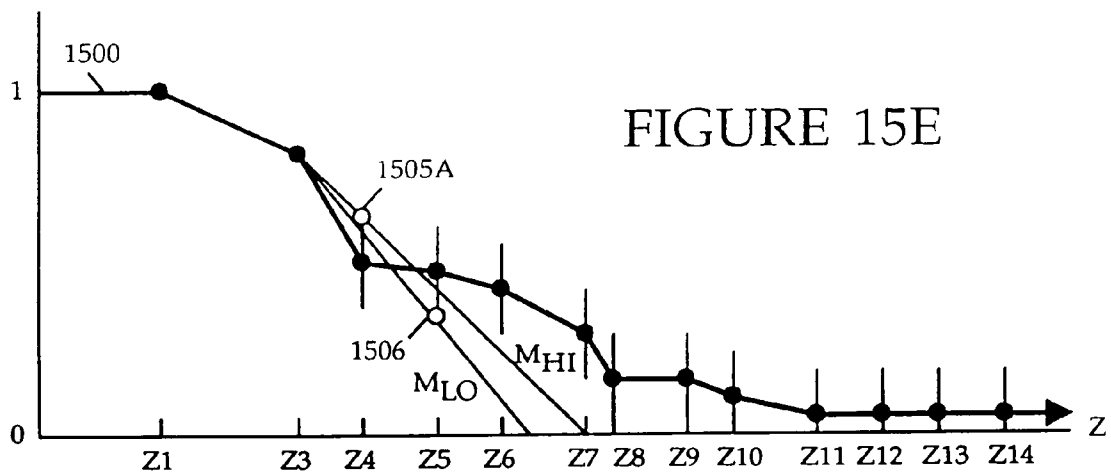
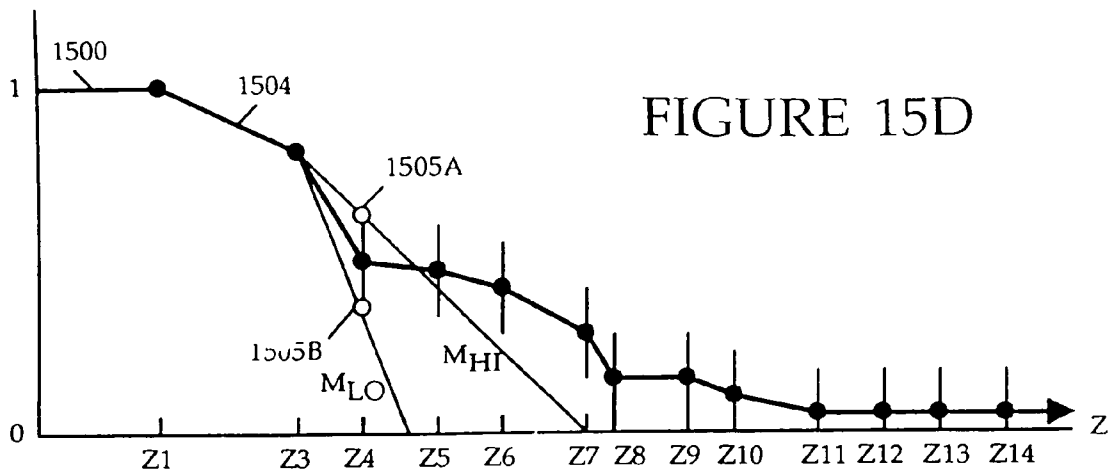
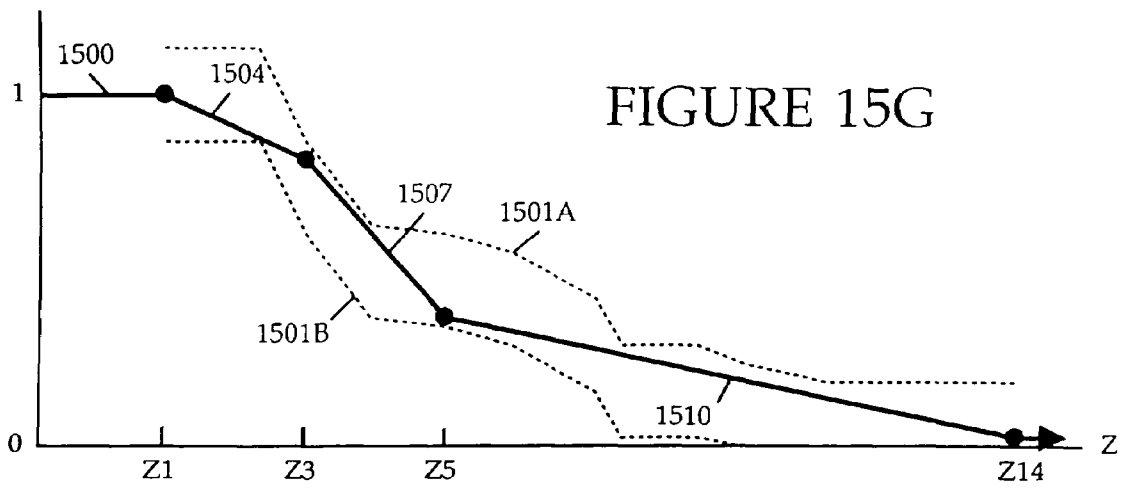


FIGURE 14









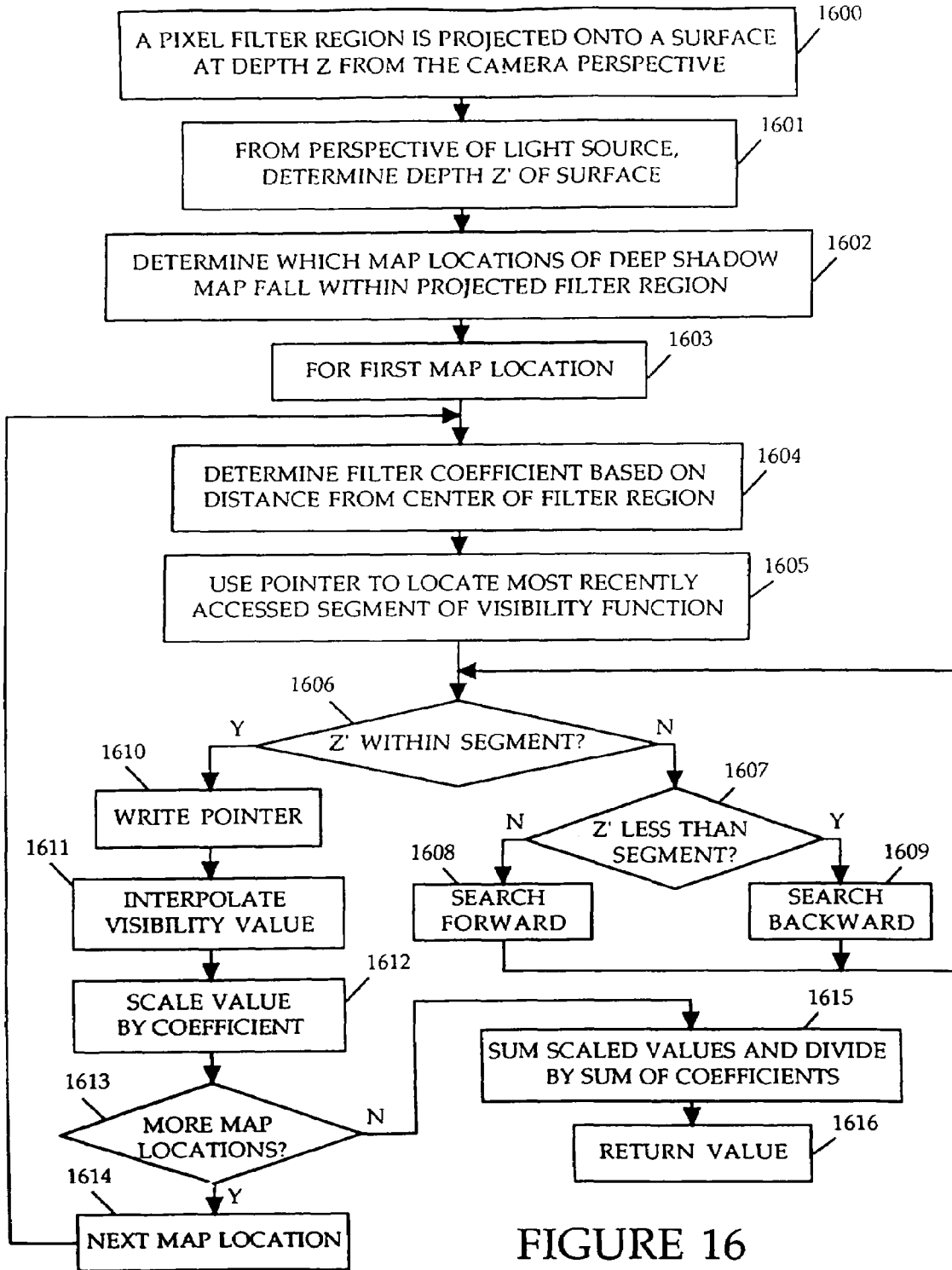


FIGURE 16

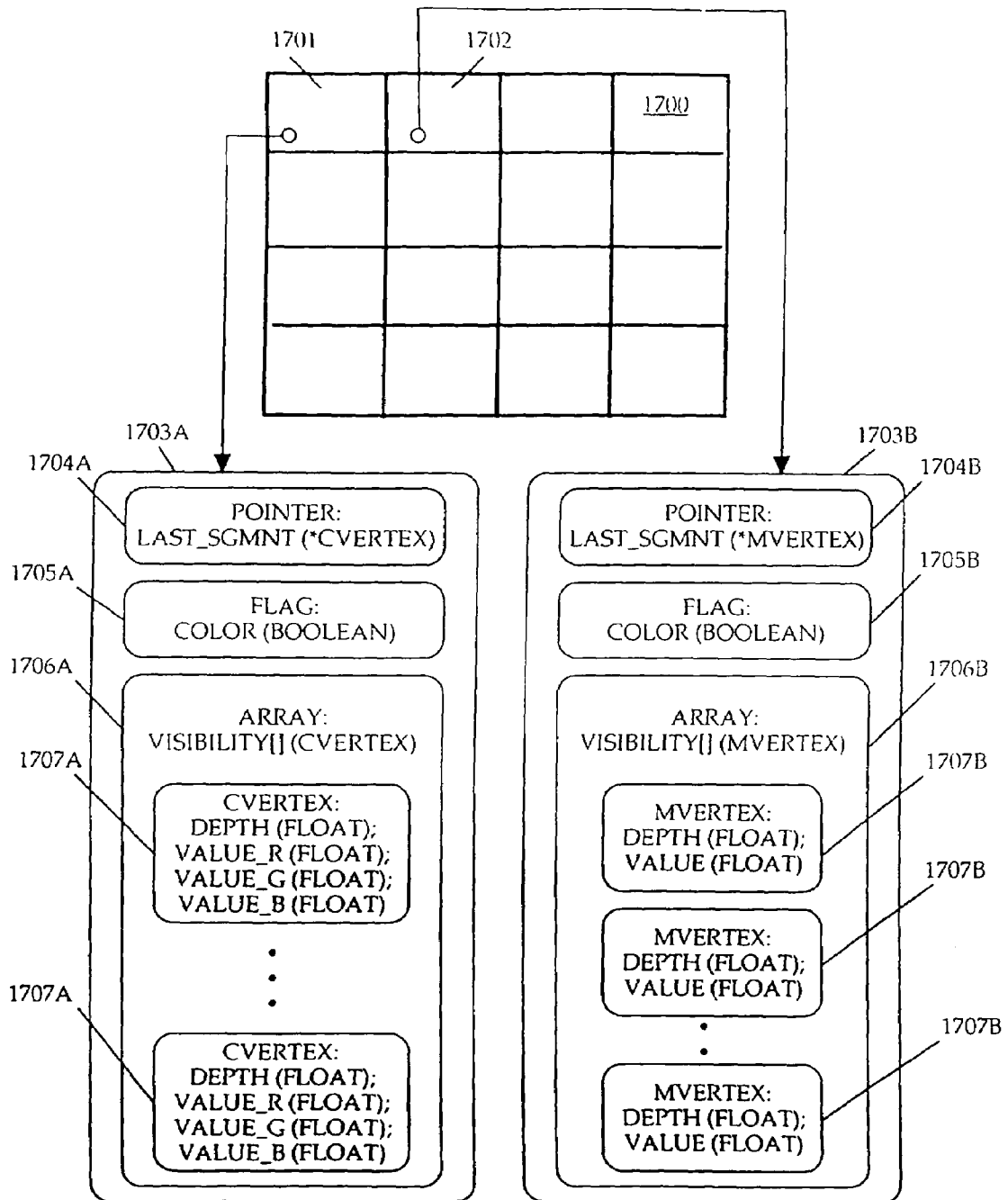


FIGURE 17

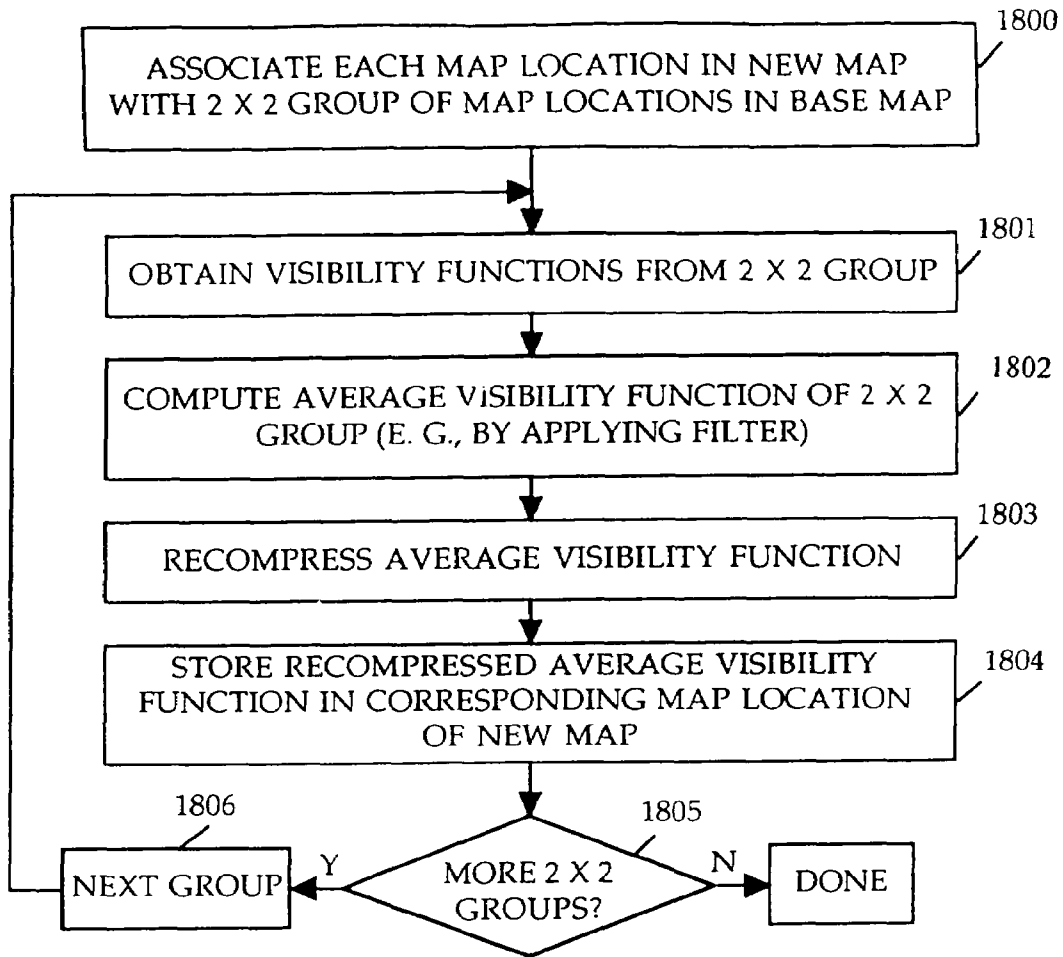


FIGURE 18A

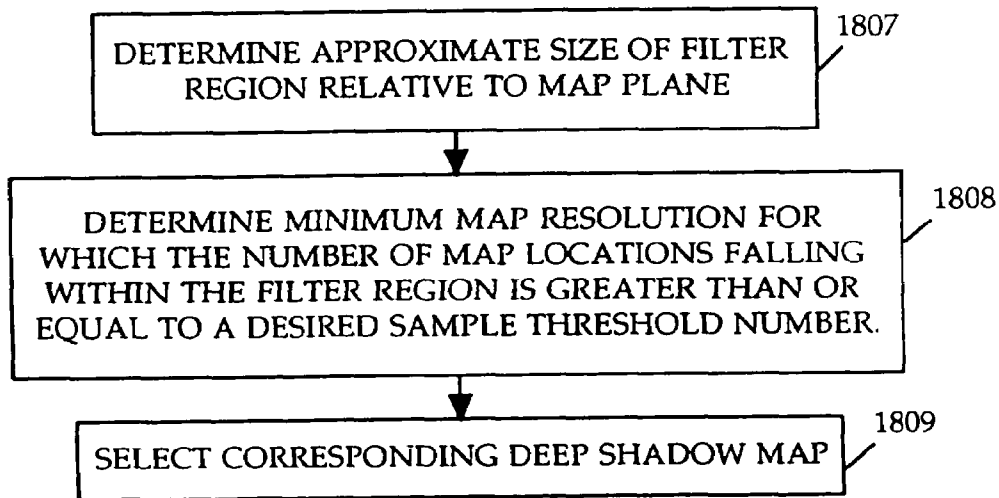


FIGURE 18B

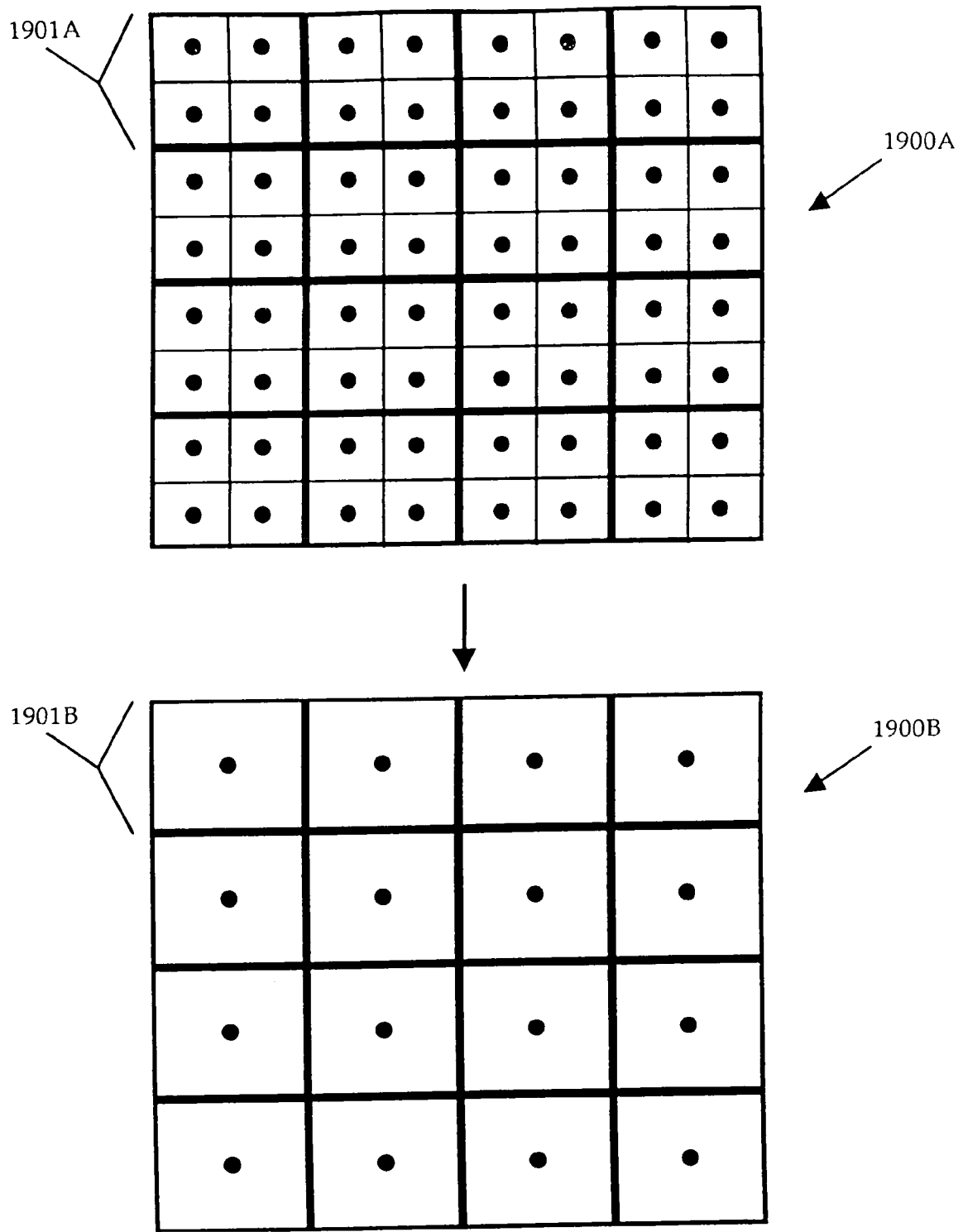


FIGURE 19

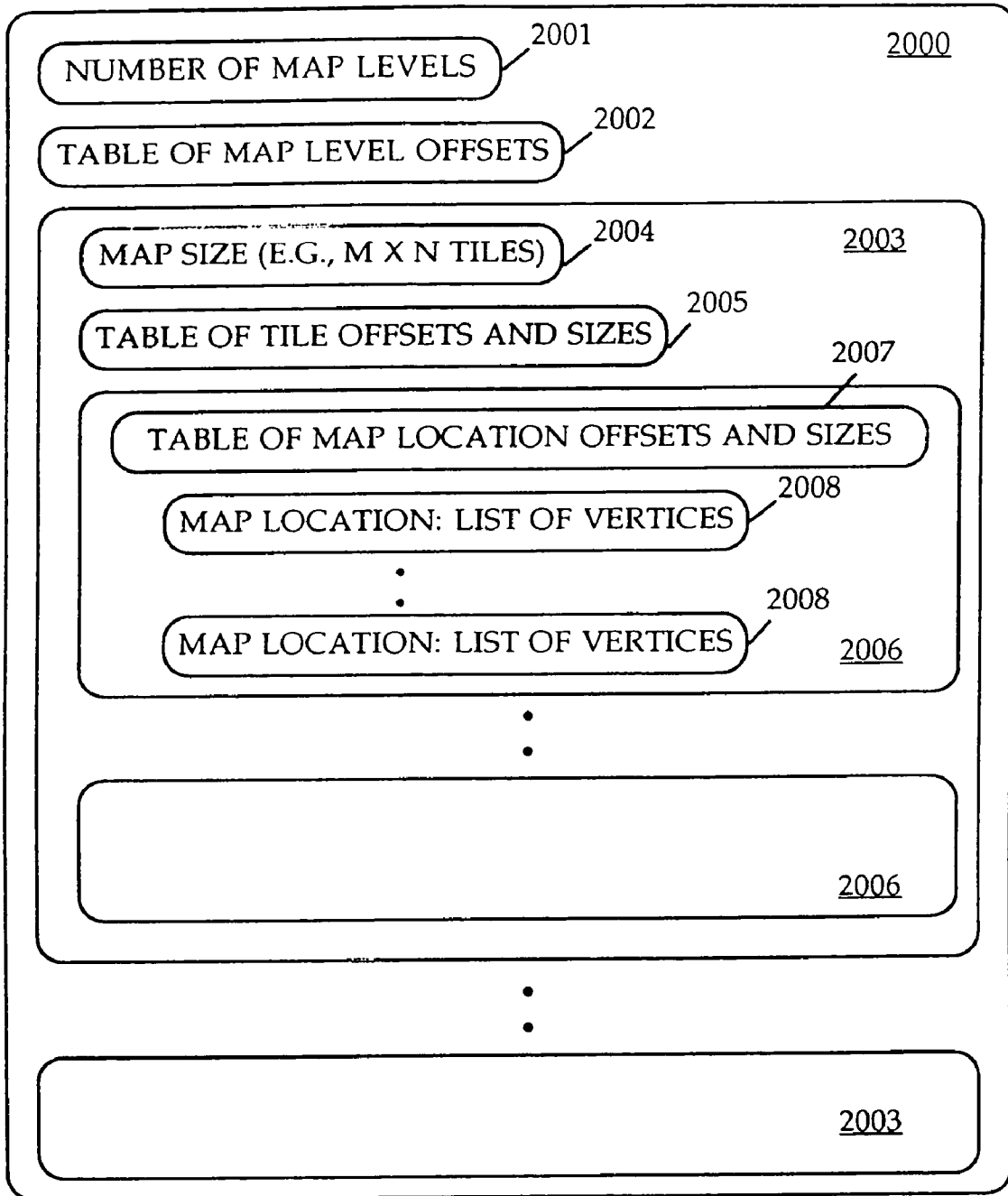


FIGURE 20



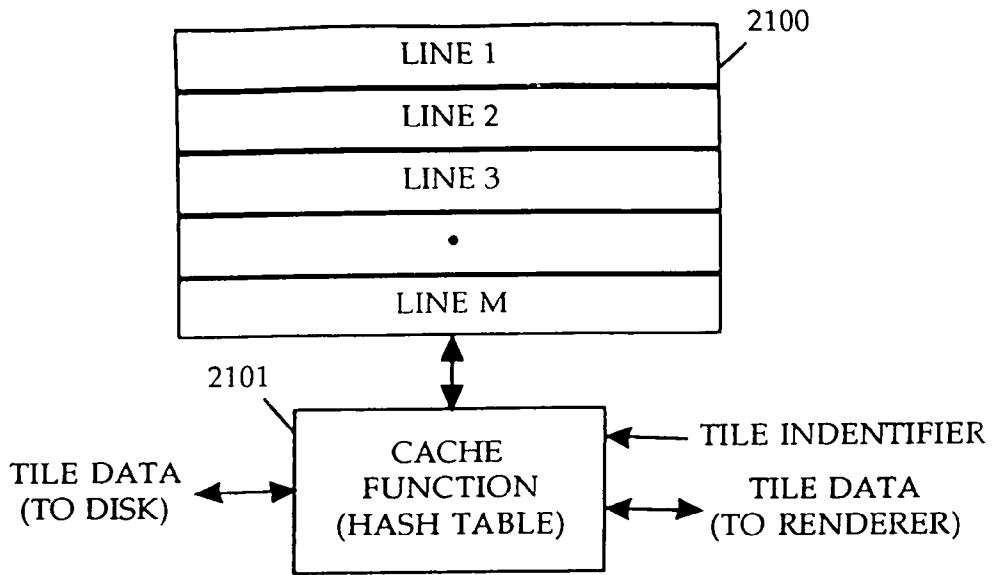


FIGURE 21

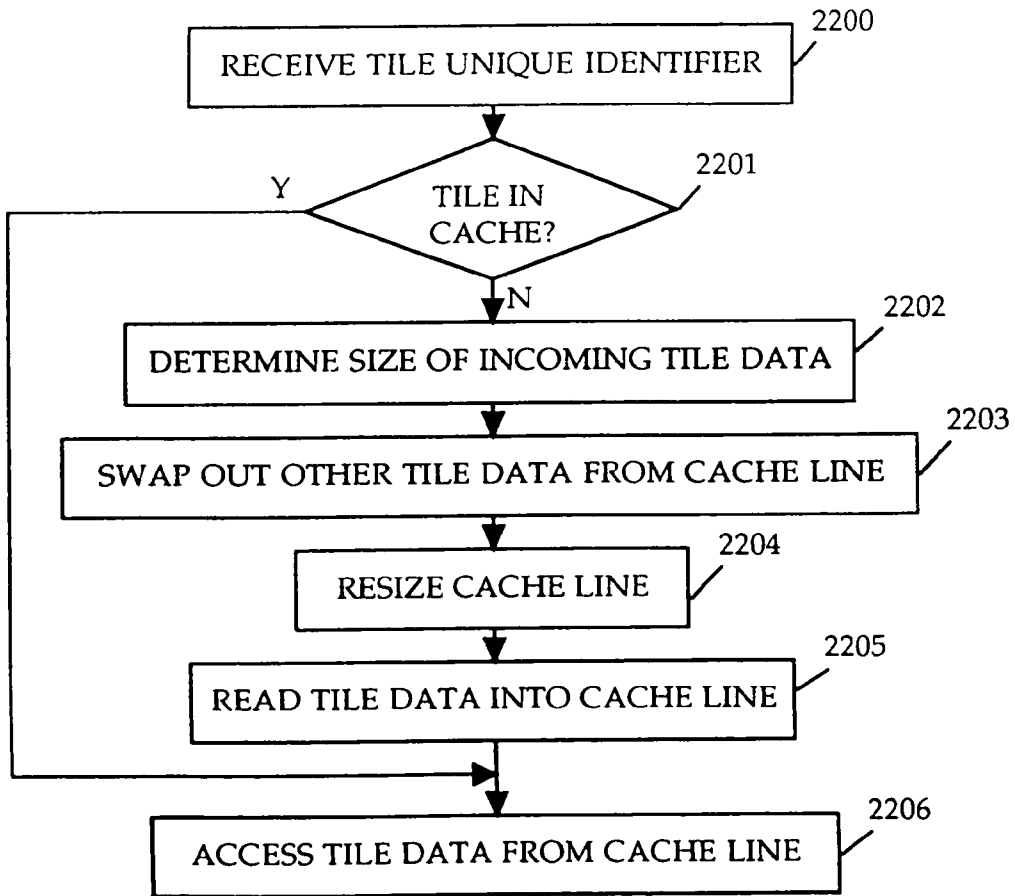


FIGURE 22

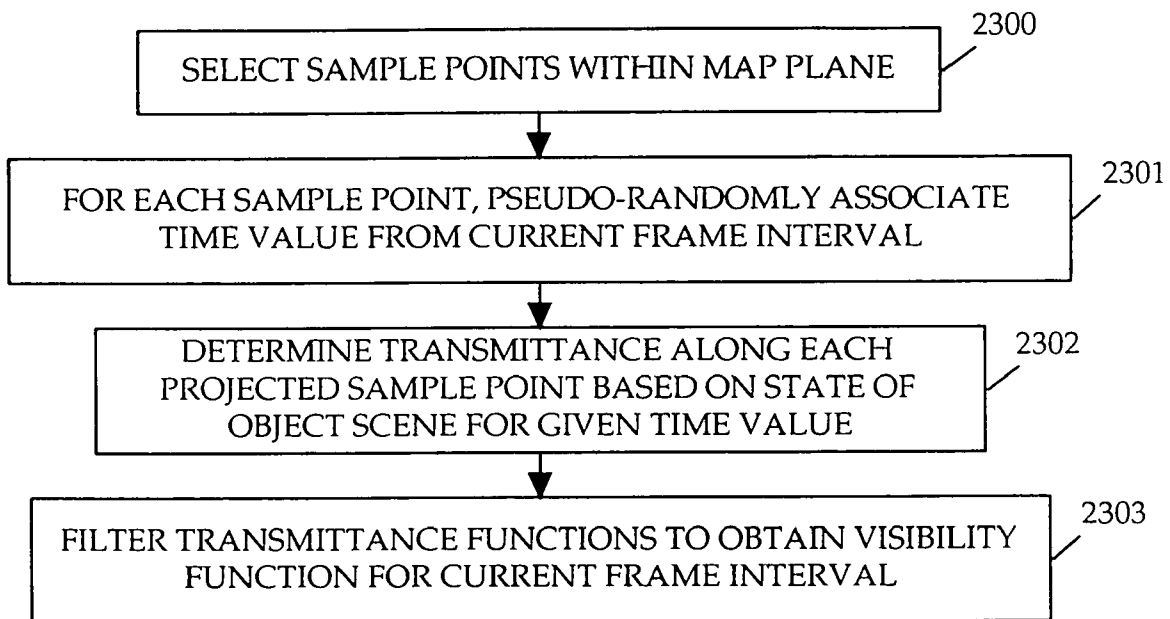
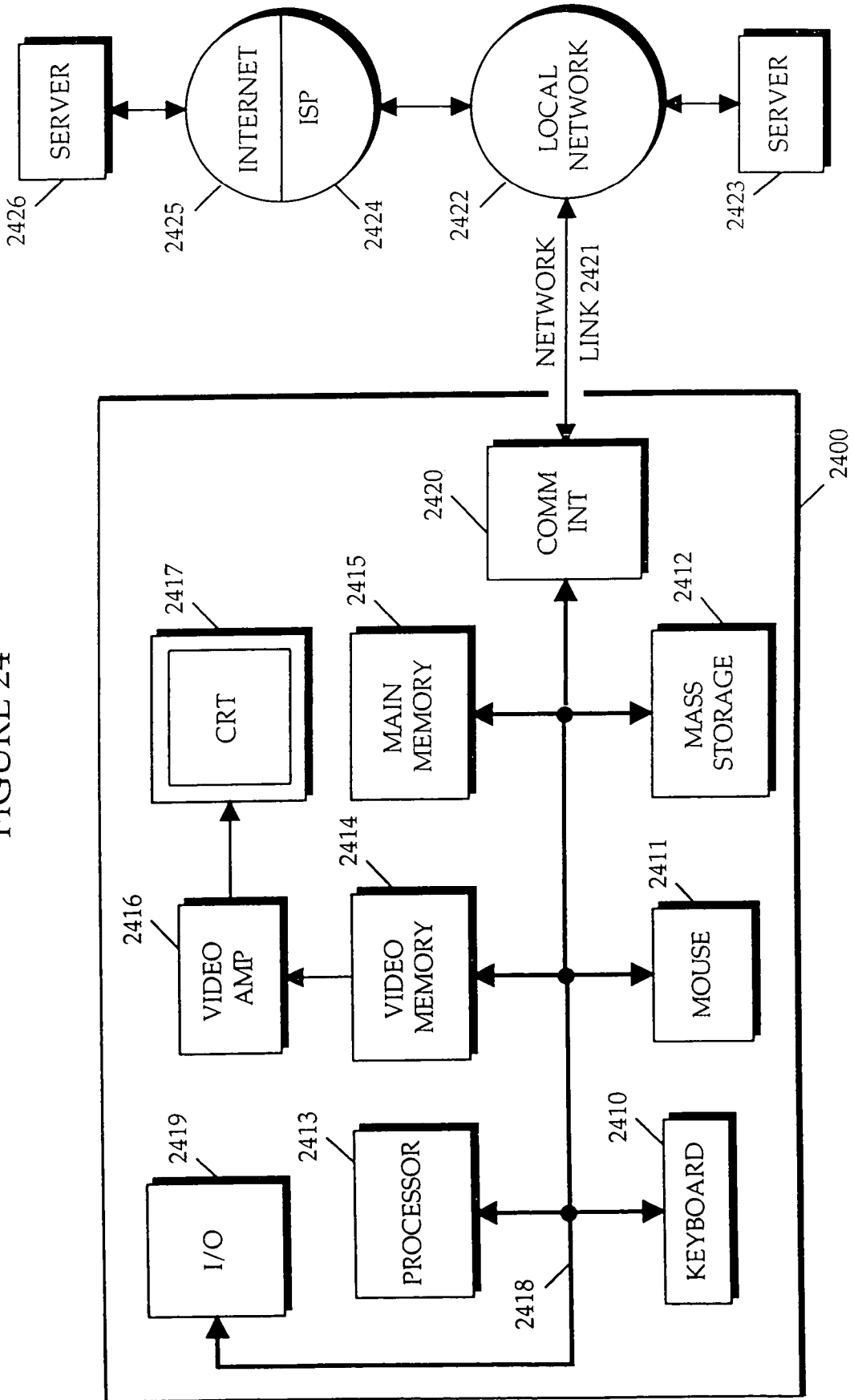


FIGURE 23

FIGURE 24



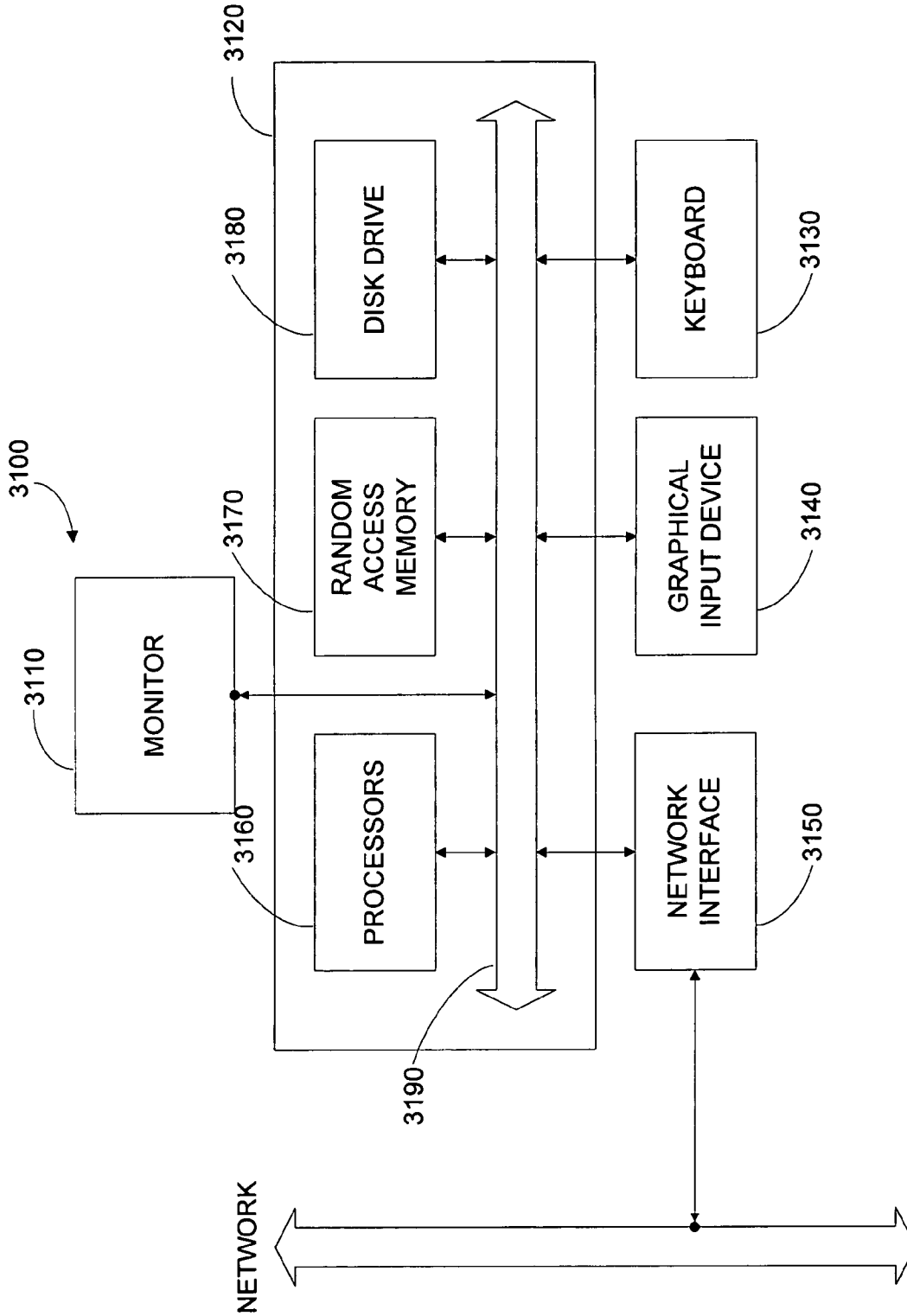


FIG. 25

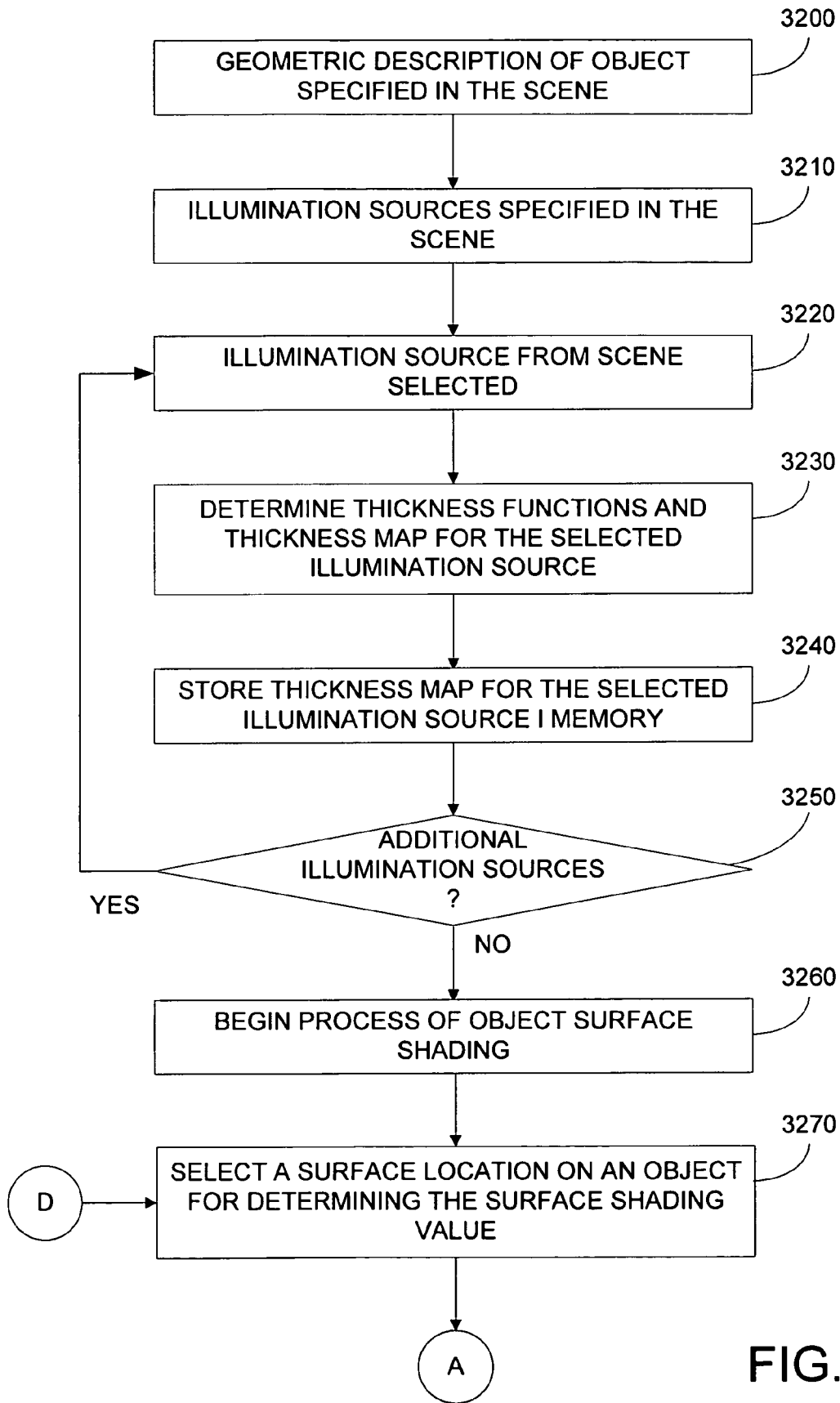


FIG. 26A

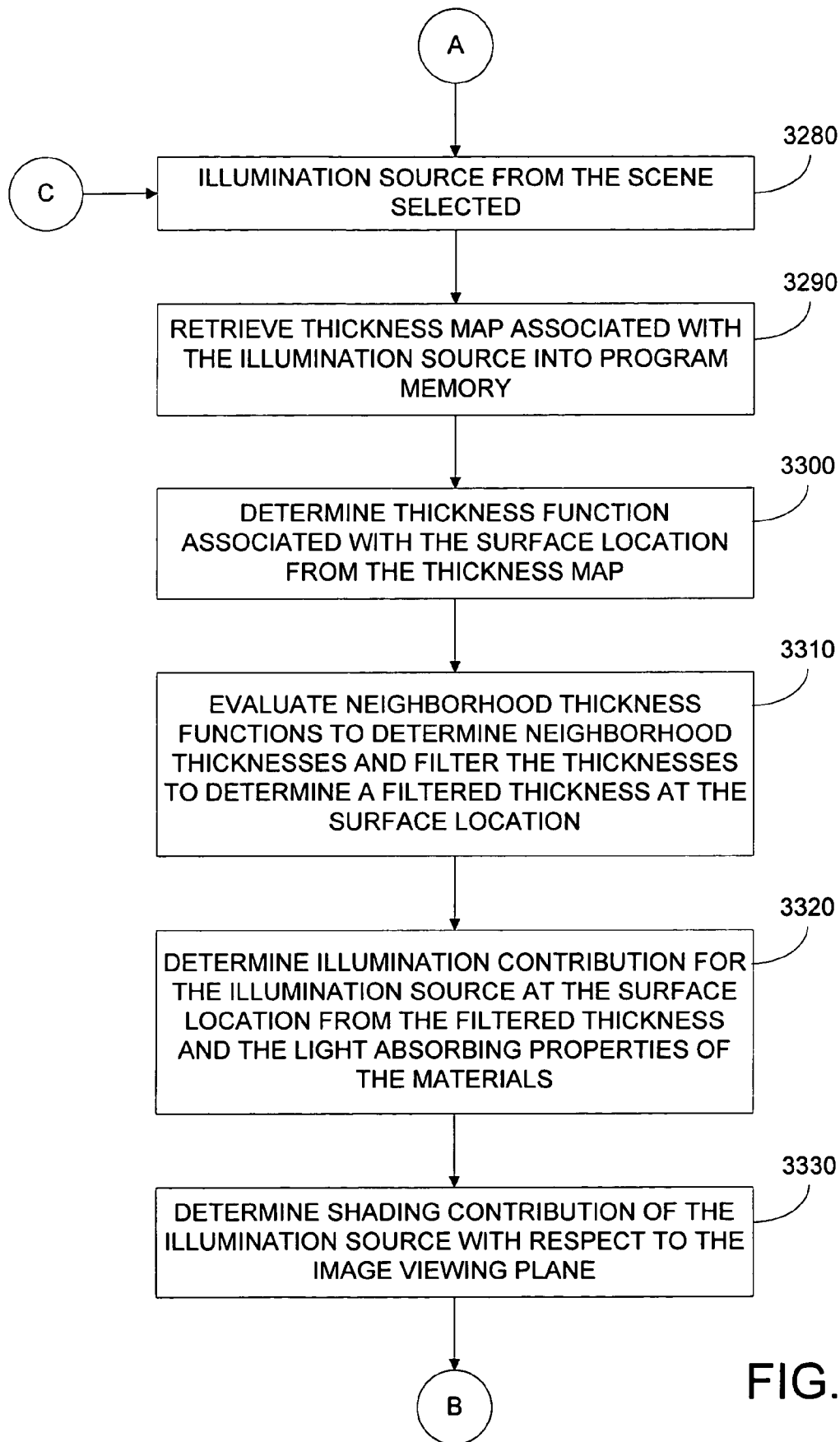


FIG. 26B

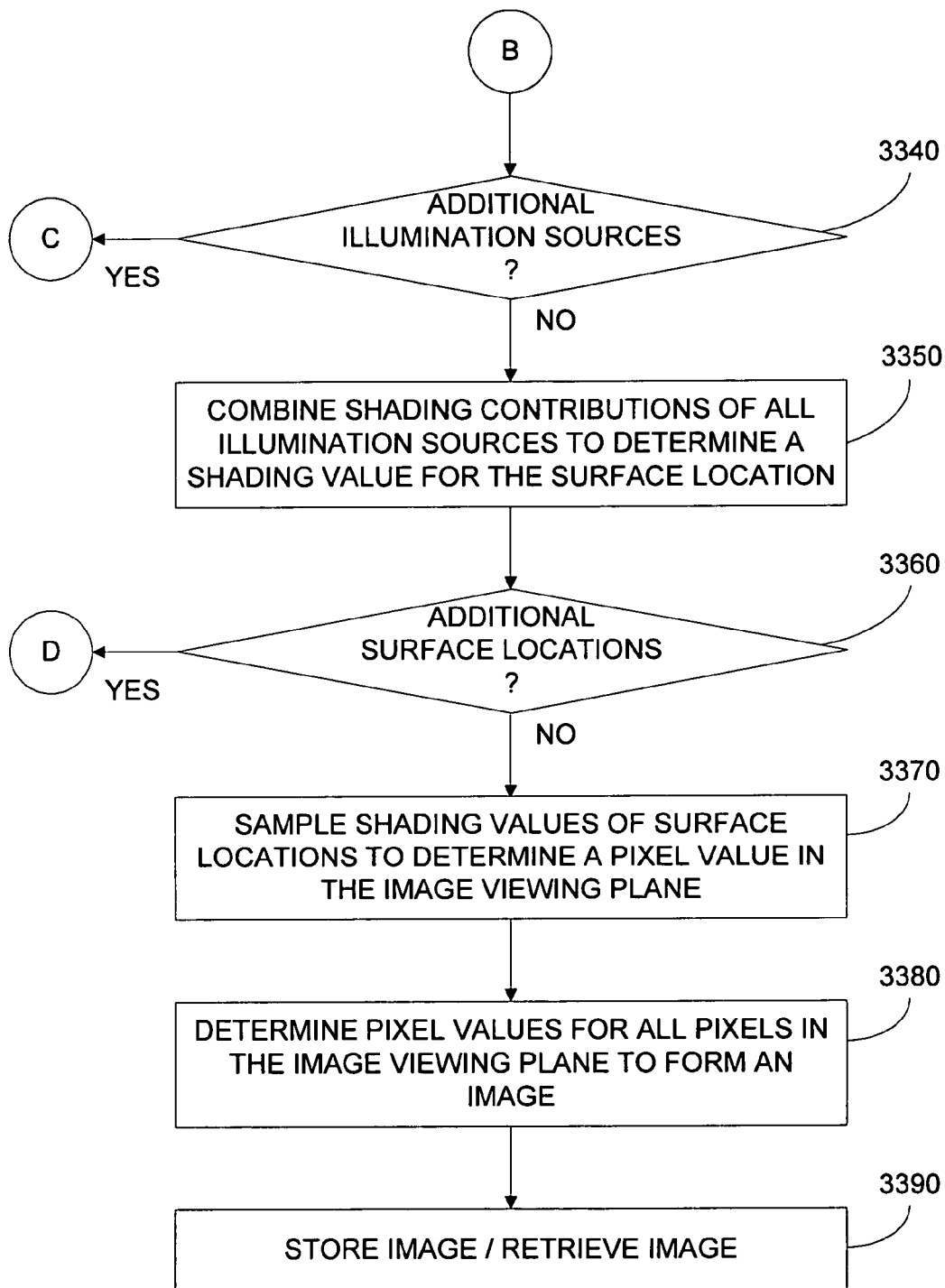


FIG. 26C

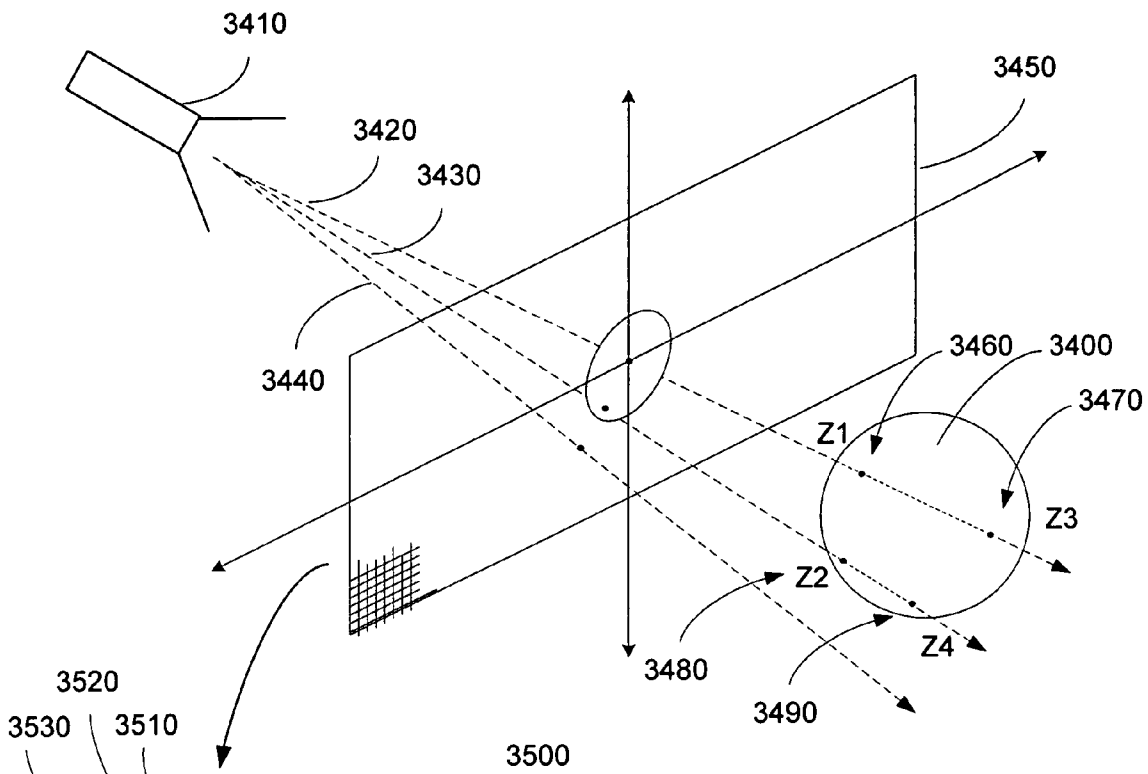


FIG. 27A

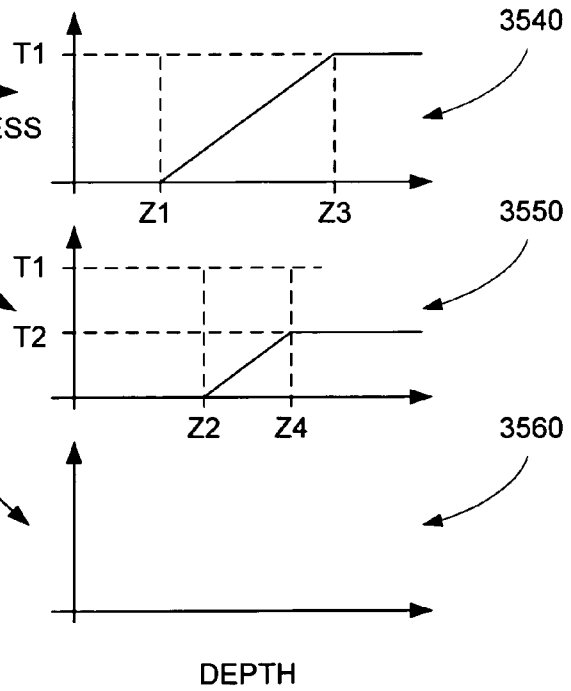
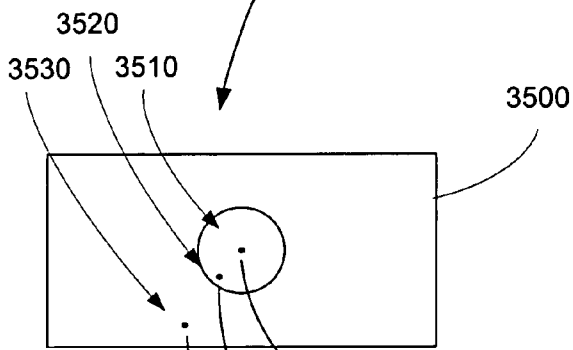


FIG. 27B



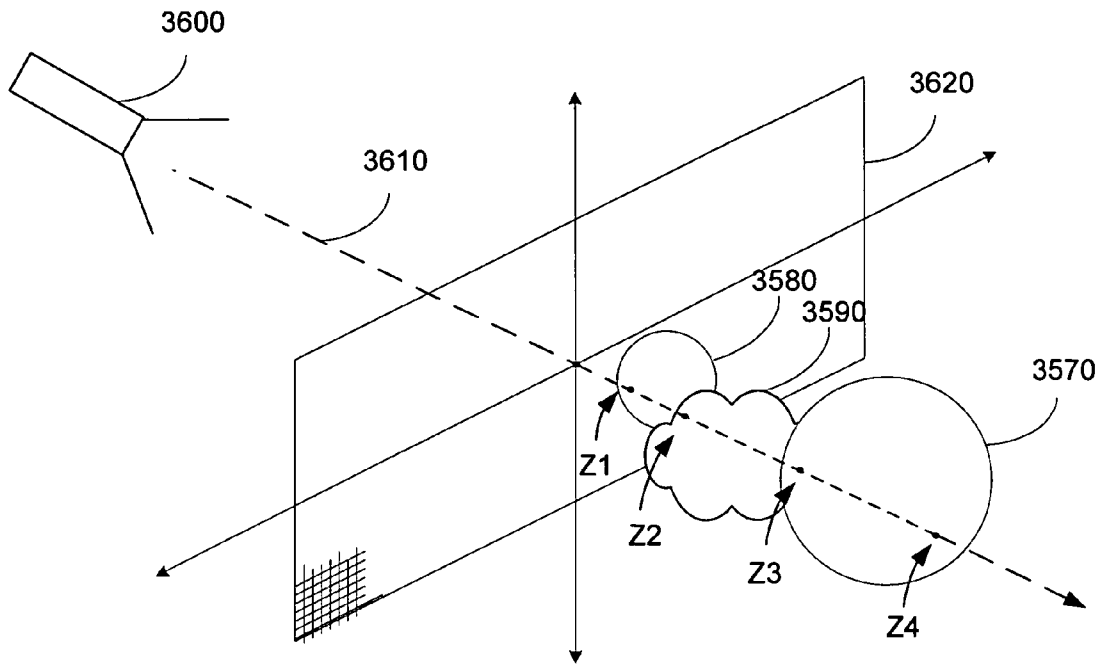


FIG. 27C

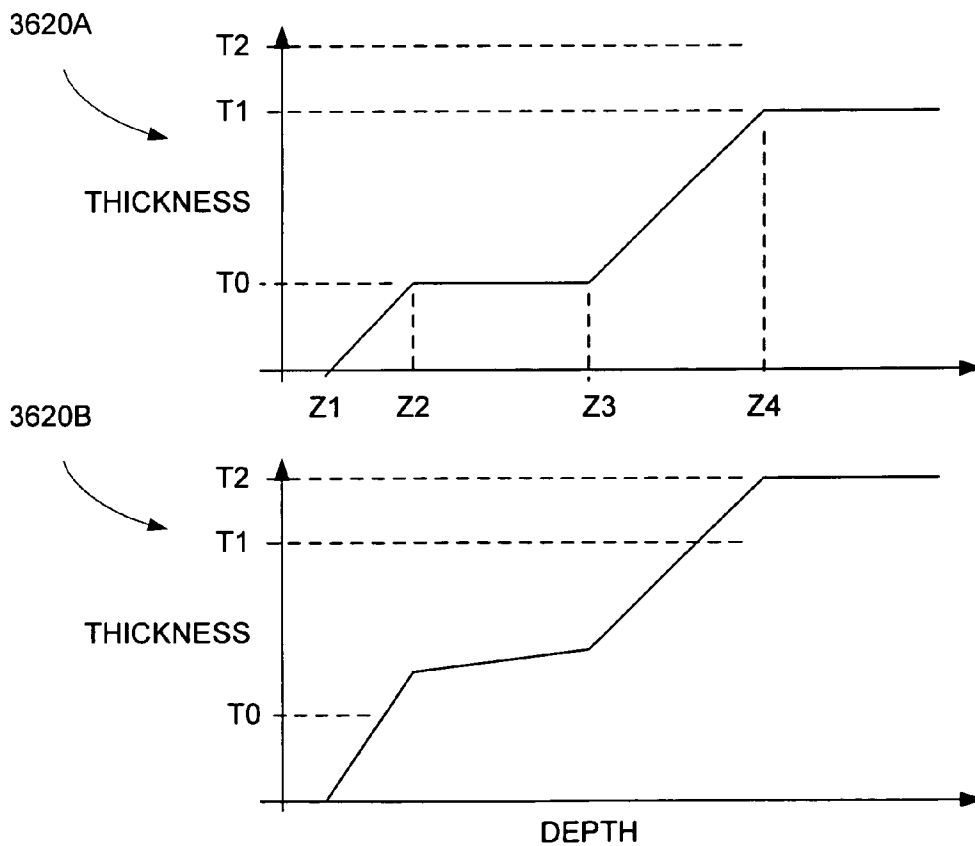


FIG. 27D

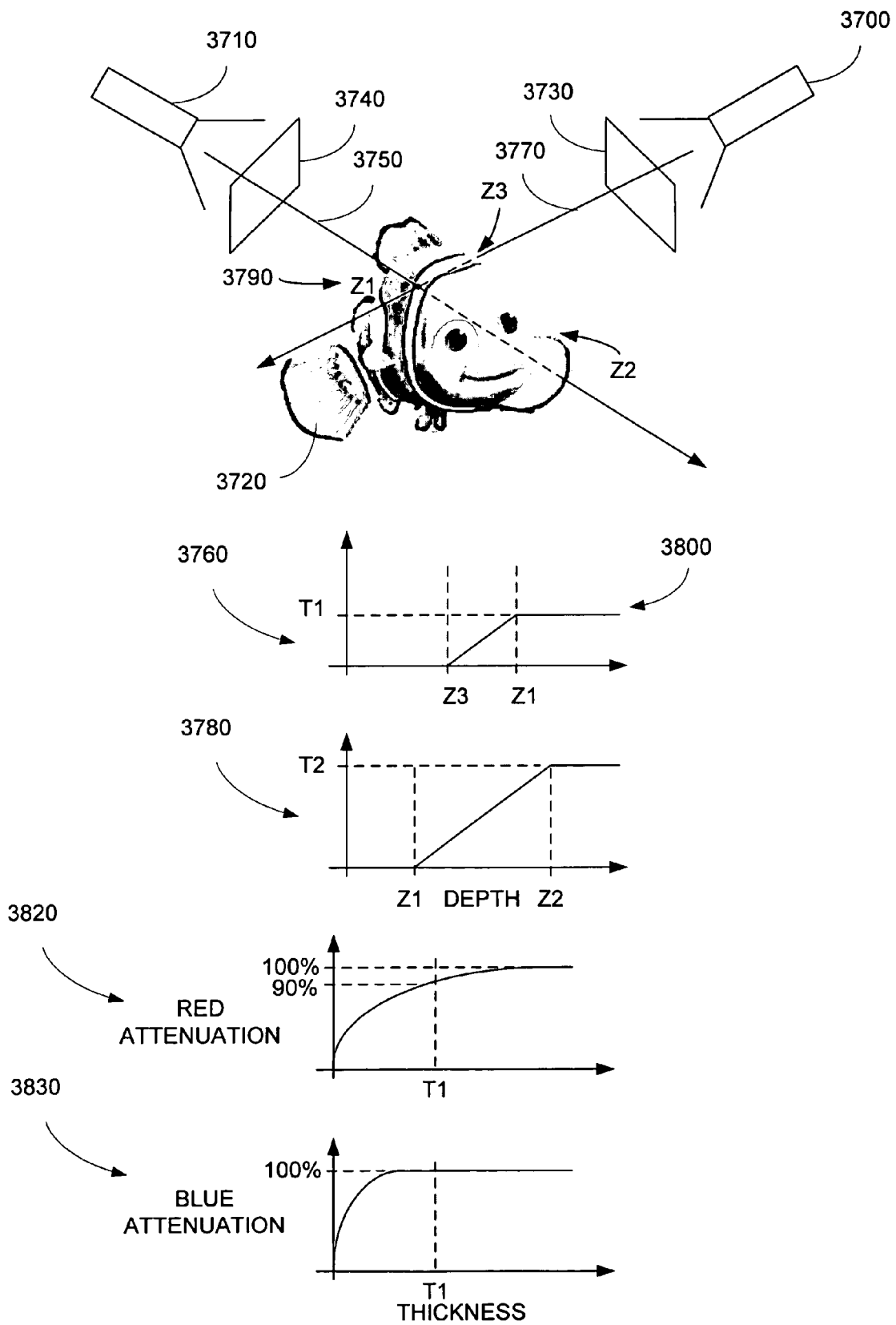


FIG. 28

**SUBSURFACE SCATTERING  
APPROXIMATION METHODS AND  
APPARATUS**

COPYRIGHT NOTICE

A portion of the disclosure of this patent document contains material that is subject to copyright protection. The copyright owner has no objection to the facsimile reproduction by anyone of the patent document or the patent disclosure as it appears in the Patent and Trademark Office patent file or records, but otherwise reserves all copyright rights whatsoever.

BACKGROUND OF THE INVENTION

This invention relates to the field of computer graphics, and, more specifically, to graphical rendering of shadows.

The present invention relates to computer animation. More specifically, the present invention relates to enhanced methods and apparatus for rendering objects, especially translucent objects, while accounting for subsurface scattering effects.

Background Art

In computer graphics, images are often created from three-dimensional objects modeled within a computer. The process of transforming the three-dimensional object data within the computer into viewable images is referred to as rendering. Single still images may be rendered, or sequences of images may be rendered for an animated presentation. One aspect of rendering involves the determination of lighting effects on the surface of an object, and in particular, the accurate representation of shadows within the rendered image. Unfortunately, typical shadow rendering techniques do not satisfactorily support rendering of finely detailed elements, such as fur or hair. Also, because surfaces are generally classified as either "lit" or "unlit," shadows from semitransparent surfaces and volumes, such as fog, cannot be accurately represented. To illustrate these problems with known shadowing techniques, a general description of image rendering is provided below with reference to a common method for rendering shadows known as "shadowmaps."

Image Rendering

Typically, rendering is performed by establishing a viewpoint or viewing camera location within an artificial "world space" containing the three-dimensional objects to be rendered. A "view plane," comprising a two-dimensional array of pixel regions, is defined between the viewing camera location and the objects to be rendered (also referred to herein as the "object scene"). To render a given pixel for an image, a ray is cast from the viewing camera, through the pixel region of the view plane associated with that pixel, to intersect a surface of the object scene. Image data associated with the surface at that point or region is computed based on shading properties of the surface, such as color, texture and lighting characteristics. Multiple points, sampled from within a region of the object scene defined by the projection of the pixel region along the ray, may be used to compute the image data for that pixel (e.g., by applying a filtering function to the samples obtained over the pixel region). As a result of rendering, image data (e.g., RGB color data) is associated with each pixel. The pixel array of image data may be output to a display device, or stored for later viewing or further processing.

In photorealistic rendering, as part of the determination of lighting characteristics of a point or points on a surface, shadowing effects are considered. That is, a determination is made of whether each light source in the object scene contributes to the computed color value of the pixel. This entails identifying whether the light emitted from each light source is transmitted unoccluded to the given point on the surface or whether the light is blocked by some other element of the object scene, i.e., whether the given point is shadowed by another object. Note that a light source may be any type of modeled light source or other source of illumination, such as the reflective surface of an object.

An example of a rendering scenario is illustrated in the diagram of FIG. 1. A camera location **100** (or viewpoint) is identified adjacent to an object scene comprising objects **104** and **105**. A light source **101** is positioned above the object scene such that object **104** casts shadow **106** upon the surface of object **105**. Camera location **100** and light source **101** have different perspectives of the object scene based on their respective locations and view/projection direction. These differing perspectives are shown in FIG. 1 as separate coordinate systems (x, y, z) and (x', y', z'), respectively. For the rendering operation, a view plane **102** is positioned between the camera location and the object scene. View plane **102** is two-dimensional in x and y with finite dimensions, and comprises an array of pixel regions (e.g., pixel regions **103A** and **103B**). Each pixel region corresponds to a pixel of the output image.

To sample the object scene for pixel region **103A**, ray **107A** is projected from camera location **100**, through pixel region **103A**, onto surface **105** at sample point **108A**. Similarly, for pixel region **103B**, ray **10713** is traced from camera location **100**, through pixel region **103B**, onto surface **105** at sample point **108B**. The surface properties at the sample point are evaluated to determine the image data to associate with the corresponding pixel. As part of this evaluation, the rendering process determines whether the sample point is lit or shadowed with respect to each light source in the scene.

In the example of FIG. 1, sample point **108A** lies within shadow **106** cast by object **104**, and is therefore unlit by light source **101**. Thus, the surface properties evaluated for sample point **108A** do not consider a lighting contribution from light source **101**. In contrast, sample point **108B** is not shadowed. The surface properties evaluated for sample point **108B** must therefore account for a lighting contribution from light source **101**. As previously indicated, multiple samples may be taken from within each projected pixel region and combined within a filter function to obtain image data for the corresponding pixel. In this case, some samples may lie within a shadow while other samples within the same pixel region are lit by the light source.

Shadow Maps

To improve rendering efficiency, the process of determining shadows within an object scene may be performed as part of a separate pre-rendering process that generates depth maps known as "shadow maps." A later rendering process is then able to use simple lookup functions of the shadow map to determine whether a particular sample point is lit or unlit with respect to a light source.

As shown in FIG. 2, a shadow map is a two-dimensional array of depth or z-values (e.g.,  $Z_0$ ,  $Z_1$ ,  $Z_2$ , etc.) computed from the perspective of a given light source. The shadow map is similar to an image rendered with the light source acting as the camera location, where depth values are stored at each array location rather than pixel color data. For each

(x,y) index pair of the shadow map, a single z value is stored that specifies the depth at which the light emitted by that given light source is blocked by a surface in the object scene. Elements having depth values greater than the given z value are therefore shadowed, whereas elements that have depth values less than the given z value are lit.

FIG. 3 illustrates how a shadow map is created for a given light source (represented herein as a point source for sake of illustration). Where multiple light sources are present, this technique is repeated for each light source. A finite map plane 300 is positioned between a light source 301 and the object scene comprising surface 302. Map plane 300 represents the two-dimensional (x,y) array of sample points or regions. A ray 305 is cast from light source 301 through sample region 303 to find a point 304 on surface 302 that projects onto the sample region. Sample point 304 is selected as the point on the first encountered surface (i.e. surface 302) that projects onto the sample region. For sample point 304, the z value ( $Z_{MAP}$ ) is determined in the light source's coordinate system and stored in the shadow map at the (x,y) location corresponding to the sample region 303 of map plane 300. Objects that intersect the sample region are considered fully lit (value of "1") for z values less than  $Z_{MAP}$  (i.e., objects in front of surface 302), and considered completely unlit (value of "0") for z values greater than  $Z_{MAP}$  (i.e., objects behind of surface 302).

A process for creating a shadow map known as ray casting is shown in FIG. 4. As shown, a sample location in the shadow map is selected for pre-rendering in step 400. In step 401, the pre-rendering process traces a ray from the light source location through the corresponding sample region of the map plane to determine and select a point on the object scene (i.e. first encountered surface) that projects onto the sample region. In step 402, for the sample point selected from within the sample region, the associated z value of the first surface encountered by the projection is stored in the sample location of the shadow map. (If no surface is intersected, a maximum z value may be used.) In step 403, if no more sample locations require pre-rendering for shadow data, the shadow map is complete for the current light source (step 405). If, in step 403, one or more sample locations within the shadow map remain unrendered, the next sample location is selected in step 404, and the process returns to step 401.

Although ray casting method of shadow map generation is discussed in this overview for simplicity, it should be noted that, in practice, methods like rasterization techniques (e.g. z-buffer) are often used.

The above ray casting process may be repeated for each light source within the object scene. Once pre-rendering is complete and each light source has a completed shadow map, standard rendering may be performed from the perspective of the camera location as previously described with respect to FIG. 1. FIG. 5 illustrates one possible method by which a rendering process may utilize pre-rendered shadow maps.

The method of FIG. 5 is applied after a sample point has been identified within a projected pixel region, during the lighting phase of rendering. In step 500, a first light source is selected for consideration. In step 501, the (x, y, z) coordinate location of the sample point from the camera's perspective is transformed into an (x', y', z') location from the perspective of the given light source. For the given (x', y') coordinates of the sample point, a value  $Z_{MAP}$  is obtained from the light source's associated shadow map in step 502.

In step 503, the z' coordinate of the sample point is compared with  $Z_{MAP}$ . If z' is greater than  $Z_{MAP}$ , in step 504,

a lighting value of "0" is passed to the general rendering process, indicating that the sample point is unlit with respect to the current light source. Step 504 then proceeds to step 507. However, if z' is less than or equal to  $Z_{MAP}$  in step 503, a lighting value of "1" is passed to the general rendering process in step 505, indicating that the sample point is lit with respect to the current light source. In step 506, the current light source contribution is computed for determining the shading of the current sample point. The light source contribution may be computed, for example, based upon factors such as the color and intensity of the light source, the distance of the light source from the sample point, the angle of incidence of the light ray with the surface, and the lighting characteristics of the surface (e.g., color, opacity, reflectivity, roughness, surface angle with respect to camera, etc.). From step 506, the method proceeds to step 507.

In step 507, if there are other light sources to consider, the next light source is selected in step 508, and the method returns to step 501. If, in step 507, there are no further light sources to consider, all computed light source contributions are combined in step 509 to determine the color output for the current sample (in addition to other rendering processes such as texture mapping).

As previously stated, a pixel region may comprise multiple samples computed in the manner described above. A filtering function is used to combine the samples into a single color value (e.g., RGB) for a pixel, typically assigning weighting coefficients biased towards the center of the pixel region.

Traditional shadow maps need very high resolutions to accurately capture photorealistic self-shadowing (i.e. shadows cast by portions of an object onto itself) images. Higher quality antialiased shadows are possible with a process known as percentage closer filtering, which examines depth samples within a given filter region and computes the fraction that are closer than the given depth z. Percentage closer filtering is described in a paper by William T. Reeves, et. al, entitled "Rendering Antialiased Shadows with Depth maps," Computer Graphics (SIGGRAPH '87 Proceedings), volume 21, pages 283-291, July 1987, and is incorporated herein by reference.

Percentage closer filtering relies heavily on a process known as stratified sampling, both in generating the original shadow map and in selecting a random subset of depth samples for filtering. Stratified sampling is described in a paper by Don P. Mitchell, entitled "Consequences of Stratified Sampling in Graphics," SIGGRAPH 96 Proceedings, pages 277-280, Addison Wesley, August 1996, and is incorporated herein by reference.

While shadow maps may be satisfactory for rendering shadows of large, opaque objects, shadow maps do not work well for finely detailed geometry, such as hair, or semitransparent surfaces or volumes, such as fog or smoke. This is because stratified sampling works much better near a single discontinuity (such as an isolated silhouette) than where there are many discontinuities crossing the filter region. This means that when rendering fur or other fine geometry, a much larger number of samples is needed in order to reduce noise artifacts such as sparkling to an acceptable level.

FIG. 6A illustrates an isolated silhouette edge crossing a pixel region for a shadow lookup, which is evaluated with N samples jittered over a  $\sqrt{N} \times \sqrt{N}$  grid of sample cells. Using percentage closer filtering, each sample contributes either 0 or 1 depending on the relative z values of the shadow map and the test point. The samples in the upper left are clearly lit (contributing "1"), whereas those samples in the lower right are clearly shadowed (contributing "0"). In this situa-

tion, the samples that contribute to the variance are those whose cells are crossed by the silhouette edge (indicated with cross-hatching). There are  $O(N^{1/2})$  such cells, and further analysis shows that the expected error in this case is  $O(N^{-3/4})$ . This means that near large silhouette edges, stratification yields much better results than unstratified Monte Carlo sampling, which has an expected error of  $O(N^{-1/2})$ .

In the case of hair or fur, however, the pixel region is crossed by many silhouette edges, as shown in FIG. 6B. In this case, every one of the  $N$  sample cells is crossed by an edge, and the corresponding expected error is  $O(N^{-1/2})$ . This means that, in the case of very fine geometry, stratified sampling does no better than unstratified sampling.

These error bounds have a dramatic effect on the number of samples required to reduce noise below a given threshold. For example, to achieve an expected error of 1%, approximately  $N=140$  samples are needed near an isolated silhouette, while  $N=2500$  samples are required near a point that is 50% obscured by dense fur. Furthermore, if the same amount of shadow detail is desired in both cases (i.e., a similar filter size in world space), then the underlying shadow map resolution must be increased by the same factor. To gain any benefit from stratification, the shadow map would need to be fine enough to resolve the silhouettes of individual hairs, and the filter region small enough that only a few edges cross it. Since such conditions are rarely satisfied in practice, shadow maps for high-quality hair rendering are typically large and slow.

A typical way of reducing the memory required by such large shadow maps is by compression. However, standard shadow maps do not behave well under compression. As described above, higher map resolutions are needed to reduce errors to an acceptable level. Compression in  $x$  and  $y$  would entail fewer samples and thus greater error. Compression in  $z$ , such as by reducing the number of bits representing  $z$  values in the shadow map, introduces a roundoff error in specifying the location of a first blocking surface. Where the roundoff error causes  $Z_{MAP}$  to be less than the actual value, the top surface will appear to be behind  $Z_{MAP}$ , resulting in erroneous "self-shadowing" of the top surface. Where the roundoff error causes  $Z_{MAP}$  to be greater than the actual value, surfaces that would normally be shadowed may now be considered completely lit. In either of these scenarios, visible rendering errors will result. However, lossless compression is acceptable, but the compression ratios are relatively small and provide no significant space benefit. Thus, compression is not a viable solution for standard shadow maps.

#### Other Shadow Techniques

One method for determining shadows is to perform ray casting. That is, a ray is cast to the sample point on the surface. Ray casting can generate accurate shadows, but on scenes with very complex geometry, ray casting is too expensive in terms of time and memory. It is also difficult, other than by using an expensive area light source, to soften shadows for artistic purposes, which in the case of standard shadow maps is achieved by simply increasing the filter width.

Another possible approach to shadowing is to precompute the shadow density as a 3D texture. This technique has been used with some success for clouds. The main drawback is that 3D textures have a relatively coarse resolution, as well as a limited range and low accuracy in  $z$  (which creates bias problems). A 3D texture with sufficient detail to capture accurate surface shadows would be prohibitively large.

Multi-layer Z-buffers and layered depth images are yet other methods that may be used for shadow maps. Multi-layer Z-buffers and layered depth images store information at multiple depths per pixel, but are geared toward rendering opaque surfaces from new viewpoints rather than shadow evaluation. Multi-layer depth images have been applied to the problem of shadow penumbras, but this technique otherwise has the same limitations as ordinary shadow maps.

Throughout the years, movie makers have often tried to tell stories involving make-believe creatures, far away places, and fantastic things. To do so, they have often relied on animation techniques to bring the make-believe to "life." Two of the major paths in animation have traditionally included, drawing-based animation techniques and stop motion animation techniques.

Drawing-based animation techniques were refined in the twentieth century, by movie makers such as Walt Disney and used in movies such as "Snow White and the Seven Dwarves" and "Fantasia" (1940). This animation technique typically required artists to hand-draw (or paint) animated images onto a transparent media or cels. After painting, each cel would then be captured or recorded onto film as one or more frames in a movie.

Stop motion-based animation techniques typically required the construction of miniature sets, props, and characters. The filmmakers would construct the sets, add props, and position the miniature characters in a pose. After the animator was happy with how everything was arranged, one or more frames of film would be taken of that specific arrangement. Stop motion animation techniques were developed by movie makers such as Willis O'Brien for movies such as "King Kong" (1932). Subsequently, these techniques were refined by animators such as Ray Harryhausen for movies including "The Mighty Joe Young" (1948) and Clash Of The Titans (1981).

With the wide-spread availability of computers in the later part of the twentieth century, animators began to rely upon computers to assist in the animation process. This included using computers to facilitate drawing-based animation, for example, by painting images, by generating in-between images ("tweening"), and the like. This also included using computers to augment stop motion animation techniques. For example, physical models could be represented by virtual models in computer memory, and manipulated.

One of the pioneering companies in the computer aided animation (CAA) industry was Pixar, dba Pixar Animation Studios. Over the years, Pixar developed and offered both computing platforms specially designed for CAA, and Academy-Award® winning rendering software known as RenderMan®. In the present disclosure, rendering broadly refers to the conversion of geometric data described in scenes to visual images.

One specific portion of the rendering process is known as surface shading. In the surface shading process, the surface shader software determines how much light is directed towards the viewer from the surface of objects in response to the applied light sources in a scene. Two specific parameters that are used for shading calculations includes a surface normal and a surface illumination.

The surface shading process is straight forward when shading "solid" objects, such as objects made of metal, wood, dense plastic, thick materials, and the like. However the surface shading process is much more complex when rendering objects made of translucent or thin materials, such as glass, marble, liquids, plastics, thin materials and the like.

This is because the shading process must not only consider the amount of light striking the outer surface of the object, but also any light that “shines through” the object.

Previous methods for shading translucent materials have relied complex calculations taking account of how light is absorbed and scattered through objects. In such cases the user first provides description of material properties including absorption and scattering properties of light. Next, the system uses the geometry of the scene to run complex ray-tracing operations to determine how light strikes an object. Finally, the system solves complex Poisson diffusion-type calculations, taking into account the absorption and scattering properties of the material, to determine how much light “shines through” the object.

Drawbacks to this approach include that ray-tracing and diffusion calculations are highly complex and take long times to compute. Accordingly, the user productivity drops because the user is forced to wait until computations are finish. In some cases, the user must wait over night. Other drawbacks include that if the user is not satisfied about how the final object appears in an image (e.g. the material is too dense), the user redefines the material properties (e.g. absorption and scattering properties), but then the user must again wait until the entire simulation is complete to see the results. Accordingly, any user adjustments to the scene cannot be imaged quickly.

In other previous methods, instead of performing a full simulation, the simulation is run on a subset of locations. Drawbacks to this approach include that the subset of locations typically vary from image to image. Because of this, the surface of objects tend to appear different from image to image. The problem may not be obvious when viewing a single image, however, when viewing a series of images, the surface of the object will undulate and sparkle.

In light of the above, the inventors of the present invention have determined that improved methods for rendering non-opaque objects are needed without the drawbacks illustrated above.

#### SUMMARY OF THE INVENTION

A method and apparatus for rendering shadows are described. Embodiments of the invention implement a two-dimensional array or map of depth-based functions, such as a visibility function in  $z$ . During rendering of an object scene, these functions are accessed via lookup operations to efficiently determine the function value for a sample point at a given depth. The use of visibility functions allows for partial light attenuation effects such as partially blocking surfaces, semi-transparent surfaces and volumetric elements, to be accurately modeled over a range of  $z$  values. Thus, in contrast to prior art shadow map methods in which a point on a surface is either fully lit or completely shadowed with respect to a light source, it is possible for a point on a surface to be more realistically rendered as being fractionally lit by a light source.

In one or more embodiments, each visibility function is determined from multiple transmittance functions. A transmittance function describes the light falloff along a particular ray cast from the light source onto the object scene. The visibility function for a given pixel is obtained by combining the transmittance functions along one or more rays cast through that pixel’s filter region. Along each sample ray, a surface transmittance function is computed for all surfaces intersected by the ray and a volume transmittance is generated for volumetric elements traversed by the ray. A total transmittance function for the ray is determined from the product of the surface and volume transmittance functions.

The visibility function is computed as a weighted sum of the transmittance functions obtained from the filter region, and is stored in a map location associated with the filter region. An incremental updating method is utilized for more efficient computation of the weighted sum.

In one or more embodiments, the visibility function is piecewise linear, implemented as a sequence of vertices, each comprising a depth ( $z$ ) value and corresponding function value. Compression is achieved by minimizing the number of vertices needed to represent the visibility function within a desired error tolerance. Multiple visibility functions (such as individual color visibility functions for R, G and B) may be efficiently represented by a sequence of vertices, each comprising one depth value and two or more function values respectively associated with the individual visibility functions at the given depth value. A flag may be associated with each map location to specify whether that location is monochrome (one visibility function) or color (separate RGB visibility functions).

During rendering, a visibility value is obtained from the stored map by performing a lookup in  $x$  and  $y$  to determine the specific function in the map, performing a linear or binary search of the corresponding sequence of vertices to locate the linear segment containing the desired depth or  $z$  value, and interpolating the function value along that linear segment. Efficient lookups are facilitated by storing a pointer to the most recently accessed segment, and initiating a subsequent search from that segment.

In one or more embodiments, multiple maps are stored at different resolutions. Each new map level is obtained, for example, by averaging and downsampling the previous level by a factor of two in  $x$  and  $y$ . Each map element is defined by taking the average of four visibility functions, and recompressing the result. Mip-mapping techniques may then be applied for more efficient shadow lookups during rendering.

To improve data access during the rendering process, portions of a map may be cached. The cache contains multiple cache lines that are each capable of storing a tile of map data. A map tile may comprise, for example, a two-dimensional subset of map locations. Because different visibility functions may contain varying numbers of vertices, the storage allocation size of map tiles may also vary. For more efficient memory performance, the sizes of cache lines may be dynamically resized as map tiles are swapped, to reflect the individual storage requirements of the current map tiles resident in the cache.

The present invention relates to computer animation. More specifically, the present invention relates to enhanced methods and apparatus for rendering objects while accounting for non-opaque objects, objects with translucent portions, or the like.

Methods and apparatus that provide inexpensive approximation of subsurface scattering of light are disclosed. The methods typically include two phases of calculations: a phase where volume information is recorded, and a phase where the final scene is rendered using lighting contributions for each of the lights in the scene.

In the first phase, “thickness maps” are generated for each light in the scene. A thickness map is generated from the perspective of the light. Further, for each “pixel” in the thickness map, a function is generated representing the accumulated thickness of objects that intersect a ray cast from the light at that pixel. In one embodiment, the thickness calculations rely on the geometry of the object to be closed and not self-intersecting.

During the second phase, the contribution to the scene from a light is calculated using the thickness map that has been generated. For each point to be shaded, thickness information around the region of the point is read from the thickness map and is filtered to calculate an average thickness for the point. This thickness, combined with common surface information such as the normal and color of the surface are used to approximate the contribution from that light. In some embodiments, scattering differences of different frequencies of illumination can be approximated using a function that interpolates through a list of user-supplied colors indexed by the thickness.

According to one aspect of the invention, a method for determining illumination of surface points of an object in a scene from lighting sources is described. One technique includes determining a first thickness map for a first lighting source for the scene, wherein the first thickness map includes a first plurality of thickness values of the object with respect to distance from the first lighting source, determining a surface point on the object, and determining a first plurality of thickness values associated with the surface point on the object in response to the first thickness map. Techniques may include determining a first filtered thickness value associated with the surface point on the object in response to the first plurality of thickness values, and determining an illumination contribution from the first lighting source at the surface point in response to the first filtered thickness value.

According to another aspect of the invention, a computer system is described. The computer system includes a memory and a processor. The memory is configured to store a first thickness map associated with a first illumination source within a scene, wherein the first thickness map includes a first plurality of thickness functions of at an object versus distance away from the first illumination source. The processor is processor coupled to the memory, and configured to retrieve the first thickness map from the memory. The processor is also configured to determine a surface point on the one object, to determine a neighborhood of surface points on the one object in response to the surface point on the one object, and to determine a plurality of thickness values of the at least one object in response to the surface point and the neighborhood of surface points and in response to the first thickness map. The processor is also configured to determine a filtered thickness value of the one object in response to the plurality of thickness values, and to determine an illumination contribution from the first illumination source at the surface point in response to the filtered thickness value of the one object.

According to yet another aspect of the invention, a computer program product for a computer system including a processor is described. The computer program product includes code that directs the processor to retrieving a first thickness map for a first illumination source for the scene, wherein the first thickness map includes an array of thickness functions, wherein each thickness functions comprises a relationship between thickness values of the object with respect to distance from the first illumination source, code that directs the processor to determine a surface point on the object, and code that directs the processor to determine a first plurality of thickness functions associated with the surface point on the object in response to the first thickness map. In various configurations, the computer program product also includes code that directs the processor to determine a first plurality of thickness values in response to the first plurality of thickness functions and in response to the surface point on the object, code that directs the processor to

determine a first filtered thickness value associated with the surface point on the object in response to the first plurality of thickness values, and code that directs the processor to determine an illumination contribution from the first illumination source at the surface point in response to the first filtered thickness value. The codes typically reside on a tangible media such as a magnetic hard disk, optical memory, semiconductor-based memory, or the like.

#### BRIEF DESCRIPTION OF THE DRAWINGS

In order to more fully understand the present invention, reference is made to the accompanying drawings. Understanding that these drawings are not to be considered limitations in the scope of the invention, the presently described embodiments and the presently understood best mode of the invention are described with additional detail through use of the accompanying drawings in which:

FIG. 1 is a diagram of an image rendering scenario within a modeled object scene.

FIG. 2 is a diagram of a shadow map of the prior art.

FIG. 3 is a diagram showing ray casting.

FIG. 4 is a flow diagram of a method for generating a shadow map.

FIG. 5 is a flow diagram of a method for performing shadow map lookups.

FIG. 6A is a diagram of shadow sampling along a single edge of a silhouette.

FIG. 6B is a diagram of shadow sampling over a filter region containing many silhouette edges.

FIG. 7 is a diagram of a deep shadow map in accordance with an embodiment of the invention.

FIG. 8A is a diagram of a visibility function over a region crossed by multiple semitransparent surfaces.

FIG. 8B is a diagram of a visibility function over a region in which partial blocking occurs.

FIG. 8C is a diagram of a visibility function over a region comprising an object with volumetric characteristics.

FIG. 9 is a flow diagram of a method for generating a deep shadow map in accordance with an embodiment of the invention.

FIG. 10 is a diagram illustrating the generation of a transmittance function in accordance with an embodiment of the invention.

FIGS. 11A-11D are flow diagrams of a method for determining transmittance in accordance with an embodiment of the invention.

FIG. 12 is a diagram of a two-dimensional filter function.

FIGS. 13A-13C are flow diagrams of methods for obtaining a visibility function by applying a filter, in accordance with one or more embodiments of the invention.

FIG. 14 is a flow diagram of a method for performing compression of a visibility function in accordance with an embodiment of the invention.

FIGS. 15A-15G are diagrams illustrating the compression of a visibility function, in accordance with an embodiment of the invention.

FIG. 16 is a flow diagram of a method for implementing deep shadow map lookups in accordance with an embodiment of the invention.

FIG. 17 is a diagram of a shadow map implementation for monochrome and color shadows in accordance with an embodiment of the invention.

FIG. 18A is a flow diagram of a method for generating multiple levels of deep shadow maps in accordance with an embodiment of the invention.

FIG. 18B, is a flow diagram of a method for selecting a map level during a lookup in accordance with an embodiment of the invention.

FIG. 19 is a diagram of a mip-mapping implementation of deep shadow maps in accordance with an embodiment of the invention.

FIG. 20 is a diagram of a file format for deep shadow maps in accordance with an embodiment of the invention.

FIG. 21 is a block diagram of a cache implementation in accordance with an embodiment of the invention.

FIG. 22 is a flow diagram of a caching method with cache line resizing in accordance with an embodiment of the invention.

FIG. 23 is a flow diagram of a method for implementing motion blur of shadows in accordance with an embodiment of the invention.

FIG. 24 is a general block diagram of one embodiment of a computer system in which embodiments of the present invention may be implemented.

FIG. 25 is a block diagram of typical computer rendering system according to an embodiment of the present invention;

FIGS. 26A-C illustrate a block diagram of a process flow according to an embodiment of the present invention;

FIGS. 27A-D illustrate an example of an embodiment of the present invention; and

FIG. 28 illustrates an example according to an embodiment of the present invention.

## DETAILED DESCRIPTION OF THE INVENTION

### Chapter 1: Method and Apparatus for Rendering Shadows

The invention is a method and apparatus for rendering shadows. In the following description, numerous specific details are set forth to provide a more thorough description of embodiments of the invention. It will be apparent, however, to one skilled in the art, that the invention may be practiced without these specific details. In other instances, well known features have not been described in detail so as not to obscure the invention.

In this specification, "map location" is used interchangeably with "pixel" to mean an element of any shape or form in the image that is in consideration.

#### Deep Shadow Map Overview

Embodiments of the invention employ a new form of shadow map, referred to herein as a "deep shadow map," to provide greater flexibility and realism in the rendering of shadows. As opposed to shadow maps of the prior art that treat shadows in a binary manner (i.e., a surface is either lit or unlit) based on a single stored depth value, deep shadow maps permit partial shadowing to be represented explicitly as a function that varies with depth. A deep shadow map stores a fractional visibility function (hereinafter "visibility function") that records the approximate amount of light that passes through the pixel and penetrates to each depth. The visibility function takes into account not only the opacities of the surfaces and volume elements encountered, but also their coverage of the filter region. Partial shadowing facilitates accurate and efficient rendering of shadows caused by "real world" lighting conditions such as partially blocking elements, semitransparent surfaces and volumetric elements.

An important feature of deep shadow maps is generality: deep shadow maps support ordinary surfaces, volumetric effects, dense fur, and even motion blur, effects that would normally be handled using different techniques. With deep

shadow maps, these effects can all be combined in a single compact data structure, and rendered efficiently under a wide range of viewing and filtering conditions.

A deep shadow map can be viewed as a two-dimensional array of piecewise linear one-dimensional functions. The representation is sparse in  $z$ , which allows it to take advantage of any smoothness in the raw data, while it is discrete in  $x$  and  $y$  in order to facilitate fast lookups. The domain can be mapped to a frustum or an orthographic space, and has the advantage of having an arbitrary extent and resolution in one of its dimensions. Further, three-dimensional filtering can be implemented, since the adjacent data values in  $z$  can be found without searching and the representation is sparse in this direction. Deep shadow maps are a useful representation for arbitrary volumetric data: fog densities, approximate illumination information, etc.

#### Visibility Functions

In one embodiment of the invention, a deep shadow map is implemented as a rectangular array of elements, where every element stores a visibility function. This implementation is illustrated in FIG. 7 as a two-dimensional array in  $x$  and  $y$ , in which each array element comprises a depth-based visibility function  $V(z)$  (e.g.,  $V_{0,0}(z)$ ,  $V_{0,1}(z)$ , etc.). The rectangular array of the deep shadow map corresponds to the map plane located between the light source and the object scene, with each map location (i.e., array element) being associated with a two-dimensional filter region of the map plane. To better understand visibility functions, consider a beam of light that starts at the light source origin ( $z=0$ ), and passes through a given pixel of the filter region. For that pixel, the visibility function value at a given depth is the fraction of the light beam's initial power that penetrates to that depth. Note that the light beam is not necessarily square; the beam can be shaped and weighted according to any desired pixel filter. Further, the filter regions for adjacent pixels may overlap in some embodiments.

FIGS. 8A-8C illustrate (from side-view) several examples of visibility functions for a light beam passing through a pixel of the deep shadow map given different forms of light attenuating circumstances. Specifically, FIG. 8A illustrates a sequence of semitransparent surfaces stacked in front of the light beam; FIG. 8B illustrates the effect of multiple opaque objects partially blocking the light beam at different depths; and FIG. 8C illustrates light attenuation through a volumetric element such as fog. In each case, the visibility function is defined from a value of "1," indicating no light attenuation, decreasing to "0," indicating complete blocking of the light beam. It will be obvious that the invention may also be practiced with different numerical values assigned to these conditions.

In FIG. 8A, light source **800** projects light beam **810** through a stack of semitransparent surfaces, **801-803**. It is assumed for simplicity in this example that the surfaces are planar and constant in  $z$ . The beam's power is reduced as it passes through each consecutive semitransparent surface. As shown, the visibility function steps down at depth  $Z_{S1}$  when surface **801** is intersected. The amount of attenuation at  $Z_{S1}$  is dependent upon the opacity of surface **801**. Unlike prior art shadowing methods, if the opacity of surface **801** is not equal to "1" (i.e., not completely opaque), the visibility value after  $Z_{S1}$  is nonzero. At depths  $Z_{S2}$  and  $Z_{S3}$ , the visibility function is subject to further attenuation steps based upon the level of opacity of surfaces **802** and **803**, respectively. Thus, the attenuation contributions of each successive semitransparent surface are accounted for in the visibility function. In contrast, because only a single depth



value is stored, a shadow map of the prior art would represent the light beam as completely blocked at depth  $Z_{S1}$ , introducing lighting errors at depths beyond  $Z_{S1}$ .

In FIG. 8B, light source **800** projects light beam **810** through a region of an object scene impinged upon by opaque objects **804-807**. In this situation, the visibility function is reduced as a function of the beam cross-section blocked by the blocking object. As the remaining cross-sectional area of the beam diminishes, the visibility function decreases as well. In the illustrated example, beam **810** is impinged upon by object **804** beginning at depth  $Z_{A1}$ , UP to a maximum cross-sectional blockage at depth  $Z_{A2}$ . The visibility function then remains constant until depth  $Z_{B1}$ , at which point the visibility function again drops in value through depth  $Z_{B2}$ , the depth of maximum blockage from object **805**. A similar reduction is experienced between depths  $Z_{C1}$  and  $Z_{C2}$  based upon encroachment of object **806** on the remaining beam cross-section. From depth  $Z_{D1}$  to depth  $Z_{D2}$ , the visibility function decreases to zero as object **807** blocks the remaining portion of the projected beam. Beyond  $Z_{D2}$ , there is no light contribution from light source **800** due to the accumulated blockage by opaque objects **804-807**.

Note that a shadow map of the prior art would represent the scenario of FIG. 8B with a single depth value  $z$  wherein the visibility transitions instantaneously from 1 to 0, disregarding any effects due to the partial blocking. Such a limited representation introduces significant error in the shadow rendering process. To decrease this error, a shadow map of the prior art would need to be of fine enough resolution to resolve each of the blocking objects, increasing memory requirements as well as rendering time.

In FIG. 8C, light source **800** projects light beam **810** through a volumetric element **808** such as fog, which reduces the power of the light beam as a continuous function of depth. The visibility function is constant at 1 until light beam **810** encounters the leading edge of volumetric element **808** at depth  $Z_{V1}$ . The visibility decreases continuously from depth  $Z_{V1}$  until the beam exits the trailing edge of volumetric element **808** at depth  $Z_{V2}$ , after which the visibility function is again constant. The rate of decrease in beam power within the volumetric element **808** may vary based upon depth-dependent functions of the volumetric element, such as fog density. Such characteristics can be accurately represented with a visibility function as shown. In shadow maps of the prior art, such volumetric elements must be treated as opaque objects, or not represented in the shadow map at all.

#### Transmittance and Prefiltering

Considering a ray of light that starts at the light source origin and passes through the point  $(x, y)$  on the image plane. Some fraction of the light emitted along this ray will be attenuated by surfaces or by volumetric scattering and absorption. The fraction of light that penetrates to a given depth  $z$  is known as the transmittance  $\tau(x, y, z)$ . For deep shadow maps,  $\tau$  is referred to as a "transmittance function" when considering the transmittance at a fixed image point  $(x, y)$  as a function of  $z$ .

In one or more embodiments of the invention, the visibility function for a given pixel is based on transmittance. The visibility function for each map location is obtained by filtering the nearby transmittance functions, and resampling at the center of the pixel. This can be better understood by considering a particular depth  $z$ . The transmittance at every point in this  $z$ -plane is given by  $\tau(x, y, z)$ , and the visibility function  $V_{i,j}$  for each pixel in the deep shadow map is obtained by filtering these values as follows:

$$V_{i,j}(z) = \int_{-r}^r \int_{-r}^r f(s, t) \tau\left(i + \frac{1}{2} + s, j + \frac{1}{2} + t, z\right) ds dt$$

where  $(i+1/2, j+1/2)$  is the center of the region associated with the pixel  $(i, j)$ ,  $f(s, t)$  is the desired bandlimiting filter (centered around the origin), and  $r$  is the filter radius. This definition is similar to ordinary image filtering, except that it applies to every  $z$  value separately.

An advantage of deep shadow maps over regular shadow maps is that prefiltering is supported. Prior art techniques for generating shadow maps do not support prefiltering because the shadow maps contain only single depth values at each pixel. Attempts to "filter" depth values result in much greater errors in shadow rendering. Thus, to maintain desired error levels in the rendered output, all samples (depth values) obtained for the prior art shadow map must be carried over into the pixel rendering process.

With deep shadow maps, each pixel summarizes a large number of depth samples due to prefiltering of the transmittance functions during the pre-rendering process. When a visibility function is evaluated at a given  $z$  value, the result is substantially the same as if percentage-closer filtering was applied to all of the depth samples within the pixel's filter radius. Thus, high-quality filtering can be performed by accessing a much smaller number of pixels during the rendering process.

Prefiltering is important, because sampling error analysis holds for both prior art shadow maps and deep shadow maps. In both cases, a large number of depth samples must be filtered in order to obtain accurate shadows of detailed geometry. While deep shadow maps do not reduce the number of depth samples that must be taken from the scene, deep shadow maps greatly reduce the amount of data that must be accessed during filtering. For example, in order to compute a shadow of dense hair with an expected error of 1%, approximately  $N=2500$  samples per pixel are needed in the prior art methods. Using a deep shadow map with 250 samples per pixel (i.e., 250 samples prefiltered to obtain the visibility function at each pixel), only  $N=10$  pixels need to be processed to achieve a similar accuracy. In contrast, with prior art shadow maps, all 2500 samples must be processed.

Prefiltering not only makes shadow lookups faster, but also allows deep shadow maps to be much smaller than the equivalent high-resolution depth map used in the prior art. This is an advantage when deep shadow maps are written, stored, and cached in memory.

As described, prefiltering allows deep shadow maps to have a much reduced resolution in  $x$  and  $y$  with respect to prior art shadow maps. Yet, the size of the deep shadow map is not merely a function of the resolution in  $x$  and  $y$ . The size is also a function of the manner in which each visibility function is represented and stored. For this reason, in one or more embodiments of the invention, visibility functions are compressed. In one compression method described later in this specification, compression is performed with respect to desired error constraints in the function value at each depth. More specifically, error bounds are determined based upon desired percentage error values. The visibility function is then approximated with a minimum amount of data required to stay within those error bounds.

A general flow diagram of a method for generating a deep shadow map for a light source in accordance with one or more embodiments of the invention is provided in FIG. 9. In step **900**, a current map location (pixel) is selected for

15

shadow pre-rendering. In step 901, sample rays are selected from within the corresponding projected filter region of the map location. For each sample ray, the transmittance function  $\tau$  is determined in step 902. Each transmittance function  $r$  accounts for all surfaces and volumes traversed by the respective sample ray. In step 903, all of the transmittance functions are combined to form a single visibility function in  $z$ . Combination is achieved, for example, by specifying a two-dimensional filter in  $x$  and  $y$ , and applying the filter at multiple values of  $z$ . In step 904, the resulting visibility function is compressed, and, in step 905, the compressed visibility function is stored in the given map location.

#### Computation of Fractional Visibility

Each element (e.g., each surface or volume) that affects transmittance along a sample ray may have its own partial transmittance function computed independently. However, it may be computationally more efficient to determine the partial transmittance functions for multiple elements in one process. The total transmittance function along the ray is obtained from the product of those partial transmittance functions. In the embodiment described below, a single surface transmittance function is computed that accounts for all surface elements traversed by the ray. A separate volume transmittance function is computed that accounts for all volumetric elements. Other embodiments of the invention may compute transmittance functions for the elements traversed by the ray either individually or in any combination.

A method for determining a visibility function from multiple transmittance functions is described below with reference to FIGS. 11A-11D. In FIG. 11A, in step 1100, the map plane is diced into multiple sample regions, e.g., as a grid. This assures a minimum sample spacing for better coverage of each filter region. In step 1101, one or more sample point(s) is selected within each sample region. A simple technique is to sample at the center of each sample region, though other sample point distribution approaches (e.g., stochastic or "pseudo-random" sampling) may be used to improve sampling quality. In step 1102, a first sample point is selected for determination of its corresponding transmittance function. The order in which sample points are processed may vary. However, scanline rendering processes may be used to facilitate this operation, in which case the sample points are selected in scanline order. Note that the transmittance functions for all sample points need not be concurrently stored in memory. If pixels are processed in scanline order, it is sufficient to store enough scanlines to span the width of the applied filter function.

In step 1103, for the current sample point in the map plane, a ray is projected from the light source through the sample point to cross the object scene. In step 1104, a surface transmittance function  $\tau^S$  is determined that accounts for each surface intersected by the ray. The surface intersections can be found using either a ray tracer or an ordinary scan conversion renderer, for example. In step 1105, a volume transmittance function  $\tau^V$  is determined that accounts for each volumetric object traversed by the ray. Steps 1104 and 1105 may be performed in any order, or in parallel. In step 1106, the transmittance function of the sample point  $t$  is determined from the product of the surface transmittance function  $\tau^S$  and the volume transmittance function  $\tau^V$ .

In step 1107, if there are more samples to process, the next sample point is selected in step 1108, and the method returns to step 1103. If, however, in step 1107, no further samples need processing (e.g., sufficient scanlines are processed to

16

perform filtering for a row of map locations), in step 1109, filtering is performed to obtain visibility functions for corresponding map locations.

The step of determining the surface transmittance  $\tau^S$  is described in more detail below with reference to the flow diagram of FIG. 11B. In step 1110, the projected ray is traversed in  $z$  from the light source origin. In step 1111, the initial value of the surface transmittance function  $\tau^S(z_{i-1})$  is set equal to "1".

In step 1112, if there is a "surface hit" (i.e., the ray intersects a surface), the method proceeds to step 1113; otherwise, the method proceeds to step 1117. In step 1113, the surface characteristics are queried to determine the opacity  $O_i$  of the surface where the ray intersects at depth  $z_i$ . In step 1114, the transmittance value at  $z_i$  is determined as follows, to account for the opacity of the surface:

$$\tau^S(z_i) = (1 - O_i) \tau^S(z_{i-1})$$

Step 1116 is an optional step for ending traversal in  $z$ , once the computed transmittance function falls below a threshold value. If  $\tau^S(z_{i-1})$  is less than a threshold value  $\tau_{MIN}$ , then the computed surface transmittance function is output at step 1119. The threshold value may be predicated on an acceptable error range (e.g., conservatively assuming multiplication by a maximum value ("1") of the volume transmittance function). Once this threshold is met, it may be unnecessary to continue evaluating surface effects along this ray, especially if the last surface was opaque ( $O_i=1$ ). If the threshold is not met in step 1116, or if step 1116 is not implemented, the method proceeds to step 1117.

In step 1117, the current depth value is compared with a depth threshold value  $z_{CLIP}$ , such as the depth of a rendering clipping plane. If the depth threshold has not been met or all the surfaces have not been sampled, the method continues traversal in  $z$  in step 1118, and returns to step 1112. If, in step 1117, the depth threshold is met or all the surfaces have not been sampled, the computed surface transmittance function  $\tau^S$  is output in step 1119.

In one or more embodiments, the surface and volume transmittance functions, as well as the visibility function, are approximated with piecewise linear functions. By approximating the functions in this manner, it is possible to fully describe those functions with a sequence of vertices, in which each vertex identifies a particular depth value  $z_i$  and a function value at that depth (e.g.,  $\tau^S(z_i)$ ). In the case of the surface transmittance function, each discontinuous step caused by a surface hit may be represented by a pair of vertices having the same depth value but two different function values representing the value prior to the surface hit and the value subsequent to the surface hit. This representation results in wasted space, however, the wasted space is removed during the compression process. Note that a true step in the compressed output function would occur only for surface parallel to the  $xy$ -plane. The vertices at  $z=0$  and  $z=\infty$  are represented implicitly, and are not part of the output.

The step of determining the volume transmittance function  $\tau^V$  is described in further detail below with reference to the flow diagrams of FIGS. 11C-11D. At step 1120, traversing in  $z$ , the atmospheric density is sampled at regular intervals along the projected ray to determine an extinction coefficient  $K_i$  at each depth  $z_i$ . The extinction coefficient measures the light falloff per unit distance along the ray. It is assumed that the atmospheric density of a volumetric element may be obtained (or derived) for any location in the scene. At depths where the projected ray does not lie within a volumetric element, the extinction coefficient is zero. The

extinction function  $K(z)$  is obtained by linearly interpolating from the extinction coefficients in step **1121**.

The fraction of light that penetrates to a given depth  $z$ , i.e., the volume transmittance function  $\tau^V(z)$ , is computed at step **1122** by integrating and exponentiating the extinction function as follows:

$$\tau^V(z) = \exp\left(-\int_0^z \kappa(z') dz'\right)$$

While step **1122** may be carried out by computing the integral of the extinction function directly, a simpler approximation method that yields a more tractable piecewise linear function is shown in FIG. **11D**.

The method of FIG. **11D** evaluates the transmittance value at each vertex of the extinction function, so that the volume transmittance function can be linearly interpolated from those transmittance values. In step **1123**, the incremental transmittance for each linear segment of the extinction function is calculated from the vertex extinction coefficients as follows:

$$T_i = \exp(-(Z_{i+1} - Z_i)(K_{i+1} + K_i)/2)$$

Using the incremental transmittance values, the volume transmittance function at those vertex locations is determined in step **1124** by multiplying the incremental transmittance values together. The volume transmittance at each vertex is given by:

$$\tau^V(z_i) = \prod_{j=0}^i (T_j)$$

In step **1125**, the volume transmittance function  $\tau^V$  is linearly interpolated from the computed values for  $\tau^V(z_i)$ .

An example application of the methods described above is illustrated in the diagram of FIG. **10**, with respect to generation of a transmittance function from a sample ray. In this example, a sample ray **1000** is projected from light source **1000**. In traversing the object scene, sample ray **1005** intersects four surfaces **1001-1004**, as well as a volumetric element **1006**.

Function **1007** represents the piecewise constant surface transmittance function  $\tau^S$  obtained by evaluating the surface effects at the intersections with surfaces **1001-1004**. At the depth of each surface hit, the surface transmittance function experiences a corresponding downward step, the magnitude of which is based on the opacity of the intersected surface. Each step is represented by two vertices. Thus, the surface transmittance for ray **1005**, which intersects a total of four surfaces, is fully represented by eight vertices.

Function **1008** represents the piecewise linear extinction function  $K$  obtained by sampling the atmospheric density of element **1006** along ray **1005**. Function **1009** represents the volume transmittance function  $\tau^V$  obtained by integrating and exponentiating the extinction function **1008**. Functions **1008** and **1009** share the same vertex depth locations.

Function **1010** is the total transmittance function  $\tau$  obtained by multiplying functions **1007** and **1009** together. To simplify the calculation, multiplication is performed only at depths where at least one of functions **1007** and **1009** has a vertex. Where one function has a vertex and the other does not, a function value is interpolated from the nearby vertices.

Note that the number of vertices in the output transmittance function **1010** is equal to the sum of the number of vertices in functions **1007** and **1009**.

5 Filtering Implementation

As previously alluded to, individual transmittance functions are combined to form a single visibility function by means of a two-dimensional filter. The application of the filter is generally described by the following equation:

$$V_{i,j}(z) = \sum_{k=1}^n \omega_k \tau_k(z)$$

where “ $n$ ” is the number of transmittance functions within the filter radius around  $(i+1/2, j+1/2)$ , and  $\omega_k$  is the normalized filter weight for the corresponding image sample point  $(x_k, y_k)$ . The resulting visibility function  $V_{i,j}$  accounts not only for the light attenuation due to semitransparent surfaces and volumetric objects such as fog. By virtue of the spatial sampling in  $x$  and  $y$ , the visibility function also accounts for the fractional coverage of these features.

An example of a  $4 \times 4$  filter is shown in FIG. **12**. The center of the coefficient grid represents the center of the filter region  $(i+1/2, j+1/2)$ . Those samples closest to the center are scaled by coefficient “A.” Samples within the grid areas beyond the “A” regions in the  $x$  or  $y$  direction are scaled by coefficient “B,” whereas samples in the grid areas at the outside corners are scaled by coefficient “C.” Filter coefficients applied to the transmittance functions are typically weighted towards the center of the filter region (i.e.,  $A > B > C$ ). The output of the filter is normalized by dividing the summed result by the sum of the filter coefficients, which, for this example, is  $4A + 8B + 4C$ . The output of the filter is thus a weighted average of the input transmittance functions at each depth  $z$ . Note that other filtering methods could be used, including those in which the filter value depends on the substratum sample location.

A general method for filtering the transmittance samples is illustrated in the flow diagram of FIG. **13A**. The light transmitted at the source (i.e.,  $z=0$ ) is transmitted by definition with a transmittance of “1” for any sample point. Thus, in step **1300**, the visibility value  $V(0)$  is set to “1.” In step **1301**, the set of vertices for all of the transmittance functions that fall within the filter region is identified and sorted in depth order, and, in step **1302**, a first vertex is selected from the set.

In step **1303**, the depth  $z_i$  of the current vertex is determined, and, in step **1304**, the filter is applied to all transmittance functions at that depth to determine the corresponding visibility value  $V(z_i)$ . The result is stored as an output vertex  $(z_i, V(z_i))$ . Application of the filter entails interpolating each transmittance value at depth  $z_i$ , scaling each transmittance value by the corresponding filter coefficient, summing all of the scaled values, and dividing the result by the sum of the coefficients.

In step **1305**, if there are more vertices to process, then the next vertex is selected in step **1306**, and the process returns to step **1303**. However, if there are no further vertices to consider in step **1305**, filtering is completed. The visibility function  $V(z)$  is the piecewise linear function defined by the computed output vertices.

Although each visibility function is piecewise linear, it has as many vertices as all of the contributing transmittance functions combined. This means that as the number of

sample points within the filter region increases, the number of vertices at which the filter must be applied increases proportionally. Further, the number of computations needed in a single pass of the filter also increases substantially proportional to n (i.e., there are n samples to be interpolated, scaled and summed). Thus, the complexity of the filtering operation to obtain the visibility function over all depths is a function of n<sup>2</sup>.

Though the filtering method of FIG. 13A is functional, and may be used in embodiments of the invention, an alternative method is preferred for which the cost increases much less rapidly with the size of the filter. The alternative method employs incremental updates with a constant update cost per vertex.

If the transmittance functions are piecewise constant, the output function can be efficiently computed as follows. At z=0, the weighted average is computed as V(0)=1. All of the input vertices are then processed in increasing z order, which can be done in O(log n) time per vertex by storing the next vertex of each transmittance function in a heap. For every vertex, the current visibility sum is updated by subtracting out the corresponding transmittance function's old contribution and adding in its new contribution. That is,

$$V' = V + \omega_j(t'_j - t_j)$$

where V is the old visibility function value, V' is the updated visibility function value,  $\omega_j$  is the filter weight for the chosen transmittance function,  $t_j$  is the old value of the transmittance function and  $t'_j$  is its new value. The values of the other transmittance functions are not needed until one of their respective vertices is processed.

The above method may be applied where each of the transmittance functions is piecewise constant. However, in many circumstances (e.g., where volumetric effects are considered), the transmittance functions are not piecewise constant, merely piecewise linear. For piecewise linear functions, the filter process keeps track of the output visibility function's current value and slope. The update for each vertex consists of two steps: extending the output function, using its current position and slope, to the z value of the next input vertex; and updating the current output slope. FIGS. 13B-13C provide a flow diagram of a method for filtering piecewise linear transmittance functions in accordance with one or more embodiments of the invention.

In step 1307 of FIG. 13B, the initial visibility value is set to "1." In step 1308, the initial slope  $M_v(0)$  of the visibility function is calculated as the weighted sum of the initial transmittance slopes  $M_n^r(0)$ , where the transmittance slope is given by:

$$M_n^r(z_i) = (\tau(z_{i+1}) - \tau(z_i)) / (z_{i+1} - z_i)$$

and the initial visibility function slope  $M_v(0)$  is:

$$M_v(0) = \sum_{k=1}^n \omega_k M_k^r(0)$$

In step 1309, the set containing all vertices of the filtered transmittance functions is determined and sorted in increasing depth order. In step 1310, the depth  $z_i$  of the next vertex in the set is determined. The visibility value at depth  $z_i$  is then computed in step 1311 based on the current visibility function value and slope value:

$$V(z_i) = V(z_{i-1}) + M_v(z_{i-1}) \cdot (z_i - z_{i-1})$$

In step 1312, for the transmittance function associated with the current input vertex, the prior slope value and new slope value are determined. (The prior slope value may be stored in a temporary register allocated to each transmittance function for that purpose. The temporary register is updated with the new slope after the vertex is processed.) In step 1313, if the current transmittance vertex reflects a vertical step (e.g., depth matches that of next vertex), then the process continues at step 1317 of FIG. 13C; otherwise, a new visibility slope value is calculated subtracting the prior weighted slope of the transmittance function and adding the weighted new slope of the transmittance function as follows:

$$M_v(z_i) = M_n^r(z_i) - \omega_n [M_n^r(z_{i-1}) - M_n^r(z_i)]$$

In step 1315, if there are more vertices in the input set, the next vertex is selected in step 1316, and the process returns to step 1310; otherwise, the filtering process is complete for this map location.

Steps 1317-1319 of FIG. 13C are implemented to handle vertical steps of the input transmittance functions. The result is that both input vertices defining the vertical step are processed, and two output vertices are generated. In step 1317, a second visibility function value is determined at the same depth  $z_i$  by subtracting the weighted step value of the transmittance function from the prior visibility function value (as described for piecewise constant functions). In step 1318, the slope value of the transmittance function, subsequent to the vertical step, is computed. The new visibility slope value is calculated in step 1319 by subtracting the weighted transmittance slope value prior to the vertical step and adding the weighted transmittance slope value subsequent to the vertical step. From step 1319, the process continues at step 1315 of FIG. 13B.

The above technique is much more efficient than computing the weighted averages directly (as described with respect to FIG. 13A), and makes the filtering process practical even when very large numbers of samples per map location are used.

Compression of Visibility Functions

The raw visibility functions output from the filter process described above may have a large number of vertices, depending on the filter radius and the number of samples per map location. However, the raw visibility functions are generally quite smooth, making compression a viable option. The compressed functions are stored as an array of floating-point pairs, each containing a z value and a fractional visibility V.

It is desirable that the compression method preserve depth values, since even small errors in z can lead to undesirable self-shadowing artifacts. The compression method should also be appropriate for unbounded domains ( $z \in [0, \infty)$ ). In one or more embodiments of the invention, the L<sup>∞</sup> error metric (maximum error) is used to compress functions as described below.

Given a visibility function V and an error tolerance c, the compression method outputs a new visibility function V' such that

$$|V'(z) - V(z)| \leq \epsilon \text{ for all } z$$

where V' typically has a much smaller number of control points or vertices. One aspect of this approach is that it is incremental. Vertices are read and written one at a time in increasing z order, and only a constant amount of state information is used. FIGS. 15A and 15G illustrate the difference in the visibility function before and after compression, respectively.

The general technique is to draw the longest possible line segment that stays within the error bounds. The origin of the current segment is fixed, so that only the direction and length of the segment need to be chosen. To simplify the implementation, the output  $z$  values may be restricted to be a subset of the input  $z$  values. In one or more embodiments of the invention, the output  $z$  values are restricted to be a subset of the input  $z$  values.

Let the origin of the current output segment be  $(z'_i, V'_i)$ . At every step, a range of permissible slopes  $[M_{LO}, M_{HI}]$  of the input function  $V$  imposes a constraint on the current slope range, by forcing the segment to pass through the target window defined by the wedge from the segment origin to the two points  $(z_j, V_j \pm \epsilon)$ . The current slope range is initialized to  $[-\infty, \infty]$ , and is intersected with each target window in succession until further progress would make it empty. The output is the line segment with slope  $(M_{LO} + M_{HI})/2$  terminating at the  $z$  value of the last control point visited. The endpoint of this segment becomes the origin of the next segment, and the entire process is repeated. Using the average of  $M_{LO}$  and  $M_{HI}$  helps to center the endpoint within the allowable error bounds, though any slope within the slope range would satisfy the error constraints. It would be evident to one of ordinary skill in the art that other methods (e.g., least square fit) could be used once the  $z$  values of the control points have been chosen.

A flow diagram of the compression method, in accordance with one or more embodiments of the invention, is shown in FIG. 14. In step 1400, the origin of the current output segment is set to  $(z'_i, V'_i)$ , and, in step 1401, the current slope range  $[M_{LO}, M_{HI}]$  is initialized to  $[-\infty, \infty]$ . In step 1402, the next raw input vertex  $(z_j, V_j)$  is selected for consideration.

In step 1403, a maximum test slope  $M+$  computed using the upper error bound on the current vertex is compared to the current maximum slope  $M_{HI}$ , where the maximum test slope is given as:

$$M+ = (V_j - V'_i) / (z_j - z'_i)$$

If the maximum test slope  $M+$  is less than the maximum slope  $M_{HI}$ , then a provisional maximum slope value  $M'_{HI}$  is set equal to  $M+$  in step 1404, before proceeding to step 1406. Otherwise, in step 1403, if the maximum test slope  $M+$  is greater than  $M_{HI}$ , then the provisional maximum slope  $M'_{HI}$  is set equal to  $M_{HI}$  in step 1405, prior to proceeding to step 1406.

In step 1406, a minimum test slope  $M-$  computed using the lower error bound on the current vertex is compared to the current minimum slope  $M_{LO}$ , where the minimum test slope is given as:

$$M- = (V_j - V'_i) / (z_j - z'_i)$$

If the minimum test slope  $M-$  is greater than the minimum slope  $M_{LO}$ , then a provisional minimum slope value  $M'_{LO}$  is set equal to  $M-$  in step 1407, before proceeding to step 1409. Otherwise, in step 1406, if the minimum test slope  $M-$  is less than  $M_{LO}$ , then the provisional minimum slope  $M'_{LO}$  is set equal to  $M_{LO}$  in step 1408, prior to proceeding to step 1409.

In step 1409, the provisional minimum slope value  $M'_{LO}$  is compared to the provisional maximum slope value  $M'_{HI}$ . If  $M'_{LO}$  is less than (or equal to)  $M'_{HI}$ , then the provisional slope range is nonzero, and, in step 1410, the provisional maximum and minimum slope values,  $M'_{HI}$  and  $M'_{LO}$ , become the new maximum and minimum slope values,  $M_{HI}$  and  $M_{LO}$ . Step 1410 then returns to step 1402 to consider the

next raw input vertex. (If there are no other input vertices, the process jumps to step 1412 to determine the last output vertex.)

If, in step 1409,  $M'_{LO}$  is greater than  $M'_{HI}$ , the provisional slope range is empty, and the new endpoint must be computed from the prior vertex point. Accordingly, in step 1411, the process returns to depth  $z_j$  of the prior vertex. In step 1412, the new output segment is defined as the segment originating at vertex  $(z'_i, V'_i)$ , having a slope equal to  $(M_{LO} + M_{HI})/2$ , and having a new endpoint at depth  $z_j$ . In step 1413, the new endpoint is designated as the origin of the next output segment. The process then returns to step 1400 to determine the next output segment.

Application of the above compression method to a sample function is illustrated in FIGS. 15A-15G. In FIG. 15A, visibility function 1500 is shown as a piecewise linear function having fourteen vertices at depths Z1 through Z14. An upper error bound 1501A is illustrated at a constant positive offset from function 1500. Similarly, a lower error bound 1501B is illustrated at a constant negative offset from function 1500.

To begin compression, the vertex at depth Z1 is set as the origin of an output segment to be determined. In FIG. 15B, maximum and minimum slope values ( $M_{HI}$  and  $M_{LO}$ , respectively) are determined based on upper error bound 1502A and lower error bound 1502B of the vertex at depth Z2. At depth Z3, the minimum slope  $M_{LO}$  is maintained because it is within the error bounds at that depth. However, the maximum slope must now be redefined using the upper error bound at depth Z3. In FIG. 15C, it is shown that the slope range has been restricted to the maximum slope determined by upper error bound 1503 of the vertex at depth Z3, and the minimum slope determined by lower error bound 1502B. Considering the upper and lower error bounds of the vertex at depth Z4 yields an empty set with respect to the new slope range. Thus, the endpoint of the current output segment is determined at depth Z3 using the centerpoint of the slope range from FIG. 15C.

FIG. 15D shows the new output segment 1504, having endpoints at depths Z1 and Z3. The endpoint at depth Z3 now becomes the origin of the next output segment. Thus, a new slope range is determined from upper error bound 1505A and lower error bound 1505B of the vertex at depth Z4. As illustrated in FIG. 15E, a nonzero slope range can be determined using the upper error bound 1505A of the vertex at depth Z4 and lower error bound 1506 of the vertex at depth Z5. The error bounds of the vertex at depth Z6 do not fall within the slope range. Thus, the new segment endpoint is calculated at depth Z5, using the midpoint of the slope range. The new output segment 1507 is shown in FIG. 15F.

In FIG. 15F, by applying the slope range determination steps from the new output vertex at depth Z5, a maximum slope is determined from the upper error bound 1508 of the vertex at depth Z11, whereas the minimum slope is determined from the lower error bound 1509 of the final vertex at depth Z14. The last output vertex is thus calculated at depth Z14. The new output segment 1510 is shown in FIG. 15G. Also, error bounds 1501A and 1501B are shown to illustrate that the new piecewise linear output function defined by the four new vertices at depths Z1, Z3, Z5 and Z14, satisfies the error constraints placed on the compression method.

The compression method described above is fast, simple to implement, and utilizes constant storage. Approximations can be slightly improved by doing a least-square fit once the  $z$  values of the output vertices have been fixed. However, the

computed vertices satisfy the given error criteria and generate very good approximations in practice.

#### Performing Lookups During Rendering

The foregoing description refers to methods and apparatus for generating deep shadow maps as part of a pre-rendering operation. The following description provides methods for utilizing the pre-rendered deep shadow maps during a pixel rendering process.

Deep shadow map lookups are handled by applying a reconstruction and resampling filter to the visibility function values at a constant depth. FIG. 16 provides a flow diagram of a method for performing deep shadow map lookups in accordance with one or more embodiments of the invention.

In step 1600, a pixel filter region is projected onto a surface at depth  $z$  as seen from the camera perspective. Surface samples within the filter region will be used to determine the pixel value associated with that filter region. As part of the rendering process, the lighting characteristics of the surface (in the form of a filtered visibility value) are obtained via deep shadow map lookup as described in steps 1601 to 1616.

In step 1601, the depth  $z'$  of the surface (within the projected filter region) is determined from the perspective of the light source, and, in step 1602, those deep shadow map locations that fall within the projected filter region are identified. This may be accomplished, for example, by associating a bounding box with the projected filter region, and filtering those map locations that fall within the bounding box.

In step 1603, a first map location is selected to be processed, and, in step 1604, a filter coefficient is determined for the current map location. For example, the filter coefficient could be based upon the distance of the map location from the center of the projected filter region (or bounding box) in the map plane. In step 1605, a pointer associated with the map location is used to identify the last segment (or vertex) accessed in a prior lookup operation. Some embodiments may omit the use of this pointer, in which case, any vertex in the stored visibility function may be used as a starting point. However, since many shadow lookups are performed at nearby  $z$  values, use of such a pointer can reduce the average cost of visibility function evaluations by directing the start of a depth search to the region of the visibility function most likely to contain the target depth.

In step 1606, the lookup process determines whether the current segment of the visibility function contains a value for the target depth  $z'$  (e.g., by comparing the target depth with the vertices forming the endpoints of the current segment). If the current segment does not contain the depth value  $z'$ , a linear search (other search methods could also be used) is performed on the sequence of visibility vertices, as shown by steps 1607-1609. In step 1607, if the target depth  $z'$  is less than the depths included in the current segment, the sequence of vertices is traversed backward (i.e., toward  $z=0$ ) in step 1609, and the process returns to step 1606 to see if the new segment contains the target depth value. However, if, in step 1607, the target depth is greater than the depth of the current segment, then, in step 1608, the sequence of vertices is traversed in the forward direction (i.e., toward  $z=\infty$ ). From step 1608, the process returns to step 1606.

If, at step 1606, the target depth  $z'$  does reside within the current segment, the associated pointer is updated to point to the current segment in step 1610. In step 1611, the visibility value is interpolated from the current segment using the depth value  $z'$ , and, in step 1612, the interpolated value is scaled by the corresponding weighted coefficient. In step

1613, if there are further map locations to process within the projected filter region, the lookup process turns its focus to the next map location in step 1614, and the lookup process returns to step 1604.

If, in step 1613, there are no further map locations to process, the scaled values derived in step 1612 are summed together in step 1615, and the result divided by the sum of the coefficients. In step 1616, the lookup process returns the computed value from step 1615 as the resampled visibility value. The pixel rendering process can then consider the fractional visibility value in determining the given light source's contribution to the shading of the surface.

#### Storage of Deep Shadow Maps

The following is a description of data representations and storage formats that may be used to implement deep shadow maps in accordance with one or more embodiments of the invention. It will be apparent to one skilled in the art that, in various embodiments, the deep shadow maps described herein may be implemented with a variety of data structures and file formats without departing from the scope of the invention.

#### Multi-Channel Maps and Colored Shadows

In the foregoing description, deep shadow maps are described in terms of vertices having a depth value and a function value. The concepts described, however, may be extended to encompass any number of functions by implementing the deep shadow maps with multiple channels. This is accomplished by associating multiple function values with each depth such that the pair  $(z, V)$  becomes the multi-channel tuple  $(z, V_1, V_2, \dots, V_N)$ . The multi-channel representation may be used to describe multiple functions for the same sample point, such as color-based visibility functions for the same sample ray, or it may be used to describe a single function (or multiple functions) for multiple sample points, such as a monochrome transmittance or visibility function for each sample point or map location in a  $2 \times 2$  neighborhood (also referred to as a "quad"). Note that these techniques are not possible with shadow maps of the prior art.

Color-based visibility functions are useful for determining colored shadows, i.e., shadows cast by surfaces which have color-dependent transmittances. For example, a colored surface might be opaque to certain colors while being substantially transparent to other colors. This multi-channel representation allows for this color-dependent visibility behavior to be efficiently modeled.

Quad processing can be advantageous from a concurrent memory access standpoint. Four neighboring functions may be accessed at the same map location, and depth searching for multiple neighboring samples at the same depth can be accomplished with a single search. Further bilinear interpolation techniques (or trilinear interpolation where mip-mapping techniques are used) may be efficiently implemented using quad visibility functions.

The common point between functions represented in a multi-channel map is that the vertices for all of the functions occur at the same depth values. The compression process operates on all the channels simultaneously, and starts a new segment for each function whenever any of the functions would exceed its error threshold. An advantage to this approach is that some amount of additional data compression is achieved. For example, a deep shadow map with three channels is only twice as large as a single-channel map, yet contains three times the number of functions. In practice, the number of vertices needed to represent the functions may increase due to the added constraint upon the compression

process, in that the compression process must maintain error bounds on all of the associated functions simultaneously.

As an example application of multi-channel maps, FIG. 17 illustrates an implementation of monochrome and color visibility functions within a single deep shadow map, in accordance with one or more embodiments of the invention. FIG. 17 contains a deep shadow map 1700 comprising an array of map locations such as map locations 1701 and 1702. As shown, map location 1701 has an associated multi-channel function representation 1703A, whereas map location 1702 has an associated single-channel function representation 1703B.

Multi-channel representation 1703A comprises an array or list of function vertices 1706A, containing one or more color vertex elements 1707A. Each color vertex element (CVERTEX) 1707A contains a depth value (DEPTH), a red visibility value (VALUE\_R), a green visibility value (VALUE\_G) and a blue visibility value (VALUE\_B). DEPTH, VALUE\_R, VALUE\_G and VALUE\_B are shown as floating point data types, though other data types may be used in other embodiments.

Also associated with multi-channel representation 1703A, in this embodiment, are pointer 1704A and flag 1705A. (Note that pointer 1704A and flag 1705A need not reside within the same data structure as vertex elements 1707A.) Pointer 1704A (LAST\_SGMNT) is a pointer to a color vertex element (CVERTEX) 1707A, specifically, the color vertex element last accessed in a depth search of map location 1701. As stated previously with respect to FIG. 16, pointer 1704A is used in some embodiments to reduce the average cost of depth searches by providing a more likely initial starting point for the search.

Flag 1705A (COLOR) is used to specify whether the associated representation (1703A) is a color representation (i.e., multi-channel) or a monochrome representation (single channel). A simple Boolean value may be used as the flag, in which case a "TRUE" value might indicate representation 1703A is a color or multi-channel representation. Other types of flags might also be used, such as an integer whose value indicates the type of representation or the number of channels in the representation. This flag enables a single deep shadow map to use multiple representation types (e.g., three-channel and single-channel), and to differentiate between them.

Single-channel (or monochrome) representation 1703B comprises an array or list of function vertices 1706B, containing one or more monochrome vertex elements 1707B. Each monochrome vertex element (MVERTEX) 1707B contains a depth value (DEPTH) and a visibility value (VALUE). As with vertex elements 1707A, DEPTH and VALUE are shown as floating point data types, though other data types may also be used.

As with representation 1703A, associated with multi-channel representation 1703B are pointer 1704B and flag 1705B. Pointer 1704B (LAST\_SGMNT) is a pointer to a monochrome vertex element (MVERTEX) 1707B, specifically, the monochrome vertex element last accessed in a depth search of map location 1702.

As with flag 1705A, flag 1705B (COLOR) is used to specify whether the associated representation (1703B) is a color representation (i.e., multi-channel) or a monochrome representation (single channel). In this case a "FALSE" value might indicate representation 1703B is a monochrome or single-channel representation.

Mip-Mapping with Deep Shadow Maps

Mip-mapping is an imaging technique commonly applied to texture data. With this technique, the same texture is stored at multiple resolutions to accommodate different pixel resolutions within a rendered image (e.g., near surfaces have a higher pixel resolution than surfaces further away from the camera location). When the texture is mapped to a surface, the texture map level is used that has the minimum resolution necessary to match the pixel resolution of the surface. This reduces the amount of filtering that must take place during the mapping operation to bring the base level texture samples to the resolution of the surface pixels.

Shadow maps of the prior art do not permit mip-mapping because depth values cannot be filtered without introducing significant shadowing error. Prior art shadow maps are thus limited to single high-resolution maps, if visual quality is to be maintained. Unlike the prior art, deep shadow maps comprise filtered functions from which lower resolution maps may be obtained without significant degradation in output quality. Thus, in one or more embodiments of the invention, mip-mapping is employed to improve rendering efficiency. Multi-level or mip-mapped deep shadow maps can be filtered in like manner to mip-mapped textures, including application of anisotropic filters, lerping (i.e., linearly interpolating) between levels, etc.

FIG. 18A is a flow diagram illustrating a method for generating multi-level deep shadow maps in accordance with one or more embodiments of the invention. Given a base map at a base resolution, the following method generates a new map level that is reduced in resolution by a factor of two in x and y. The method of FIG. 18A may be applied recursively to build a set of map levels with successively lower resolution.

In step 1800, given a base map, each map location in the new map is associated with a 2x2 group of map locations in the base map. In step 1801, the four visibility functions corresponding to a 2x2 group of base map locations are accessed for downsampling in x and y. The average visibility function is computed from the four base visibility functions in step 1802, for example, by applying the filtering process of FIGS. 13B-13C using equally weighted coefficients. In step 1803, the average visibility function is recompressed, e.g., per the method described with respect to FIG. 14, and, in step 1804, the recompressed visibility function is stored in the corresponding map location of the new map level. If, in step 1805, there are more 2x2 groups of base map locations to consider, the next group is obtained in step 1806, and the method returns to step 1801; otherwise, the new map level is complete.

The effects of the map generation process of FIG. 18A are illustrated in FIG. 19. FIG. 19 shows a base map level 1900A that has been divided into 2x2 groups of map locations, such as group 1901A. The four component visibility functions of group 1901A are averaged and recompressed to form a single visibility function located at the center of map location 1901B in new map level 1900B. Because the new visibility function is ultimately based on samples filtered from the highest resolution map, benefits of the original high resolution sampling are still maintained.

To avoid an accumulation of error, the compression tolerance can be reduced on each successive map level. For example, if the error threshold is cut in half each time the averaged functions for a new map level are recompressed, the total error will be at most twice that permitted for the highest-resolution map. Due to the reduced compression tolerance, the number of vertices per visibility function can be expected to double once for every two mip-map levels

approximately. The full map set comprising all map levels is approximately  $1/(1-\sqrt{2}/4)\approx 1.55$  times as large as the base level (rather than the usual 4/3 ratio for an ordinary texture mip-map).

Alternately, each level can be computed from the highest level, in which case the error does not have to increase from level to level. This results in a smaller map, but costs more to generate.

To utilize the multiple map levels during rendering, the lookup method previously described with reference to FIG. 16 may be modified slightly to implement map level selection. For example, in one embodiment, steps 1807-1809 of FIG. 18B are performed between step 1601 and 1602 of FIG. 16.

In step 1807, the approximate size of the pixel filter region relative to the map plane is determined. This can be done, for example, by determining the maximum and minimum x and y values of the pixel filter region projected back onto the map plane. A bounding box can then be generated to approximate the filter region.

In step 1808, the minimum map resolution is determined for which the number of map locations falling within the approximated filter region is greater than (or equal to) a specified sample threshold number. The map resolution may be represented as a "level of detail" determined by the distance in absolute x and y values between successive map locations. The sample threshold number represents a tradeoff between computational rendering complexity (more samples increases resource usage and processing time) and rendering quality (more samples increases output quality). In step 1809, based on the minimum map resolution determined in the previous step, the corresponding map level is selected for use in the lookup operation (as continued in step 1602 of FIG. 16).

The mip-mapping methods described above permit deep shadow maps to take full advantage of prefiltering during the pre-rendering process to minimize the number of memory accesses needed during the pixel rendering process (subject to the sample threshold number). Thus, the rendering process can be performed more quickly with high resolution shadow rendering quality.

#### File Format for Deep Shadow Maps

Rendering is a memory intensive process. Therefore, to maximize memory efficiency, some embodiments of the invention store deep shadow maps in secondary memory, such as on a disk drive, and maintain only a subset of the map data in primary memory (e.g., application memory or RAM). This ensures that sufficient memory resources are available for other aspects of the rendering process.

An example of a possible file format for storing deep shadow maps is illustrated in FIG. 20. All of the component elements of the file format described herein may be stored in secondary memory as a single contiguous data file, for example. It will be apparent to those skilled in the art that other file formats may also be employed without departing from the scope of the invention.

In FIG. 20, a file 2000 comprises an integer value 2001 representing the number of map levels included in the file, one or more map levels 2003, and a table of integer offsets identifying the starting location for each of the map levels 2003.

Each map level 2003 comprises a map size value 2004, a table 2005 of integer tile offsets and sizes, and one or more tiles 2006. Map size value 2004 identifies the dimensions of the map level in terms of tiles (e.g.,  $22\times 16$  tiles). Table 2005 lists the starting offsets, as well as the tile size (e.g., in bytes), for each of the tiles 2006 within the given map level.

A tile, in this instance, is a subset of contiguous map locations within a given map. Typically, the tile is two-dimensional (in x and y) in its configuration.

Each tile 2006 comprises a table 2007 of integer map location offsets and sizes, as well as one or more map locations 2008. Table 2007 lists the starting offsets, as well as the map location size (e.g., in vertices or vertex tuples) for each of the map locations in the tile. As described previously, each map location is a list of vertices, wherein each vertex comprises a depth value and one or more function values. The file format may be traversed to obtain desired deep shadow map data by reading the appropriate integer offset values at each level to navigate to the address of the target data.

#### Tiling and Caching

In one or more embodiments, a data cache is implemented within primary memory to store tiles of shadow map data during processing. Only those tiles currently or recently accessed are maintained in the cache, minimizing the shadow map footprint within the primary memory.

A block diagram of a cache implementation is provided in FIG. 21. As shown, a portion of primary memory is allocated as multiple cache lines 2100. Each cache line is configured to contain a tile of data from a deep shadow map. Cache function 2101 is associated with cache lines 2100 to manage access to the data within the cache lines, as requested by a rendering application, and to implement a cache line replacement policy between cache lines 2100 and the tile data stored in secondary memory (e.g., in a file on a disk or other permanent storage).

Cache function 2101 contains a hash table which takes as input a unique tile identifier (e.g., a map ID, map level number and tile number) supplied by the rendering application and determines whether the corresponding tile is in one of cache lines 2100. In the event of a cache "hit" (i.e., the requested tile is in one of cache lines 2100), the corresponding tile data is made available to the rendering application. In the event of a cache "miss" (i.e., the tile is not present in one of cache lines 2100), one of the resident tiles is evicted from cache lines 2100 in accordance with the particular cache line replacement policy. The requested tile data is then read into the vacated cache line from secondary memory in what is referred to as a cache line "fill."

One aspect of deep shadow maps that the cache implementation must consider is that deep shadow map files require varying amounts of storage. This is because varying numbers (and sizes) of vertices may be used to represent visibility functions within map locations. This size issue may be handled by determining a maximum tile size based on a maximum permitted number of vertices in each map location, in which case the compression process may be configured to enforce the new constraint. The cache lines may then be set to accommodate the maximum tile size.

Another mechanism for handling the tile sizing issue is to implement dynamic cache line sizing within the cache implementation. The cache is then free to grow to meet the needs of the data being cached. Because the cache size is flexible and does not need to meet the requirements of a worst-case tile size scenario at all times, more efficient memory usage can be achieved.

FIG. 22 illustrates one embodiment of a caching method that implements dynamic cache line resizing in accordance with one or more embodiments of the invention. In step 2200, the cache function 2101 receives a unique identifier for a tile of data. As stated above, this identifier may



comprise, for example, a map ID, map level number and tile number. In step **2201**, if cache function **2101** determines that the requested tile data is in one of the cache lines, the requested tile data is output in step **2206** to the requesting application (e.g., the renderer). Though not shown, more specific address information, such as a map location identifier and vertex number), may be used to access a particular map location or vertex tuple.

If, in step **2201**, cache function **2101** determines that the requested tile data is not resident in one of the cache lines (e.g., by querying the hash table), then, the method continues in step **2202**, where the size of the requested tile is determined (e.g., from table **2005** of the map data file). One of the resident tiles is evicted from a specified cache line in step **2203**, and, in step **2204**, the specified cache line is resized according to the size data determined in step **2202**. In step **2205**, the requested tile is read into the resized cache line from secondary memory, and, in step **2206**, the rendering application accesses the tile data from the cache.

Note, it is sufficient for the cache line to be resized when the current cache line size is smaller than the tile size. However, it is not necessary for the cache line to be resized if the current size of the cache line is bigger than the tile size. In one embodiment, the cache line is resized for each new tile. In another embodiment, the cache line is resized only when the tile size is larger than the current cache line size. In other embodiments, a cache line is always resized to accommodate a larger tile size, but is resized to a smaller tile size only if the tile size is significantly smaller or if the cache line has been consistently smaller over a period of time or a number of prior cache line fills.

#### Motion Blur

A desired imaging effect in animation is motion blur. When shadows are not motion blurred, strobing and other unwanted artifacts can occur. Unlike prior art shadow maps, deep shadow maps allow motion blur to be added without incurring an extra filtering cost. With deep shadow maps, motion blur can be implemented by associating a random time with every sample point in the map plane (and its corresponding transmittance function). When the samples are filtered together into visibility functions, the samples account for the average coverage over time as well as over the image plane.

Associating a random time with every depth value in a shadow map of the prior art is very expensive, because large filter widths are needed for adequate anti-aliasing and all filtering must wait until the depth samples are converted at pixel rendering time. In contrast, deep shadow maps do much of this filtering in advance, and thus reduce the number of pixels that need to be accessed for each lookup at pixel rendering time.

FIG. **23** is a flow diagram of a sampling method for accomplishing motion blur of shadows in accordance with one or more embodiments of the invention. In step **2300**, the map plane is diced into sample regions and sample points are selected from within those regions. In step **2301**, a pseudo-random time value from the current frame interval is associated with each sample point. In step **2301**, the transmittance function along each projected sample point is determined based on the state of the object scene at the instant specified by the time value associated with the respective sample point. In step **2303**, the transmittance functions are filtered to produce a visibility function averaged in space over the filter region and averaged in time over the current frame interval. Further filtering may be performed in the pre-rendering process to generate multiple

map levels in accordance with the mip-mapping techniques described herein, with the result that the output image includes shadows that are motion blurred without the need for additional high resolution filtering at pixel rendering time.

Motion blurred shadows produced with one or more of the embodiment described above are more correct when the receiving object is stationary with respect to the shadow camera. In particular, moving objects cast incorrect shadows onto other moving objects (and onto themselves). The deep shadow map effectively blurs an object's shadow over the entire shutter interval, allowing one object to cast shadows onto other objects at different times.

#### Computer Execution Environment (Hardware)

An embodiment of the invention can be implemented as computer software in the form of computer readable code executed on a general-purpose computer. Also, one or more elements of the invention may be embodied in hardware configured for such a purpose, e.g., as one or more functions of a graphics hardware system.

An example of a general-purpose computer **2400** is illustrated in FIG. **24**. A keyboard **2410** and mouse **2411** are coupled to a bi-directional system bus **2418**. The keyboard and mouse are for introducing user input to the computer system and communicating that user input to processor **2413**. Other suitable input devices may be used in addition to, or in place of, the mouse **2411** and keyboard **2410**. I/O (input/output) unit **2419** coupled to bi-directional system bus **2418** represents such I/O elements as a printer, A/V (audio/video) I/O, etc.

Computer **2400** includes video memory **2414**, main memory **2415** and mass storage **2412**, all coupled to bi-directional system bus **2418** along with keyboard **2410**, mouse **2411** and processor **2413**. The mass storage **2412** may include both fixed and removable media, such as magnetic, optical or magneto-optical storage systems or any other available mass storage technology. Bus **2418** may contain, for example, thirty-two address lines for addressing video memory **2414** or main memory **2415**. The system bus **2418** also includes, for example, a 64-bit data bus for transferring data between and among the components, such as processor **2413**, main memory **2415**, video memory **2414** and mass storage **2412**. Alternatively, multiplex data/address lines may be used instead of separate data and address lines.

In one embodiment of the invention, the processor **2413** is a microprocessor manufactured by Motorola, such as one of the PowerPC family of processors, or a microprocessor manufactured by Intel, such as the 80x86, or Pentium family of processors, or a SPARC™ microprocessor from Sun Microsystems™, Inc. However, any other suitable microprocessor or microcomputer may be utilized. Main memory **2415** is comprised of dynamic random access memory (DRAM). Video memory **2414** may be, for example, a dual-ported video random access memory. One port of the video memory **2414** is coupled to video amplifier **2416**. The video amplifier **2416** is used to drive the cathode ray tube (CRT) raster monitor **2417**. Video amplifier **2416** is well known in the art and may be implemented by any suitable apparatus. This circuitry converts pixel data stored in video memory **2414** to a raster signal suitable for use by monitor **2417**. Monitor **2417** is a type of monitor suitable for displaying graphic images. Alternatively, the video memory could be used to drive a flat panel or liquid crystal display (LCD), or any other suitable data presentation device.

Computer **2400** may also include a communication interface **2420** coupled to bus **2418**. Communication interface

2420 provides a two-way data communication coupling via a network link 2421 to a local network 2422. For example, if communication interface 2420 is an integrated services digital network (ISDN) card or a modem, communication interface 2420 provides a data communication connection to the corresponding type of telephone line, which comprises part of network link 2421. If communication interface 2420 is a local area network (LAN) card, communication interface 2420 provides a data communication connection via network link 2421 to a compatible LAN. Communication interface 2420 could also be a cable modem or wireless interface. In any such implementation, communication interface 2420 sends and receives electrical, electromagnetic or optical signals which carry digital data streams representing various types of information.

Network link 2421 typically provides data communication through one or more networks to other data devices. For example, network link 2421 may provide a connection through local network 2422 to local server computer 2423 or to data equipment operated by an Internet Service Provider (ISP) 2424. ISP 2424 in turn provides data communication services through the world wide packet data communication network now commonly referred to as the "Internet" 2425. Local network 2422 and Internet 2425 both use electrical, electromagnetic or optical signals which carry digital data streams. The signals through the various networks and the signals on network link 2421 and through communication interface 2420, which carry the digital data to and from computer 2400, are exemplary forms of carrier waves transporting the information.

Computer 2400 can send messages and receive data, including program code or data, through the network(s), network link 2421, and communication interface 2420. In the Internet example, remote server computer 2426 might transmit a requested code for an application program through Internet 2425, ISP 2424, local network 2422 and communication interface 2420.

The received code may be executed by processor 2413 as it is received, and/or stored in mass storage 2412, or other non-volatile storage for later execution. In this manner, computer 2400 may obtain application code (or data) in the form of a carrier wave.

Application code may be embodied in any form of computer program product. A computer program product comprises a medium configured to store or transport computer readable code or data, or in which computer readable code or data may be embedded. Some examples of computer program products are CD-ROM disks, ROM cards, floppy disks, magnetic tapes, computer hard drives, servers on a network, and carrier waves.

The computer systems described above are for purposes of example only. An embodiment of the invention may be implemented in any type of computer system or programming or processing environment.

Thus, a method and apparatus for rendering shadows have been described in conjunction with one or more specific embodiments. The invention is defined by the claims and their full scope of equivalents.

Chapter II: Subsurface Scattering Approximation Methods and Apparatus

FIG. 25 is a block diagram of typical computer rendering system 3100 according to an embodiment of the present invention.

In the present embodiment, computer system 3100 typically includes a monitor 3110, computer 3120, a keyboard 3130, a user input device 3140, a network interface 3150, and the like.

In the present embodiment, user input device 3140 is typically embodied as a computer mouse, a trackball, a track pad, wireless remote, and the like. User input device 3140 typically allows a user to select objects, icons, text and the like that appear on the monitor 3110.

Embodiments of network interface 3150 typically include an Ethernet card, a modem (telephone, satellite, cable, ISDN), (asynchronous) digital subscriber line (DSL) unit, and the like. Network interface 3150 are typically coupled to a computer network as shown. In other embodiments, network interface 3150 may be physically integrated on the motherboard of computer 3120, may be a software program, such as soft DSL, or the like.

Computer 3120 typically includes familiar computer components such as a processor 3160, and memory storage devices, such as a random access memory (RAM) 3170, disk drives 3180, and system bus 3190 interconnecting the above components.

In one embodiment, computer 3120 is a PC compatible computer having multiple microprocessors such as Xeon™ microprocessor from Intel Corporation. Further, in the present embodiment, computer 3120 typically includes a UNIX-based operating system.

RAM 3170 and disk drive 3180 are examples of tangible media for storage of data including, audio/video files, computer programs, compilers, embodiments of the herein described invention including geometric description of objects, object relationships and algorithms of scattering versus depth, thickness maps, thickness functions, object data files, shader descriptors, a rendering engine, output image files, texture maps, displacement maps, scattering lengths, absorption data and/or transmission data of object materials, and the like. Other types of tangible media include floppy disks, removable hard disks, optical storage media such as CD-ROMs and bar codes, semiconductor memories such as flash memories, read-only-memories (ROMS), battery-backed volatile memories, networked storage devices, and the like.

In the present embodiment, computer system 3100 may also include software that enables communications over a network such as the HTTP, TCP/IP, RTP/RTSP protocols, and the like. In alternative embodiments of the present invention, other communications software and transfer protocols may also be used, for example IPX, UDP or the like.

FIG. 25 is representative of computer rendering systems capable of embodying the present invention. It will be readily apparent to one of ordinary skill in the art that many other hardware and software configurations are suitable for use with the present invention. For example, the use of other micro processors are contemplated, such as Pentium™ or Itanium™ microprocessors; Opteron™ or AthlonXP™ microprocessors from Advanced Micro Devices, Inc; PowerPC G3™, G4™ microprocessors from Motorola, Inc.; and the like. Further, other types of operating systems are contemplated, such as Windows® operating system such as WindowsXP®, WindowsNT®, or the like from Microsoft Corporation, Solaris from Sun Microsystems, LINUX, UNIX, MAC OS from Apple Computer Corporation, and the like.

FIGS. 26A-C illustrate a block diagram of a process flow according to an embodiment of the present invention. Initially one or more objects are geometrically specified in a scene to be shaded (or rendered), step 3200. Any conven-

tional methods for entering such geometric specifications are contemplated, for example, Maya, or the like. The geometric specification may include any conventional way of representing a surface, such as triangles, quadrilaterals, NURBS, or the like.

In the present embodiment, one or more lighting sources are also specified for the scene, step 3210. For example, the specification of the lights may include the direction of the lights, color of the lights, “barn-door” positions of the lights, harshness of the light, and the like.

As illustrated in FIGS. 26A-C, a first lighting source is then selected from the one or more lighting sources specified for the scene, step 3220. For the first lighting source, a “thickness map” of objects in a scene relative to the first lighting source is then determined, step 3230. In the present embodiment, the thickness map represents a two-dimensional array of thickness functions at a viewing plane in front of the illumination source. The thickness function in each array element represent a thickness as a function of distance from a viewing plane in a direction for the lighting source outwards. In embodiments of the present invention, the thickness map is a 500x500 array of thickness functions, 1 kx1 k array of thickness functions, or the like. In other embodiments, thickness maps having a greater or fewer number of thickness function locations is contemplated. In one embodiment, the thickness map is a function of x and y in the viewing plane, and z in the depth plane, i.e.  $f(x,y,z)$

In one embodiment, the thickness function represents an integral amount of light-absorbing material each ray passes through beginning at the viewing plane. In the cases where there are multiple objects in a scene, the thickness function for a given ray represents the total amount of material (from the multiple objects) the ray passes through with respect to distance from the viewing plane. In some embodiments, the thickness function is formed assuming the multiple objects have the same density or same light-scattering properties. In some embodiments, the thickness function is formed based upon material density. For example, such cases can also take into account light-absorbing properties of volumetric effects or atmospheric material, such as fog, smoke, fire, water, hair, or the like. In such cases, an increase in “thickness” per unit distance would be smaller for the less dense material, than for denser material (such as marble, flesh, or the like). Examples of thickness functions are illustrated below.

In the present embodiment, once the thickness are determined thickness map (the array of thickness functions) is stored, step 3240. The thickness map for the lighting source may be stored in RAM, hard drive, optical drive, or the like. In the present embodiment, the thickness map is later used to determine the surface shading of typically more than one object in the scene. Accordingly, the thickness map is determined and saved once, and is typically retrieved and used more than once.

In FIGS. 26A-C, after the thickness map for the first lighting source is saved, if there are any other lighting sources, step 3250, a second lighting source is selected, and the process described above is repeated with respect to the second lighting source, etc. In the present embodiment, after thickness maps are determined for all lighting sources, the process in FIGS. 26A-C continues to the shading (rendering) process, step 3260. In embodiments of the present invention, the above described steps may be performed at a different time from the below steps. For example, the thickness maps may be determined and stored by a user in a first work group, and later, the stored thickness maps may be used by a user in a different work group. In other embodiments, a user may initiate all of the herein described steps.

In the present embodiments, a first surface location on an object is selected for shading, step 3270. The coordinates of the surface location within the various coordinate systems is known, for example with respect to the camera space, and the like. Further, the surface normal, surface characteristics, and the like are also known, and are used later for the shading calculations.

Many different rendering methods may be implemented that result in the selection of the surface location on the object. Further, many different techniques for determining which object is selected from the scene are contemplated. For example, in one embodiment, only a portion of an object to be shaded is retrieved at a time. One such cases where this may happen is when using a “bucket” rendering method, as is currently used in Pixar’s rendering software Renderman™. In alternative embodiments, objects are retrieved from disk into memory and are shaded, at a time for a series of related images (a shot). Such embodiments may use the rendering and shading techniques disclosed in co-pending U.S. patent Application Ser. No. 10/428,325 filed Apr. 30, 2003, titled, “Shot Shading Method and Apparatus,” (incorporated by reference for all purposes) commonly assigned to Pixar. Accordingly, how the surface location on the object is determined and how and which portions of objects are selected are done in a variety of ways.

In FIGS. 26A-C, the next steps are to determine the surface shading value for the surface location in response to the different lighting sources in the scene. In the present implementation, this is done by first selecting a first lighting source, step 3280. In embodiments of the present invention, this may or may not be the same lighting source selected in step 3220 above. In various embodiments, the order the lighting sources are evaluated is based upon lighting hierarchy, strength of the lighting source, or the like. In other embodiments, there is no specific order the lighting sources are selected.

In the present embodiments, the thickness map associated with the lighting source is retrieved from memory, step 3290. For example, the thickness map determined in step 3230 above, for example, may be retrieved from a hard disk memory into RAM.

As described above, typically each array location in the thickness map is associated with a thickness function that is a function of distance from a lighting viewing plane in the direction away from the lighting source towards the objects in the scene. Accordingly, the surface location is mapped onto the thickness map to determine the thickness function (“center thickness function”) associated with the surface location, step 3300. In additional embodiments, thickness functions neighboring the “center thickness function” in the thickness map associated with the surface location are also identified.

Next, in this embodiment, using the thickness function, and the distance of the surface location from the illumination viewing plane, the thickness is determined at the surface location, step 3310. In embodiments of the present invention, these above steps may be merged together.

In some embodiments, in step 3300, thickness functions neighboring the “center thickness function.” are also identified. Further in step 3310, in additional embodiments, the neighboring thickness functions are also evaluated given the distance to the surface location, to determine neighboring thicknesses. In various embodiments, the neighborhood may be a 3x3 grid around the “center thickness function” in the thickness map. In embodiments of the present invention, the size of the neighborhood may vary automatically or by user selection. For example, in thinner objects, the neighborhood

may be a 3×3 array, whereas for thicker objects, the neighborhood may be a 2×2, 7×7, 9×9, etc. kernel array, or the like.

In alternative embodiments of the present invention, the surface locations and the neighboring surface locations are used to identify the “neighboring” thickness functions. In some embodiments, neighboring surface locations map onto unique thickness functions, however in other embodiments, neighboring surface locations may map to the same thickness function. An example of the latter case is when the resolution of the thickness map is much lower than the resolution of surface locations.

In embodiments of the present invention described above, the thickness at the surface location and the neighboring thickness are combined to obtain a single thickness for the object at the surface location in step 3310. Generally, the thickness at the surface location is then determined by filtering the thicknesses. For example, in some cases, the thickness is the average or weighted average of the thicknesses and the neighboring thicknesses; in other cases the thickness is any other combination (convolution) of the thicknesses such as a low-pass filter, median filter, Gaussian filter, high-pass filter and the like. In one embodiment, by filtering thicknesses from a neighborhood thicknesses, the thicknesses at surface of the object tend to average out or be blurred. Because the object thicknesses are averaged out, the illumination at a particular surface location is “softened.” This simulates the scattering of light rays through the object.

In embodiments of the present invention, the neighborhood size and the filter applied may be varied by the user to vary the scattering effect of the object material. Accordingly, if the user wants to change the scattering characteristics of the material, the user can do so by varying these parameters and without having to recalculate the thickness maps and functions. This ability greatly increases turn-around time.

In embodiments of the present invention, based upon the filtered thickness determined above, and the light absorbing properties defined for the thickness, an illumination contribution from the light source at the surface location is determined, step 3320. The light absorbing properties for the material versus thickness of the material is typically pre-specified by a user. For example, a user may specify that a percentage (e.g. 50%) of incident illumination is absorbed through a specified thickness of material. Alternatively, the user may specify that a percentage (e.g. 33%) of incident illumination is absorbed through a unit thickness of material. Many other ways to characterize the absorption property of materials are also contemplated. In the present embodiment, based upon the absorption characteristics of the material for a particular thickness, and given the filtered thickness determined in step 3310 above, the illumination contribution at the specified surface location can easily be determined. Examples of this will be given below. In light of the above, one of ordinary skill in the art would recognize that instead of absorbing properties versus thickness, one could utilize relationships between light transmission properties of an object material versus thickness for embodiments of the present invention.

In other embodiments, if different materials are used to contribute to the thickness maps, the thickness function can take into account the different absorption qualities of the different materials. As an example, the thickness function may be based upon material density. For instance, atmospheric haze may provide a smaller increase in thickness in a thickness function per unit distance compared to thick smoke.

In addition, in some embodiments of the present invention, the materials that make up the calculated thickness may have different absorption properties for different frequencies of light. Accordingly, users can specify a material absorption versus thickness of material based upon frequency of light. For example, nitrogen gas scatters and absorbs blue wavelengths of light more than red wavelengths of light, accordingly absorption versus material for red light is less than absorption versus material of blue light.

In still other embodiments, combinations of different materials, and different absorption characteristics of the different materials with respect to wavelength can be used to determine the illumination contribution of the surface location.

In the present embodiment, the shading contribution of the light source in a direction of the viewer is then determined, step 3330. Conventional shading techniques may be used in embodiments of the present invention taking into account, the surface normal direction, a color of the illumination determined in step 3320, above, a color of the surface, a image viewing plane normal, and the like. Other parameters are also contemplated and used in other embodiments of the present invention.

In FIGS. 26A-C, once the shading contribution from a first light source at the surface location has been determined, if there are other light sources, step 3340, the process above repeats for the remaining illumination sources.

Once the shading contributions of all illumination sources at the surface location have been determined, the shading contributions are then combined, step 3350. In some embodiments, the combination may simply be a sum of intensities. In other embodiments, when the shading contributions have different frequency components, thus the combination may be a sum of the intensities at the different frequencies. Other conventional methods for combining the shading values may also be used. In additional embodiments of the present invention, a weighted combination of the illumination contributions can be used.

In the present embodiment, the process above may be repeated for other surface locations on an object in the scene, step 3360, to obtain combined shading values for such surface locations. In one embodiment, stochastic sampling techniques pioneered by Pixar, such as U.S. Pat. No. 4,897, 806 may then be used to sample the combined shading values of surface locations, to form a value for a pixel in an image, step 3370. Such techniques are incorporated into the Renderman® rendering software. The use of other rendering software and hardware are contemplated in other embodiments of the present invention.

This process is repeated for all pixels in the image, typically until values for all pixels in the image are determined, step 3380.

In one embodiment, the resulting image may be further processed and then recorded onto a tangible media such as a strip of film, a magnetic memory (hard disk), an optical memory (DVD, VCD), or the like. Subsequently, the image may be retrieved from the tangible media and output to users (e.g. animator, audience member, and the like.), step 3390.

FIGS. 27A-D illustrate an example of an embodiment of the present invention. More specifically, FIGS. 27A-D illustrates thickness map and thickness function representations.

In FIG. 27A, an object 3400 is shown illuminated by a lighting source 3410. Also shown are a number of rays, including rays 3420, 3430, and 3440 that are projected from lighting source 3410 through a lighting viewing plane 3450. As shown in FIG. 27A, ray 3420 initially intersects object 3400 at point z1 3460, passes through object 3400, and exits

at point z2 3470. Further, ray 3430 initially intersects object 3400 at point z3 3480, passes through object 3400, and exits at point z4 3490. In this example, ray 3440 does not pass through object 3400.

FIG. 27B illustrates a thickness map 3500 generated at viewing plane 3450. In this example, ray 3420 is mapped to location 3510, ray 3430 is mapped to location 3520, and ray 3440 is mapped to location 3530. Also illustrated are thickness functions 3540-3560 corresponding to locations 3510-3530, respectively. As can be seen, in these example, the amount of light varies with respect to distance.

In the example of FIG. 27C, two objects 3570 and 3580 are illustrated with an atmospheric or volumetric effect 3590, in between. Also illustrated is a lighting source 3600 and a projected ray 3610. As can be seen, ray 3610 penetrates object 3580, passes through volume 3590, and then penetrates object 3570. In the example of FIG. 27D example thickness functions 3620A-B are shown.

In a first example, thickness function 3620A is shown with material density of objects 3570 and 3580 being the same, and volume 3590 not attenuating ray 3610. In a second example, thickness function 3620B is shown with the material density of objects 3570 and 3580 being different (having different slopes), and the material density of volume 3590 adding to the thickness.

FIG. 28 illustrates an example according to an embodiment of the present invention. In this example, two lights 3700 and 3710 are illustrated illuminating an object 3720. In this example, a thickness map 3730 and 3740 are formed with respect to object 3720. As shown, a ray 3750 in thickness map 3730 passes through object 3720 and a thickness function 3760 is determined. Further, a ray 3770 in thickness map 3740 passes through object 3720 and a thickness function 3780 is determined.

In this example, a shading value for the point z1 3790 on the surface of object 3720 is to be determined. In one embodiment, for light 3700, thickness function 3760 is mapped to point z1 3790, and the thickness is T1 3800. Next, for light 3710, thickness function 3780 is mapped to point z1 3790, and in this case, the thickness is 0, i.e. the light is not attenuated.

In the present embodiment, the absorption characteristics of the material are typically specified by the user. The absorption characteristics and the thickness of the material are then used in this embodiment to determine the amount of light remaining at a point, after the light passes through the specified thickness of material. In embodiments of the present invention, the absorption characteristics of the material may be linearly dependent or non-linearly dependent upon material thickness (depth).

In the example of FIG. 28, the absorption characteristics of the material of object 3720 is referred to. As shown in graphs 3820 and 3830, the absorption of the material of light is dependent upon the frequency of light. Specifically, graph 3820 illustrates the attenuation of red light with respect to thickness, and graph 3830 illustrates the attenuation of blue light with respect to thickness. Additional graphs may be specified for other colors, such as green, yellow, or the like. In this example, at thickness T1 3800, it can be seen that red wavelengths of light are not completely attenuated, whereas at thickness T1 3800, blue wavelengths of light are substantially attenuated. Thus, according to this example, if light source 3700 outputs red and blue lights at the same intensity, at point z1 3790, the illumination contribution from light source 3700 would be red light at 10% of the initial red intensity. Further, if light source 3710 outputs blue and red lights at the same intensity, at point z1 3790, the illumination

contribution from light source 3710 would be red and blue light at the initial intensities. The illumination contributions are then combined with the surface normals, the viewer normal, and the like to determine a shading value at point z1 3790.

Embodiments of the present invention are very useful in cases where light is attenuated, but not necessarily fully blocked by objects in a scene. For example, embodiments may be applied to objects such as fish, bones, jellyfish, octopus, anemones, glass block, and other materials that have translucent qualities. Similarly, embodiments may be applied to other translucent materials, such as atmospheric effects such as rain, fog, clouds, and the like, volumetric effects such as hair, feathers, fur, and the like.

Many changes or modifications are readily envisioned. For example, in one embodiment, one ray from an illumination source to the surface location may be used to determine the illumination contribution at a surface location. In other embodiments, rays from the illumination source to the surface location and neighboring surface locations are used to determine the illumination contribution at the surface location. By using a neighborhood approach, a filter (such as a low-pass filter, median filter, Gaussian filter, high-pass filter and the like) is applied to the neighborhood of illumination contributions on the surface location in interest.

As an example, when using a single ray to determine the illumination contribution, an illumination ray may strike a fish bone or other internal organ and be absorbed. As this would be repeated for other surface locations, the result would be a sharp silhouette of the fish bones or the like, on the side of the fish away from the light. By considering illumination contributions of a neighborhood of surface locations and filtering them, a result would be a softer silhouette of the fish bones on the side of the fish away from the light. In embodiments of the present invention, the size of the neighborhood may vary automatically or by user selection. For example, in thinner objects, the neighborhood may be a 3x3 array, whereas for thicker objects, the neighborhood may be a 4x4, 5x5, 11x11, etc. array, or the like. In embodiments of the present invention, the neighborhood size and the filter applied may be varied by the user to vary the diffuse effect of the object. By allowing the user to easily vary these parameters, this reduces the requirement to recalculate thickness maps and thickness functions, every time the material scattering characteristics change.

In light of the above disclosure, one of ordinary skill in the art would recognize that the shaded value of a surface location may be determined from direct illumination of the surface location of the object and illumination passed through the object. The combination of both of these types of illumination can be used to determine a final illumination value at the surface location. In embodiments of the present invention, any linear or non-linear combination of these values may be used. In further embodiments, a weighting of these values may be performed by the user. For example, the user may determine that an object "glows too much" accordingly, the user may lessen the illumination contribution weighting due to a backlight, or the like. By allowing the user to easily vary the illumination contribution, this reduces the requirement to re-calculate thickness maps and thickness functions, based upon different material absorption characteristics.

In some embodiments of the present invention where light at different frequencies are absorbed at different rates, the absorption at a given light frequency may be based upon absorption of primary color components. As an example, for a particular material, an absorption relationship for red light,

green light, and blue light may be provided by the user. Next, to determine how the material absorbs yellow light, the yellow light is represented as a red light of a particular intensity and a green light of a particular intensity. Based upon the given material thickness, the amount of red and green light absorbed (and remaining) are determined. Finally, the illumination contribution is a combination of the remaining red light and green light intensities. As an example, if a yellow light is directed towards the rear of an object made of green jade, because red wavelengths are absorbed by the jade, the light that shines through the front of the object will be greenish.

In additional embodiments, the user may specify the color of light transmitted according to thickness of material. For example, the absorption relationship for the material may specify that for a first thickness, the illumination contribution will be red, for a second thickness, the illumination contribution will be green, and for a third thickness, the illumination contribution will be blue. In such cases the absorption relationship effectively specifies a color "filter" in response to object thickness. For example, if the illumination source is white light, if an object has a first thickness, the illumination contribution is red, if the object has a second thickness, the illumination contribution is green, and the like. As another example, if the illumination source is purple light, if the object has a first thickness, the illumination contribution is red, if the object has a second thickness, there is no illumination contribution, and if the object has a third thickness, the illumination contribution is blue.

In other embodiments of the present invention, thickness functions, such as illustrated in the above figures need not be actually represented by a mathematical function. Instead, in some embodiments, the thickness functions can simply be a table of entries including a distance and a thickness value. In some embodiments, the surface shading, i.e. the color of the surface of an object is important. Thus, in such cases, only the distance from the illumination viewing plane, and the thickness at that point are relevant for illumination contribution purposes. As an example, in FIG. 27D, for thickness map 3620A, the illustrated thickness function may simply be represented as a series of number pairs:  $\{(z_1, T_0), (z_2, T_0), (z_3, T_0), (z_4, T_1)\}$ . A simple counter could be used to indicate if a point is within an object or outside an object.

In light of the above disclosure, the inventors believe that fast and high quality shading of non-opaque objects can now be performed. Typical non-opaque object material may include waxy or fleshy items such as skin, wax, fruit, bones, etc. as well as thin objects, or the like.

In the above embodiments, certain assumptions and techniques are applied that reduce the amount of mathematical calculations compared to the prior art. The shading values produced using embodiments of the present invention will not necessarily be mathematically correct, however is acceptable for animation purposes. Additionally, it is believed that objects shaded using embodiments of the present invention will have characteristics uniquely identifiable from a mathematically correct simulation.

Embodiments of the present invention may be applied to any number of rendering platforms and for a variety of purposes. For example, embodiments may be used on engineering workstations for development purposes, on visualization systems for artists and animators, in rendering farm machines for final production, on computer graphics boards and the like. Accordingly, the concepts disclosed above are extremely valuable in a variety of applications.

Further embodiments can be envisioned to one of ordinary skill in the art after reading this disclosure. In other

embodiments, combinations or sub-combinations of the above disclosed invention can be advantageously made. The block diagrams of the architecture and flow charts are grouped for ease of understanding. However it should be understood that combinations of blocks, additions of new blocks, re-arrangement of blocks, and the like are contemplated in alternative embodiments of the present invention.

The specification and drawings are, accordingly, to be regarded in an illustrative rather than a restrictive sense. It will, however, be evident that various modifications and changes may be made thereunto without departing from the broader spirit and scope of the invention as set forth in the claims.

What is claimed is:

1. A method for determining illumination of surface points of an object in a scene from lighting sources comprises:

determining a first thickness map for a first lighting source for the scene, wherein the first thickness map includes, for a plurality of rays from the first lighting source, respective thickness functions, each thickness function representing thickness values of the object with respect to distance from the first lighting source along the respective ray;

determining a surface point on the object;

determining, for a first plurality of surface points in the neighborhood of the surface point, a first plurality of thickness values associated with the first plurality of surface points on the object in response to the first thickness map;

determining a first filtered thickness value associated with the surface point on the object in response to the first plurality of thickness values; and

determining an illumination contribution from the first lighting source at the surface point in response to the first filtered thickness value.

2. The method of claim 1 wherein determining the illumination contribution further comprises calculating the illumination contribution in response to the first filtered thickness value and a thickness value relationship for the object selected from the group: thickness value versus absorption relationship, thickness value versus transmission relationship.

3. The method of claim 2 wherein the first plurality of thickness values of the object with respect to the first lighting source vary in direction away from the first lighting source.

4. The method of claim 3 wherein determining the first plurality of thickness values comprises determining a first plurality of thickness values of the object between the first lighting source and the plurality of surface points in the respective directions.

5. The method of claim 1 further comprising:

determining a second thickness map for a second lighting source for the scene, wherein the second thickness map includes, for a plurality of rays from the second lighting source, respective thickness functions, each thickness function representing thickness values of the object with respect to the second lighting source along the respective ray;

determining, for a second plurality of surface points in the neighborhood of the surface point, a second plurality of thickness values associated with the second plurality of surface points on the object in response to the second thickness map;

41

determining a second filtered thickness value associated with the surface point on the object in response to the second plurality of thickness values; and

determining an illumination contribution from the second lighting source at the surface point in response to the second filtered thickness value. 5

6. The method of claim 5 further comprising determining a shading value for the surface point on the object in response to an illumination contribution selected from the group: the illumination contribution from the first lighting source, the illumination contribution from the second lighting source, the illumination contribution from the first lighting source and the illumination contribution from the second lighting source. 10

7. The method of claim 1 further comprising:  
determining a shading value for the surface point on the object in response to the illumination contribution from the first lighting source;  
determining a value for a pixel in an image in response to the shading value; and  
storing a representation of the image in a tangible medium. 20

8. The method of claim 7 further comprising outputting the representation of the image from the tangible medium to one or more viewers. 25

9. A computer system comprises:

a memory configured to store a first thickness map associated with a first illumination source within a scene, wherein the first thickness map includes, for a plurality of rays from the first lighting source, respective thickness functions of at least one object, each thickness function representing thickness values of the object versus distance away from the first illumination source along the respective ray; and

a processor coupled to the memory, wherein the processor is configured to  
retrieve the first thickness map from the memory,  
determine a surface point on the at least one object,  
determine a neighborhood of surface points on the at least one object in response to the surface point on the at least one object,  
determine, for the neighborhood of surface points, a plurality of thickness values of the at least one object in response to the neighborhood of surface points and in response to the first thickness map,  
determine a filtered thickness value associated with the surface point of the at least one object in response to the plurality of thickness values, and  
determine an illumination contribution from the first illumination source at the surface point in response to the filtered thickness value of the at least one object. 35 40 45 50

10. The computer system of claim 9 wherein:  
the memory is also configured to store a relationship between thickness values of the at least one object versus a characteristic selected from the group: illumination attenuation, illumination transmission, and  
the processor is configured to determine the illumination contribution in response to the filtered thickness value and in response to the relationship. 60

11. A computer system comprises:

a memory configured to store:  
a first thickness map associated with a first illumination source within a scene, wherein the first thickness map includes a first plurality of thickness functions of at least one object versus distance away from the first illumination source, 65

42

a first relationship between thickness values of the at least one object versus a characteristic selected from the group: illumination attenuation in a first color component, illumination transmission in the first color component, and

a second relationship between thickness values of the at least one object versus a characteristic selected from the group: illumination attenuation in a second color component, illumination transmission in the second color component; and

a processor coupled to the memory, wherein the processor is configured to  
retrieve the first thickness map from the memory,  
determine a surface point on the at least one object,  
determine a neighborhood of surface points on the at least one object in response to the surface point on the at least one object,  
determine a plurality of thickness values of the at least one object in response to the neighborhood of surface points and in response to the first thickness map,  
determine a filtered thickness value of the at least one object in response to the plurality of thickness values,  
determine an illumination contribution from the first illumination source at the surface point in response to the filtered thickness value of the at least one object and in response to the first and second relationships. 70

12. The computer system of claim 11 wherein the first color component and the second color component are selected, without replacement from the same one of the color component groups consisting: {red, green, blue}, {cyan, magenta, yellow}.

13. The computer system of claim 11 wherein the first relationship and the second relationship are different.

14. The computer system of claim 13 wherein each of the first plurality of thickness functions of the object versus distance away from the first illumination source comprise a table of thickness values of the object versus distance from the first illumination source.

15. The computer system of claim 9 wherein the processor is also configured to determine a shading value for the surface point in response to the illumination contribution for the first illumination source at the surface point.

16. A computer program product for a computer system including a processor includes:

code that directs the processor to specify an object;  
code that directs the processor to retrieve a first thickness map for a first illumination source for the scene, wherein the first thickness map includes, for a plurality of rays from the first lighting source, respective thickness functions, wherein each thickness function comprises a relationship between thickness values of the object with respect to distance from the first illumination source along the respective ray;  
code that directs the processor to determine a surface point on the object;  
code that directs the processor to determine, for a first plurality of surface points in the neighborhood of the surface point, a first plurality of thickness functions associated with the surface point on the object in response to the first thickness map;  
code that directs the processor to determine a first plurality of thickness values in response to the first plurality of thickness functions; 75

43

code that directs the processor to determine a first filtered thickness value associated with the surface point on the object in response to the first plurality of thickness values; and

code that directs the processor to determine an illumination contribution from the first illumination source at the surface point in response to the first filtered thickness value;

wherein the codes reside on a tangible medium.

17. The computer program product of claim 16 wherein code that directs the processor to determine an illumination contribution comprises code that directs the processor to determine the illumination contribution from the first illumination source at the surface point in response to the first filtered thickness value and a relationship for the object selected from the group: absorption versus thickness value, transmission versus thickness value.

18. The computer program product of claim 17 wherein the first plurality of thickness values comprise amounts of material of the object between the first illumination source and the surface point on the object and surface points in a neighborhood of the surface point on the object.

19. The computer program product of claim 17 wherein: the relationship for the object comprises an absorption amount of a primary component of light versus thickness value; and

the primary component of light is selected from the group: red, green, blue.

20. The computer program product of claim 18 further comprising code that directs the processor to determine the first thickness map for the first illumination source for the scene.

21. The computer program product of claim 19 further comprising:

code that directs the processor to determine a shading value at the surface point in response to the illumination contribution from the first illumination source; code that directs the processor to determine a pixel value in response to the shading value; and

code that directs the processor to store a representation of a frame of animation including the pixel value in a tangible medium.

22. A method for determining illumination of surface points of an object in a scene from lighting sources comprises:

determining a first thickness map for a first lighting source for the scene, wherein the first thickness map includes, for a plurality of rays from the first lighting source, respective thickness functions, each thickness function representing thickness values of the object with respect to distance from the first lighting source along the respective ray;

determining a surface point on the object;

determining, for a first plurality of surface points in the neighborhood of the surface point, a first plurality of thickness values associated with the first plurality of surface points on the object in response to the first thickness map;

determining a first filtered thickness value associated with the surface point on the object in response to the first plurality of thickness values; and

44

determining an illumination contribution from the first lighting source at the surface point in response to the first filtered thickness value and further in response to a relationship characterizing the passage of at least first and second color components of light from the first lighting source through the object.

23. The method of claim 22 wherein the relationship for the object is selected from the group: thickness value versus absorption relationship for the first and second color components, thickness value versus transmission relationship for the first and second color components.

24. A computer program product for a computer system including a processor includes:

code that directs the processor to retrieve a first thickness map for a first illumination source for the scene, wherein the first thickness map includes, for a plurality of rays from the first lighting source, respective thickness functions, wherein each thickness function comprises a relationship between thickness values of the object with respect to distance from the first illumination source along the respective ray;

code that directs the processor to determine a surface point on the object;

code that directs the processor to determine, for a first plurality of surface points in the neighborhood of the surface point, a first plurality of thickness functions associated with the first plurality of surface points on the object in response to the first thickness map;

code that directs the processor to determine a first plurality of thickness values in response to the first plurality of thickness functions and in response to the surface point on the object;

code that directs the processor to determine a first filtered thickness value associated with the surface point on the object in response to the first plurality of thickness values; and

code that directs the processor to determine an illumination contribution from the first illumination source at the surface point in response to the first filtered thickness value and further in response to a relationship characterizing the passage of at least first and second color components of light from the first lighting source through the object;

wherein the codes reside on a tangible medium.

25. The method of claim 1 wherein the first plurality of surface points in the neighborhood of the surface point includes the surface point.

26. The method of claim 1 wherein the first plurality of surface points in the neighborhood of the surface point does not include the surface point.

27. The computer program product of claim 16 wherein the first plurality of surface points in the neighborhood of the surface point includes the surface point.

28. The computer program product of claim 16 wherein the first plurality of surface points in the neighborhood of the surface point does not include the surface point.

\* \* \* \* \*